Optimisation of the Process Parameters of the Resin Film Infusion Process.

Christopher J von Klemperer

Centre of Composite Materials and Structures
School of Mechanical Engineering
University of Natal
Durban
1999

Thesis submitted in fulfilment of the academic requirements for the degree of Doctorate of Philosophy in the School of Mechanical Engineering, University of Natal, Durban.

October 1999

Abstract

The resin film infusion process or RFI is a vacuum assisted moulding method for producing high quality fibre reinforced components. The goals of this research have been to investigate this new process, with the aim of determining how the process could be used by the South African composites industry. This included factors such as suitable materials systems, and optimum process parameters.

The RFI process is a new composite moulding method designed to allow fibre reinforced products to be manufactured with the ease of pre-preg materials while still allowing any dry reinforcement material to be used. The high pressures required for traditional manufacturing methods such as autoclaves, matched dies and RTM can be avoided while still having very accurate control over the fibre / resin ratio.

Moreover, the RFI process is a "dry" process and hence avoids many of the environmental and health concerns associated with wet lay-up and vacuum bag techniques. Furthermore the simple lay-up process requires less skill than a wet lay-up and vacuum bag method.

Through a combination of mathematical modelling and physical testing, a material system has been identified. The primary process parameters were identified and a strenuous regime of testing was performed to find optimum values of these parameters. These results were finally feed back into the development of the mathematical model.

Declaration

I, Christopher J. von Klemperer student number 911 429791, hereby declare that this dissertation is my own unaided work, unless otherwise stated. It is being submitted for the Degree of Doctorate of Philosophy in Mechanical Engineering to the University of Natal, Durban. Neither this dissertation nor any part thereof has been submitted for any degree or examination at any other university.

Acknowledgements

I would like to thank:

Prof. VE Verijenko, my supervisor for all the direction, encouragement and invaluable input during the course of this research.

Igor Sevostianov for the initial direction and continued guidance with the development of the mathematical model.

Amith Singh, Sailesh Gangaram, Sibusiso Zulu, Vincent Mbatha, Prinal Patel and Nirvan Sookay; the 1998 and 1999 final year RFI project students for assistance with all the sample manufacture and testing.

Kate Hall and Hafeeza Mahomed at AMT Durban for assistance with the material systems and supplies of Redux.

Administration staff, lecturers and workshop technicians at the School of Mechanical Engineering and the Centre of Composite Materials and Structures for their advice and assistance.

My family and friends for their support and encouragement.

The NRF Competitive Industry section, Kentron, and the University of Natal for their financial support.

Contents

List of Figures

List of Tables

Principal Symbols

$\sigma_{tensile}$	Tensile stress
σ_{bend}	Bending stress
$\varepsilon_{tensile}$	Tensile strain
F	Force or applied load
A	Area
L	Length
ΔL	Change in length
I	Moment of inertia (2^{nd} moment of area)
b	Breadth
d	Depth or diameter
M	Bending moment
P	Pressure
ΔP	Pressure difference
ρ	Density
g	Acceleration due to gravity = 9.81 m/s^2
h	Height
Q	Flow rate
Δz	Thickness
k	Permeability
T	Temperature
μ	Absolute viscosity

(Symbols used in the chapter on Mathematical Modelling are described in the text.)

List of Abbreviations

RFI	Resin Film Infusion process.
RTM	Resin Transfer Moulding.
GRP	Glass Reinforced Plastic
PVC	Ply-Vinyl-Chloride.
SCRIMP	Seemann Composites Resin Infusion Moulding Process.
AMT	Advanced Materials Technologies. (Retailer)
CSIR	Centre for Scientific and Industrial Research. (South Africa)
PLC	Programmable Logic Controller.
0°	Stacking sequence consisting of one unidirectional laminate.
0°/90°	Stacking sequence consisting of 2 laminae at 90° to each other.
FAN	Flow Analysis Technique.
FEM	Finite Element Method.
1-D	One dimensional.
2-D	Two dimensional.
3-D	Three dimensional.

1. Aim

The aim of this project is to study the Resin Film infusion moulding process with the goal of optimising the materials used and the process parameters. This was investigated using a combination of theoretical and experimental approaches.

2. Introduction

Increasing activity in composites manufacturing technology has focused on the development of low cost processing. Traditional methods have proven not only to be costly in terms of the tooling required but also hazardous to human health due to the vapour emissions and hazardous materials. Because of these drawbacks, the drive to find a dry material process has been gaining momentum over recent years. Resin film infusion (RFI) represents such a process.

The resin film infusion process makes use of a vacuum bag technology to debulk and compact reinforcement material and dry film, which is placed on top of the reinforcement in a single sided mould. The entire assembly is then heated to allow a thermoplastic or thermosetting resin film to become molten and flow into and throughout the preform material. A further heating stage is then required to cure the resin.

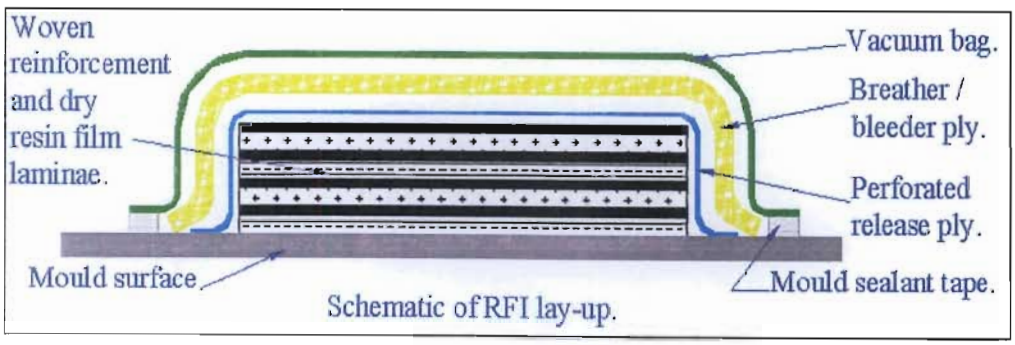

Figure 1 Schematic of basic lay-up process for RFI sample manufacture.

The research necessary to develop this process for the local composites industry consisted of three areas:

- The selection of a suitable material system
- The identification of the primary process parameters
- Optimisation of those parameters for product quality and cost.

A suitable material system would include the following:

- A dry thermosetting resin film, with good structural properties, and a cure temperature below 200°C.
- Bleeder cloths: A porous fabric to absorb excess resin as the consolidation occurs.
- Release layers: Porous release films to be placed between the component, and the breather cloths. They ensure that the resin in the component does not bond to the breather cloth, or the vacuum bag, while allowing excess resin to be drawn through into the bleeder material.
- Vacuum bag sealant tapes, which are sealant tapes used to form airtight seal between the vacuum bag and the mould.
- Peel ply fabrics: These are woven materials of Nylon or Polyester yarns, which are very strong and have good heat resistance. Their function is to provide a clean, uncontaminated surface for either secondary bonding or painting.
- Reinforcement materials, which provide the reinforcement to the composite. Ideally any of the currently available fibre reinforcement materials such as glass, carbon or aramid fibres should all be compatible with the RFI process.

The main focus of the material system research has been into finding a suitable dry resin, as the remaining materials will be similar or identical to those currently used for wet lay-up composite moulding methods. This is necessary to ensure compatibility between RFI and existing fibre composites, and help keep the costs down.

The process parameters which were investigated included the temperature profile, the dwell times to allow the molten resin to soak through the component and final curing of the component, the ramp speeds (i.e. the time to raise the temperature to dwell, and the dwell temperatures themselves). In addition the effect of vacuum pressure was investigated. The goal of this investigation was to ascertain optimum parameters, which minimised costs, with respect to the quality of the component. (The quality of the component will depend on the application, but could be the strength, mass or even the surface finish of the completed component).

In addition to physically testing materials, and processes, a mathematical model was developed. This work took place in parallel with the experimental work. The process was numerically modelled as a fluid flow problem using Darcy's law with a viscous fluid (liquid resin) passing through a porous media (woven reinforcement). This permitted factors such as void formation (caused by cavitation of the resin) and possible damage to the woven reinforcement due to the high stresses resulting from the moving resin front to be studied and the process parameters optimised. The data obtained from this research was used as the starting point for the initial experimental work. Finally the experimental work was conducted to verify and update the mathematical model with the aim of producing software which would give the optimum parameters for different applications.

3. Literature Survey

3.1. Introduction.

The choice of modern composite manufacturing methods are, as with all engineering decisions, driven by cost, quality, health and safety concerns, and a consideration of fitness for purpose. For some time now, the development of the manufacture of medium to large size structures of high fibre volume fraction (more than 45 %) has centred on resin transfer moulding techniques, compression moulding and autoclave vacuum bag methods.

Since the 1980's a variety of composite material processes has been developed with the objective of reducing manufacturing cost by replacing conventional pre-preg materials and lamination processes. These composite processes have been considered more of an art than a science and have been developed through trial and error. Utilising the concept that the viscosity of homogeneous thermosetting system can reach quite low values at elevated temperatures before cure is initiated, resin infusion into a dry fibrous preform becomes an attractive manufacturing technique especially for 3-D composite structures. This resin infusion process can provide a better alternative to the pre-pregging process. By using a resin system which exists as a dry film at room temperatures, the process can be used alone or in conjunction with pre-preg.

3.2. Stitched Composites and RTM vs. RFI

Monolithic structural composites are generally processed by laying up pre-impregnated continuous fibres (i.e. pre-preg) and curing under high temperature and pressure. Compared to the conventional pre-pregs, a knitting technology based stitching process is a relatively new way of fabrication. This stitching process was found to resolve some of the disadvantages of pre-pregs such as low resistance to "in-plane" compression loads with delamination type of damage, and low inter-laminar shear strength. In addition, stitching is found to enhance the impact resistance as well as the static-through-the-thickness mechanical properties of composites.[11,73] Stitching with pre-preg would be practically impossible, causing fibre breakage and misalignment after the stitching. With the help of textile technology and resin infusion process a "materials-by-design" concept that can design complex textile structures in the aerospace and automotive industries may be possible.[74] However, there are several technological and physical limitations that have to be resolved before such technology is put into practice.

Resin transfer moulding (RTM) is already a well established technique for high production rate of small scale complex composite pans. The degree of complexity is usually determined by moulds suitable for press forming operations.[75,76] The RTM process allows greater flexibility in designing complex shapes by varying processing conditions, preform types, and reinforcement directions. For large shapes, tooling costs can become excessive for RTM due to need to build up a structure that can resist moulding pressures. Tooling for vacuum bag methods of manufacture is of much lower cost since only a single mould face is used. A high structural stiffness (for the tooling) is not required, as ev n in the autoclave, the mould is subjected to hydrostatic, rather than differential pressure. Recently a more versatile process of resin infusion into a dry fibrous preform, called resin infusion process (RFI), has been developed to overcome the problems encountered in RTM, such as low fibre content, utilisation of expensive matched moulds, long distances for resin flow to fill out the fibrous preform, and void formation.[77,78] The RFI process was originally developed for autoclave processing using a vacuum bag/tooling combination for the manufacture of shaping pans. RFI is easily adaptable to unidirectional or woven fabric preforms forming either monolithic or honeycomb (sandwich) type structures, having either flat or curved shapes with various

types of matrices[79]. This process has the advantage of reducing the cost of manufacturing 3-D structural composites by eliminating the expensive moulds needed in RTM. In addition, three dimensional structural composites can be manufactured using a RFI process with a reduced void content.

3.3. Environmental concerns

Furthermore, with vacuum bag and wet hand lay-up methods, the operator is exposed to uncured liquid resin systems and to any volatile components they may emit into the workplace atmosphere. This is particularly a serious problem for resins cured by additional cross-linking, notably when using unsaturated polyester or vinyl ester resins which emit styrene vapour. Styrene vapour has been reported to cause detrimental effects in workers such as depression and fatigue with a slowing of reaction times[80] and in severe cases detrimental psychiatric symptoms[81]. These obviously pose a safety threat. Installing extraction fans is costly and time-consuming, For low volume production a shift to alternative resins, e.g. ambient cure epoxy or low styrene content polyester, may be a cost-effective short-term solution. In the long term the process must be re-designed to take advantage of cheaper resin systems and reduce health and safety risks.[82]

3.4. Historical development of RFI

Despite the recent interest in the vacuum resin infusion process, it was being considered as a clean alternative to hand lay-up as long ago as 1950. The Marco method[83] was designed in the USA for the manufacture of boat hulls with reduced void content and tooling costs compared to RTM manufacture. It was not widely adopted because resin and reinforcement development favoured open mould lay-up or spray deposition (for boat manufacture) in what was until recently an under-regulated industry. The Marco tooling design can be seen in Figure 2. Dry reinforcement was laid up onto the solid male tool and a semi-flexible/splash female tool was used for consolidation and to provide a seal for the application of vacuum.

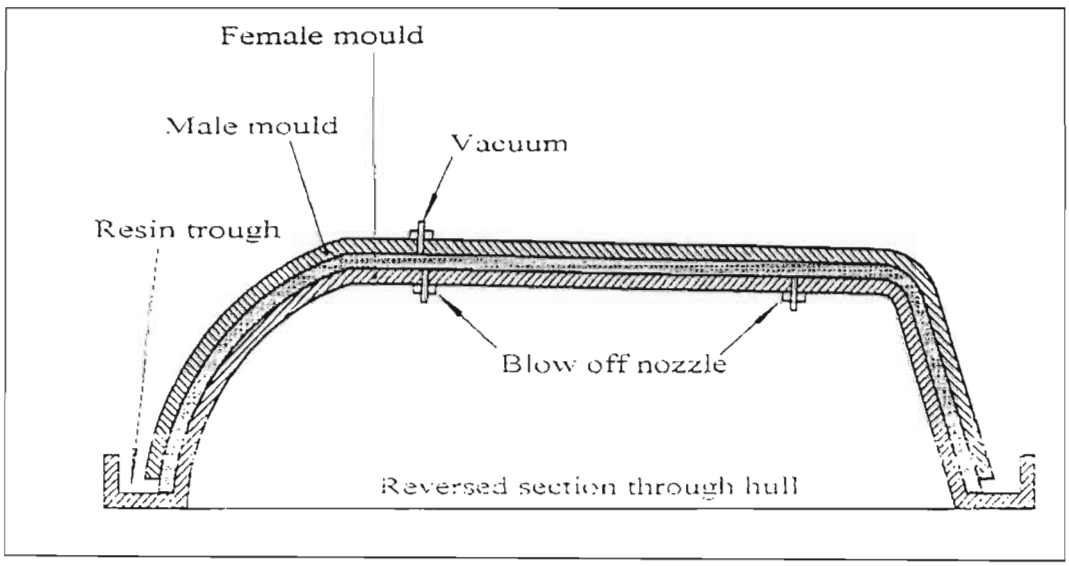

Figure 2 The Marco method of resin infusion tooling. (cir.1950)

In 1972, Group Lotus Car Ltd patented a vacuum moulding method for the production of RFI components.[64] The process consists of a closed GRP mould into which dry fibre material is placed. Before tool closure a measured amount of resin is poured onto the fibre. On closing of the tool halves the tool cavity is evacuated , drawing the tool faces together, diffusing the resin into the fibre stack.

In 1978, Gotch detailed the use of vacuum impregnation using one solid tool face and a silicone rubber diaphragm bag.[1] Liquid resin is poured onto pre-placed dry fibre before

being enclosed by the bag. Moulding quality was higher than that achieved using hand lay-up. Gotch also reported that the method removes the operator dependence of quality when compared to hand lay-up. Vacuum pressure only was used to draw resin into the tool. The elastomeric bag design was changed to solid tooling for complex shapes due to problems with the variability of fibre content and flow control. These problems were attributed to the high viscosity resins used at the time rather than to the method of manufacture itself. In 1980,[2] and later in 1985 [3] again Gotch highlighted the need for manufacturing technique which can handle the legislated lower levels for styrene vapour emissions that were being imposed in most countries of European community. He again considered the silicone vacuum bagging method detailed earlier,[1 below] but now with resin drawn into a sealed vacuum bagged tool using vacuum pressure. Gotch suggests the ideal resin viscosity for a vacuum injection system to be 100- 200 MPa.s. Commercially developed resin systems with such viscosities have been developed, stimulating further process development. The flexural strength of laminates of identical constituents manufactured by hand lay-up, cold press moulding and the vacuum bag infusion process were compared.[2] Gotch noted that values obtained from the hand lay-up process were scattered and very operator dependent whereas the values for press moulding and vacuum infusion were more consistent.[2] He found that the production rates for railway coach panels of medium complexity were typically three times greater for the vacuum infusion method than those for hand lay-up.[3 below]

In 1982, Allen et al.[4] considered the use of vacuum infusion to manufacture high fibre content composites. Closed aluminium tooling was used with consolidation via a platen press. Fibre volume fractions achieved ranged from 43% to 60% using 0°/90° plain woven E-glass reinforcement and vinyl-ester resins. Although the work did not consider flexible tooling it demonstrated that infusion of high fibre volume fraction components can be achieved at resin pressures as low as 1 bar.

In the same year Le Comte patented his "Method and apparatus for producing a thin-walled article of synthetic resin, in particular a large-sized article".[5] The patent describes a process similar to Marco method, i.e. reinforcement fabric compressed under vacuum between a solid and flexible tool face. The method can be used for the production of glass reinforced plastic boat hulls with cores and stiffeners in place (Figure 3). Tooling materials are glass reinforced plastics.[6] The resin is raised 4-5 m

above the injection point to provide some positive pressure. Le Comte has produced 50 m surface ship hulls using this method. Infusion takes approximately 10 hours before resin gel, which occurs at workshop temperatures of 18° to 20° C.

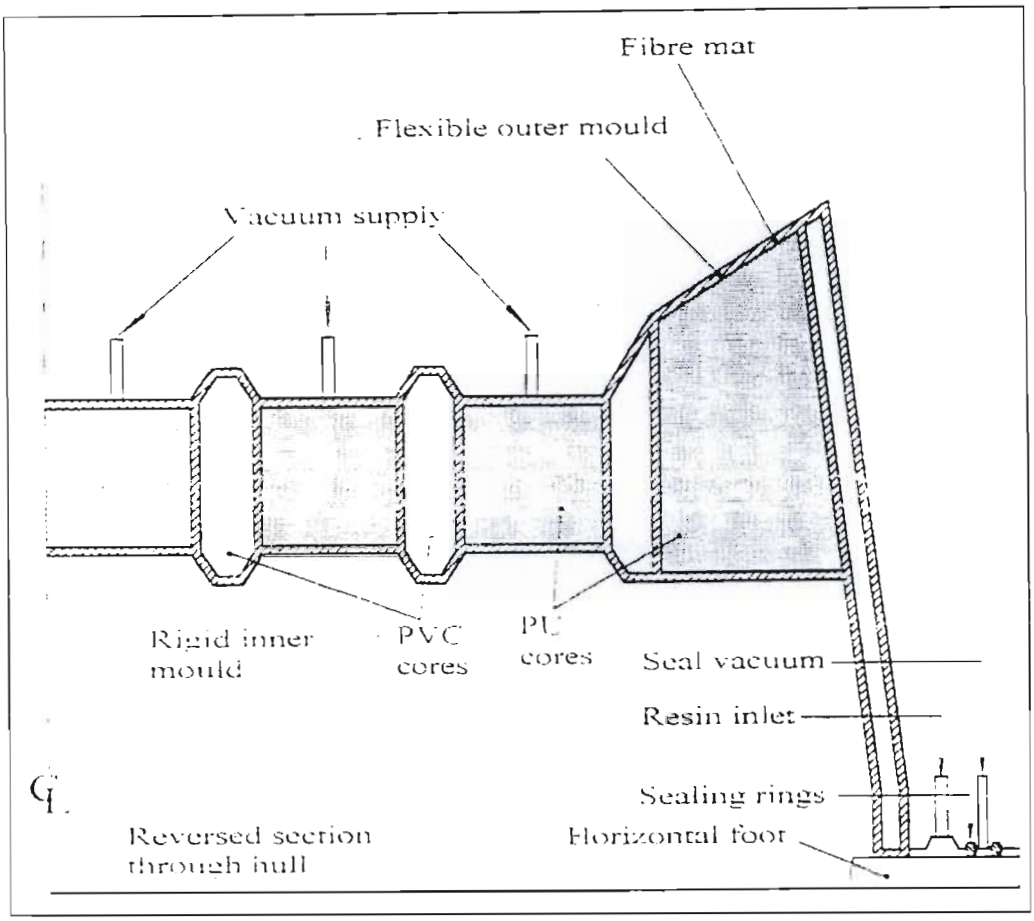

Figure 3 Section through tooling used by Le Comte.

In 1985 Tengler reported on a vacuum injection process to produce high strength carbon fibre reinforced composites.[7] He used closed aluminium tooling with the vacuum being drawn inside the cavity to facilitate consolidation and to draw resin into the tool. Double edge seals were also used to reduce air leaks. Components of 35% fibre volume fraction could be successfully manufactured but problems with the high viscosity of the epoxy resin and short gel times were encountered for mouldings of higher fibre content. This led to incompletely filled mouldings.

Adams and Roberts used the solid nickel coated metal tooling vacuum assisted resin injection method to produce solid and cored laminates.[8,9] This process was developed from their work in 1970s.[64] Once the tool cavity had been evacuated consolidation was

due only to atmospheric pressure. No mould clamping was used. This method was used to manufacture structural components such as car side-impact panels for Lotus. Cost savings were suggested when compared to RTM owing to the reduced moulding forces. They also stated that vacuum infusion saved production time when compared to pre-preg manufacture as heavy debulking operations were not required, the process being a one-shot manufacture method.

Ciba-Geigy published details of their vacuum infusion process for the manufacture of glider ailerons.[10] Tooling consisted of a solid composite female and a nylon bag male. Resin is drawn into the tool on evacuation of the tool cavity. The process, as shown in Figure 4, was developed as a manufacturing method to replace conventional hand lay-up of large parts, reducing health and safety risks and increasing production efficiency with repeatable quality. Vacuum infusion was chosen using female composite tooling with internal oil heating/cooling and silicone or PVC bagging material. Sealing of the bag was via a circumferential seal compressed by an aluminium box section and toggle clamps. Resin entered the tool via a peripheral resin channel and impregnated circumferentially toward the central vacuum ports. The use of Injectex fabrics and low viscosity epoxy resins helped resin flow.[12] It was possible to produce good quality components using this process. No mechanical properties of the components manufactured by this method have been published.

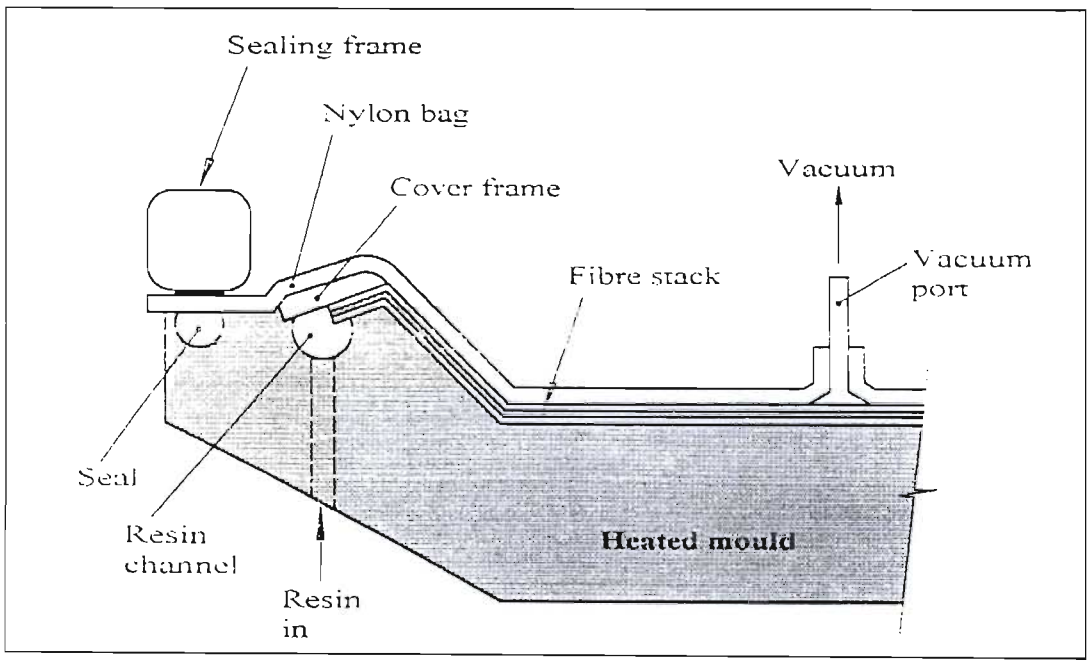

Figure 4 A schematic of the Ciba-Geigy resin infusion method.

In 1986 Letterman patented his "Resin film infusion process and apparatus".[13] Expanding on the RTM process, resin infusion can be performed in a press, vacuum oven or autoclave depending on the flow and curing characteristics of the resin to be used. As it is originally developed for autoclave processing using a vacuum bag/tooling combination in shaping a part, it is easily adaptable to unidirectional or woven fabric preforms forming either monolithic or honeycomb type structures. Schematically illustrated in Figure 5, the lay-up arrangement for an autoclave resin film infusion process is quite similar to a conventional autoclave process using pre-pregs. However, unlike the case with pre-pregs, each ply is made up of dry fibres while the resin matrix is placed at the top or the bottom of the ply stack. Bleeder plies are placed around the lay-up and are surrounded by sealant tape. The whole system including the dry preform, the resin matrix, and the bleeder plies is completely enclosed in a vacuum bag and connected through a thin breather to the vacuum line.

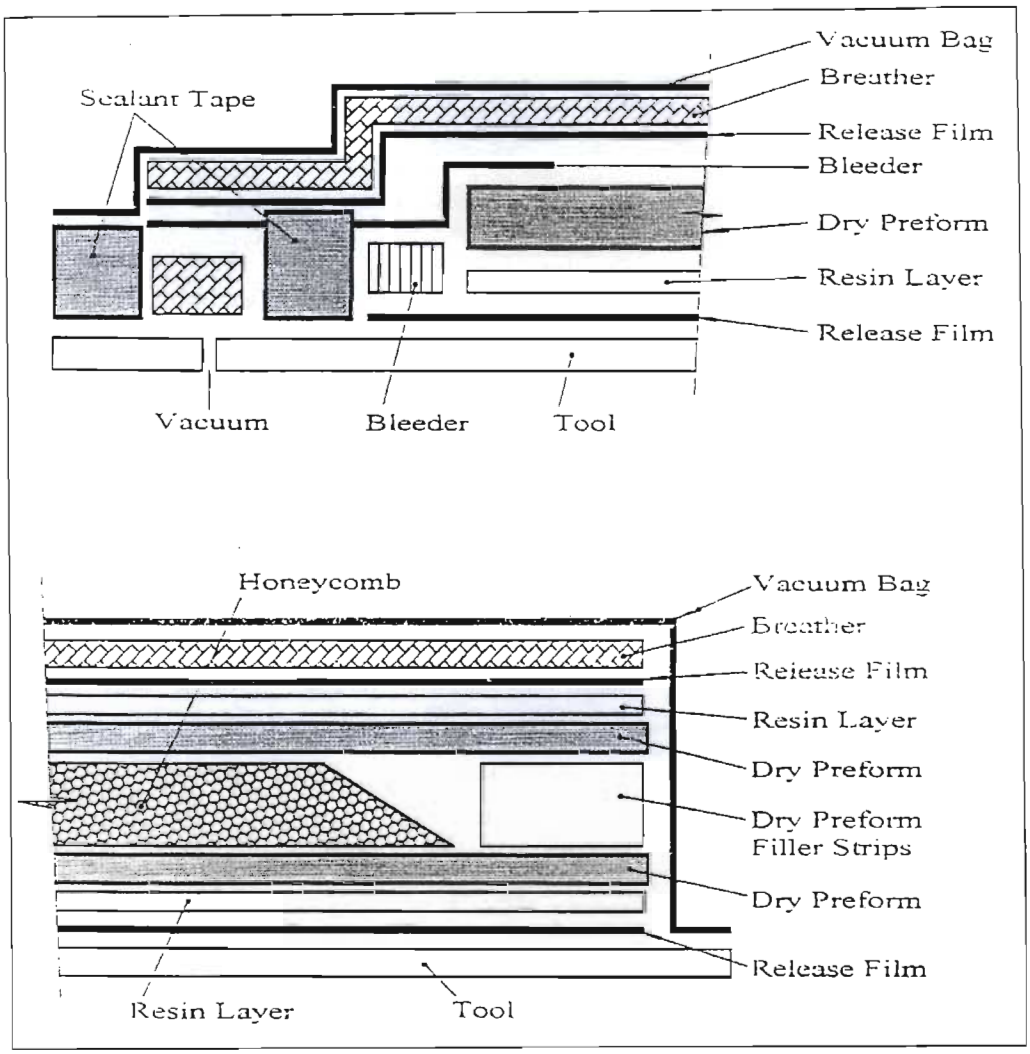

Figure 5 A lay-up of the autoclave resin infusion process for woven fabric preforms (above) and honeycomb structures (below).

3.5. Materials Systems

3.5.1. Vacuum Bag Materials.

The selection of a suitable vacuum bag material is key for any vacuum forming process, including RFI Bag, where integrity is a key factor in the process. Thin nylon bags can be prone to perforation giving rise to voids in the part, as a steady stream of air is drawn in by the vacuum. At the company DSM located in Europe, Brittles has developed a highly flexible styrene impermeable film and a low viscosity resin (Synolite 6637-W- I) with a low peak exotherm of 75° C in a laminate thickness of 4 mm.[14] Exotherm is of course component geometry dependent on the vacuum injection process. DSM has also introduced a method using a double vacuum bag. Low vacuum (0.1 bar) is initially applied to the inner bag to lightly compress the reinforcement. At this stage the fabric is manually pressed into the comers of the mould. Vacuum is then raised to 0.5 bar after which the outer bag is put in place. An even distribution of vacuum has to be achieved between the films: a breather layer (synthetic tissue is used so the resin front penetration can be seen) is laid between each film. Vacuum between the films is increased to 0.96 bar (gauge pressure). The increase in vacuum pressure between the films removes the danger of air ingress into the tool through the bag. During laminate filling the inner vacuum is maintained in order to consolidate the laminate until the resin has cured. This method was suggested by Höhfeld.[15]

Marcus described new developments in vacuum bag forming.[16] He listed the benefits of silicone bag materials as its tear resistance, re-usability and large percentage elongation (i.e. good conformity). Shepherd patented an embossed vacuum bag design, which eliminates the need for a breather layer to ensure even vacuum over the component surface.[17] Removal of the breather reduces the consumables and allows the observation of resin flow through the vacuum bag. Kohama et al. have investigated the behaviour of various bagging films when forming components with sharp radii.[18] Although the authors were studying vacuum bag forming their findings are of relevance to RFI. They used positive air pressure to force a bag into a female mould containing pre-preg. The tooling used had both convex and concave corners. Four bagging films of varying stiffness; namely, nylon, silicone rubber, polypropylene and low density polyethylene were used to examine the effect of the properties of bag material on component

thickness variation. Nylon and silicone rubber have low Young's modulus and elongation for vacuum forming. However, the properties of nylon film are extremely sensitive to moisture, while silicone rubber was found to have poor solvent resistance and high cost. Other bagging materials have higher Young's modulus than nylon and silicone. Consequently, they required higher vacuum or pressure to form complex shapes and produced components with irregular thickness. Polypropylene and low density polyethylene were both found to have heat resistance below that required for the exothermic reaction peaks of the epoxy resin used.

In 1989 Boey described a vacuum bag technique for autoclave pre-preg material using formable and reusable silicone bagging materials.[19] Although not a process involving long-range resin flow, novel techniques for bag sealing, clamping and breaching without losing vacuum are suggested (more information can be seen on Figure 6). Such techniques and ancillaries may benefit the development and applicability of the RFI.

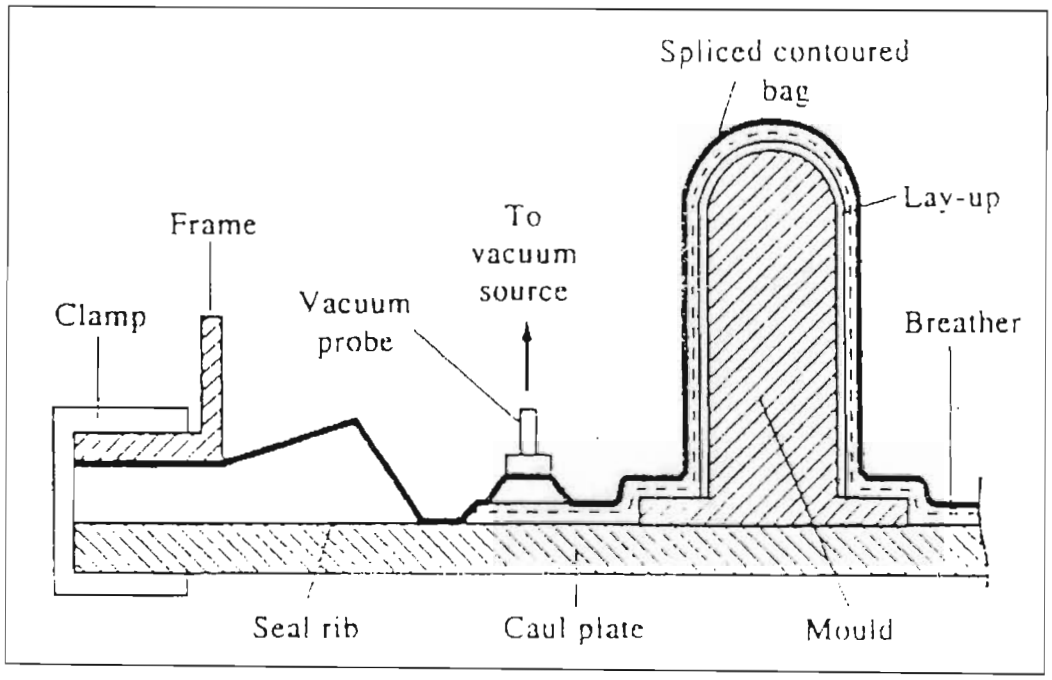

Figure 6 The novel bag sealing and clamping techniques used by Boey.

In 1990 Ahn et al. studied the bag material for the resin film infusion process.[20] They reported that the bag material varies depending on the resin processing temperature. When vacuum is drawn on the system at the beginning of the process, air and other gases are removed via the natural conduit created by the interstices between dry fibre

plies and the bleeder layers. Thus the dry fibre preform to be impregnated is under negative pressure before any resin impregnation. Various types of matrix including film, pellet and viscous liquid can be easily adopted to a specific dry fibre preform. When the resin infusion process takes place in autoclave, the mould can be easily formed by the sealant tape.

3.6. Mathematical Modelling

In 1989 and 1990 Hayward and Harris studied the effect of injection using vacuum in addition to applied injection pressure for RTM and found marked improvements in the appearance of laminate (i.e. surface finish and wetting out)) as well as flexural and short beam shear strengths.[21,22] Quality improved for all laminates regardless of the resin fibre combination used and even for modest levels of applied vacuum. The benefits of vacuum were reflected primarily in the reduction of voids. The authors also recommended turning off the vacuum when the mould is filled to prevent excess styrene being boiled off This may result in cured-in voids. In practice this may be hard to achieve because small vacuum bag or seal leaks will inevitably reduce consolidation pressure if the applied vacuum is removed.

Lundström et al. and Lundström suggest that the "boiling off" of styrene under vacuum is unlikely.[23,24] At vacuum pressure levels typical of the process, the boiling point of styrene is not reached. This is confirmed by Figure 7, which shows that the boiling pressure of pure styrene is about 0.01 MPa (90% vacuum) at 40° C. The boiling temperature increases as the vacuum level decreases to a point where the temperature required to boil styrene at 10% vacuum is in excess of 100° C. At this temperature rapid cure of the polyester resin will take place causing an increase in viscosity and a further resistance to the formation of bubbles. Lundström suggests that poor laminate quality for polyester/vinyl ester systems, normally attributed to styrene vapour, is more likely due to air as a result of mould leakage.[23,24] He suggests that double seals should be used in mould design with a greater vacuum applied between the seals than in the component area.

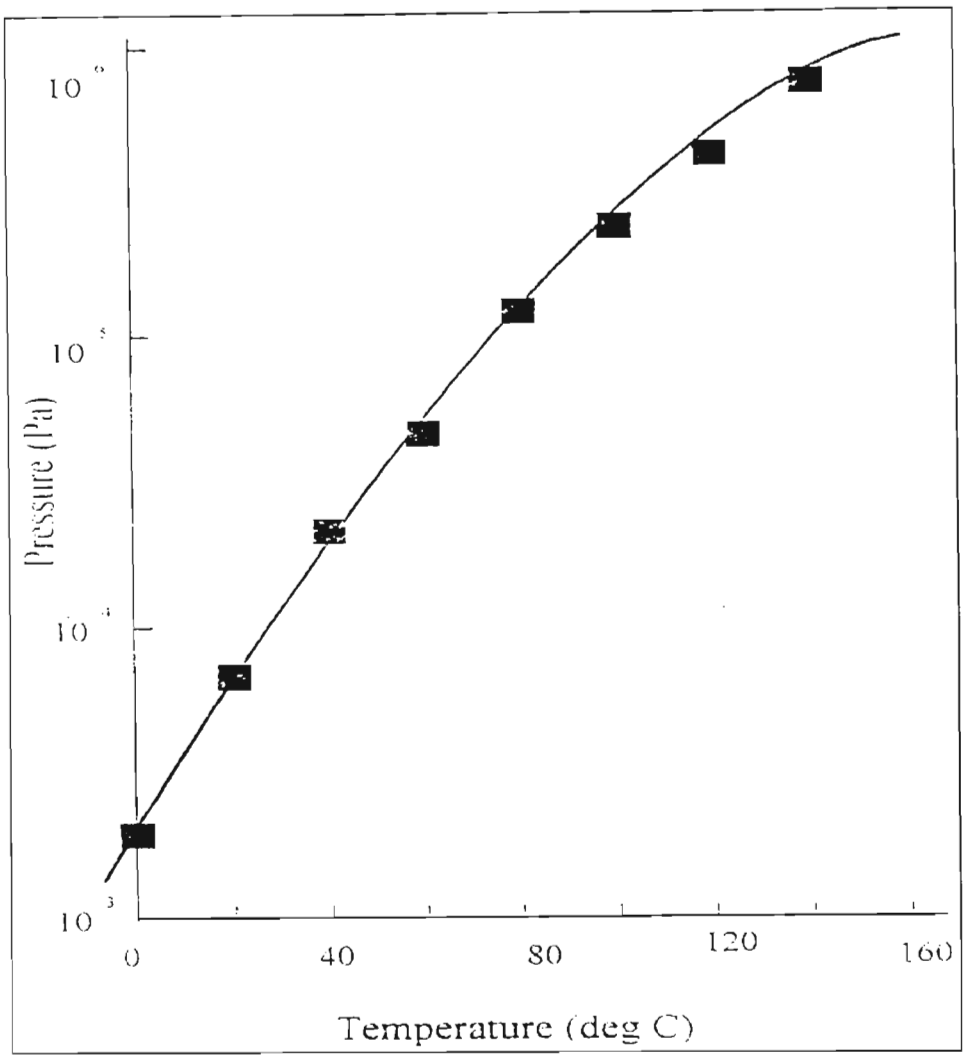

Figure 7 Pressure vs. temperature for styrene. The Transition point between liquid and vapour phases is clearly shown.

Boey in 1990 [25] and Boey and Liu in 1991 [26] used vacuum bag infusion techniques to investigate how the process can reduce laminate void content. Boey describes a vacuum infusion method utilising one solid and one bagging film tool face in which resin is drawn into the tool by evacuating the tool cavity.[25] He reports that consistently low void contents (about 1.3%) and correspondingly high and consistent flexural strengths were achieved. Void formation was also reduced when two as opposed to one vacuum port was used on a 600 mm by 300 mm flat plate moulding. In the later paper, the process was taken further by manufacturing a model smoke tunnel (Figure 8).[26] A big advantage of the vacuum process over the traditional hand lay-up method, was that the dry reinforcement could be carefully positioned before resin entered the tooling, allowing accurate placement of fibre layers. For high production runs the vacuum bag could be replaced by a flexible splash tool or re-usable bag.

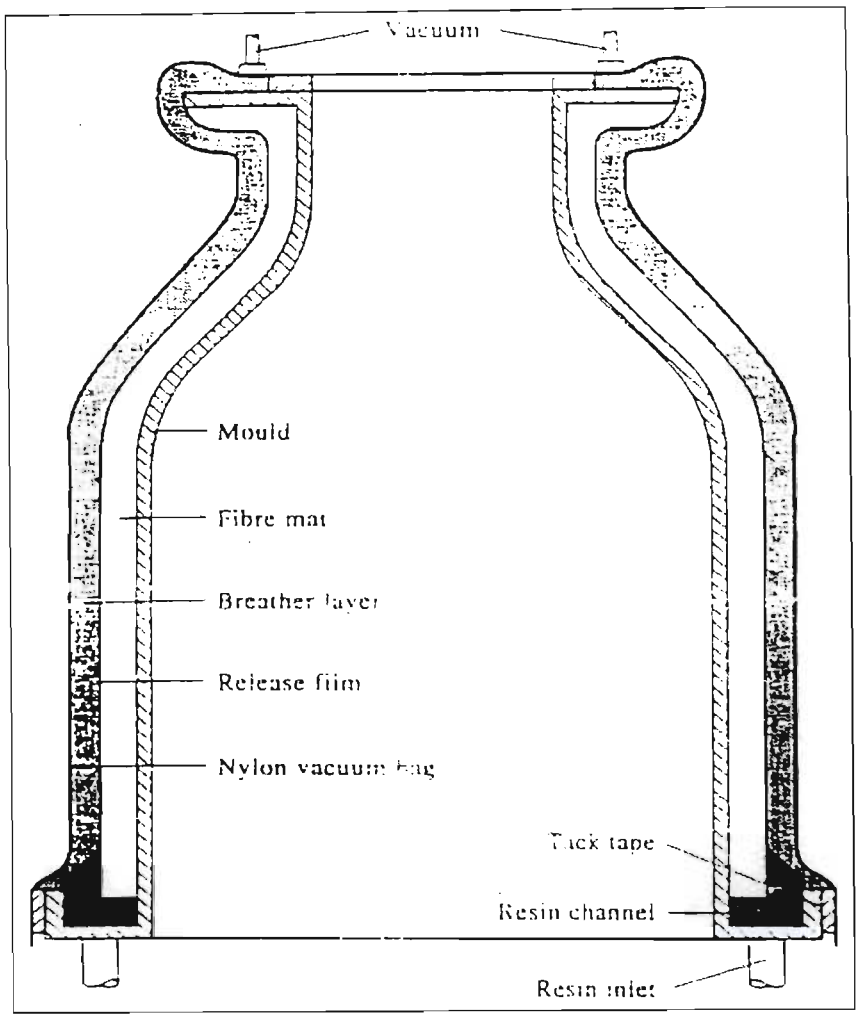

Figure 8 Schematic of resin infusion tooling used to manufacture model smoke tunnels.

Ahn et al.[20] described the typical cure cycle for the RFI process using an epoxy matrix. The resin infusion process is similar to the pre-pregging process in that the resin flows over the surface of dry fibres. On the other hand, resin infusion may be also viewed similar to the cure and consolidation processes since the viscosity of the resin changes with time and temperature due to the cure process. Therefore the resin flow as well as the reaction may need to be considered simultaneously in analysing the resin infusion process. In RFI processes using an autoclave the temperature cycle consists of heating, holding, and cooling steps simulating a typical composite processing cycle (Figure 9). Viscosity is strongly influenced by the heating rate which in turn influences the resin flow. In addition, capillary phenomena from the aligned reinforced fibres to be impregnated may also influence the matrix resin flow. Especially for the high pressures imposed by an autoclave, capillary pressures may dominate the whole resin infusion process.

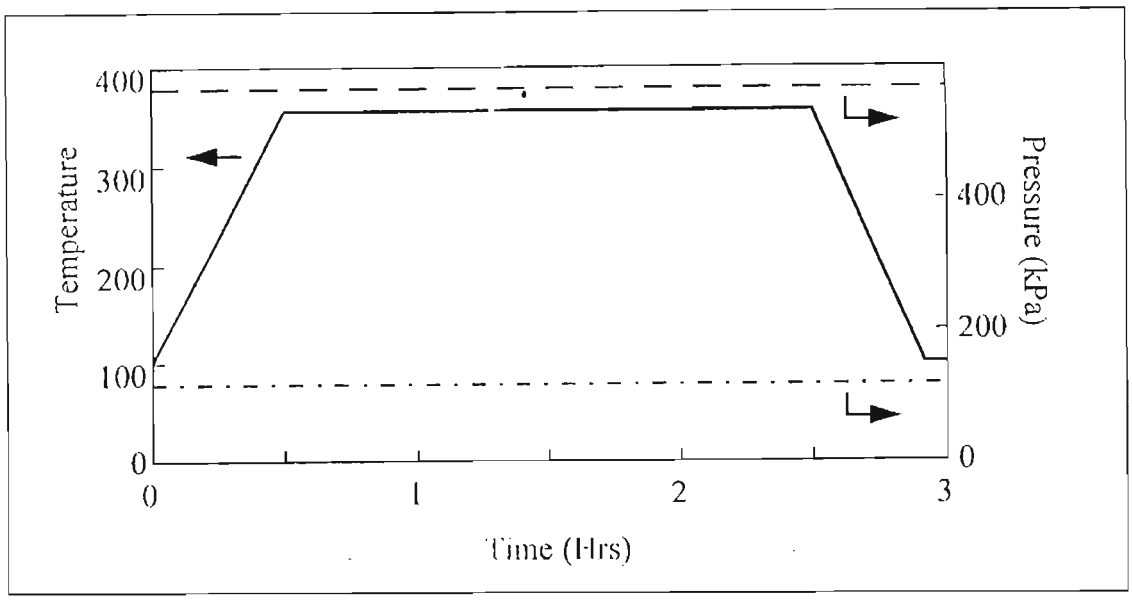

Figure 9 Typical autoclave temperature and pressure cycle for resin infusion using an epoxy resin system.

In 1991, Seemann made UK and European patent applications for a variation of the US patented Seemann Composites Resin Infusion Moulding Process (SCRIMP).[27,28,29] The process is simple and resembles other vacuum infusion techniques in that the laminate is contained under a nylon bag. Resin is drawn in under vacuum. The novel aspect of SCRIMP is the use of a mesh to distribute the resin within the tool, eliminating the need for a breather cloth. The difference between the US patent and the European applications is that the distribution medium is placed on one side of the moulding in the former and on both in the latter. The differentiating features can be seen in Figure 10. This process has been used to manufacture 15 m boat hulls, with foam cores, in a single shot. Seemann has claimed weight fractions of 26% resin for test samples manufactured using the SCRIMP process. The test material consisted of vinyl ester resin reinforced with five layers of approximately 800 g/m^2 plain weave glass fabric. The achievable fibre content figures were confirmed by Barer,[30] who currently uses the technology in the production of marine craft. The application of the technology in the manufacture of boat hulls uses a staggered resin entry system enabling large parts to be produced by sequential changes to the porting arrangement.

Lazarus highlighted the need for improved resin systems.[31] Increased gel times and reduced viscosity are required to enable larger, thicker components to be manufactured

more easily at ambient temperature. The ideal viscosity for an injection resin is suggested to be 200 - 300 MPa.s.

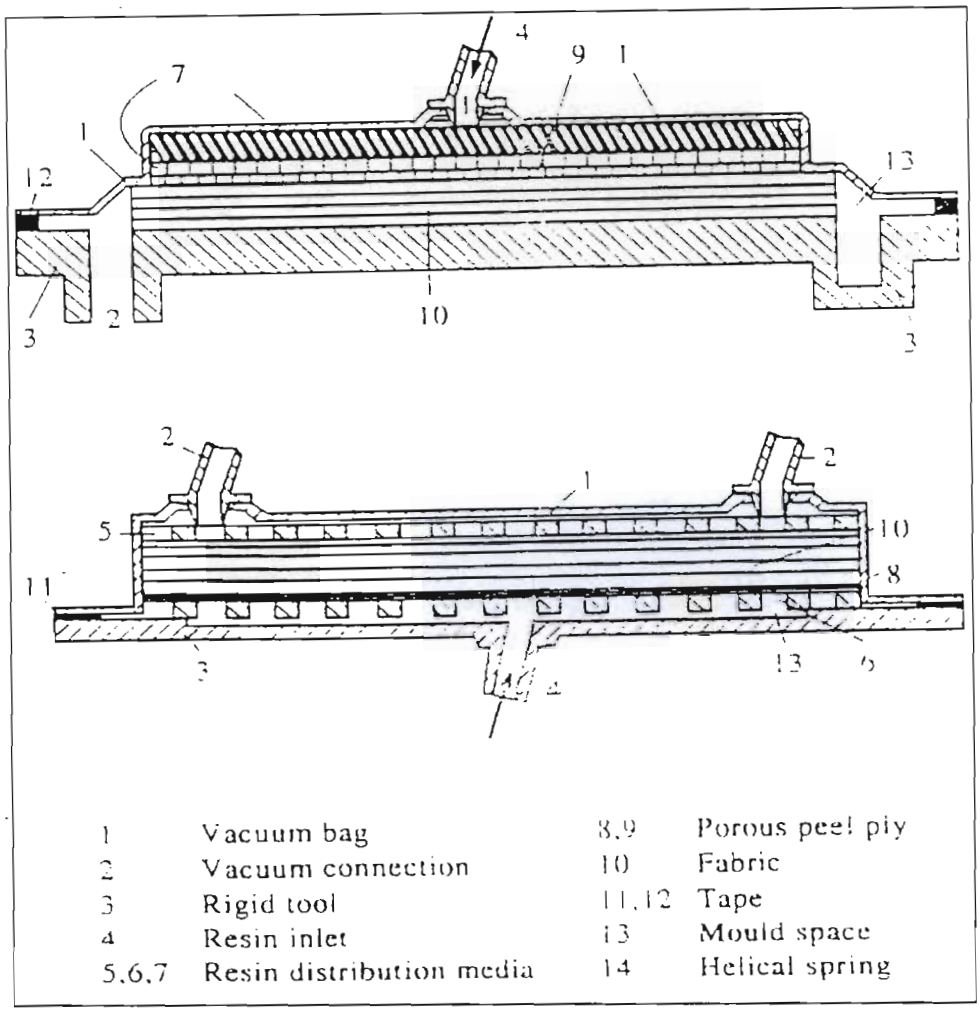

Figure 10 Schematic of the SCRIMP process, showing the US patent (above) and European patent application (below).

In 1993, Barnes and co-workers developed a hybrid SCRIMP-like system for the repair and reinforcement of steel structures including offshore oil platforms and surface vessels.[32,33,34] The method involved infusing high volume fraction carbon fibre patches directly on to the pre-preg structure with epoxy resin. Flow length could exceed 1500 mm. The steel substrate effectively acts as the solid tool surface. A good adhesive bond is required at the interface.

3.7. Damage

In 1994 and 1995 Shim et al. investigated damage formation in stitched structural composites manufactured with RFI process.[35,36] They demonstrated that the inherent anisotropy and heterogeneity of stitched composites created by the stitching process resulted in resin-rich areas which induced voids, cracks, and micro-cracks irrespective of the toughness of the resin matrix or flexibility of stitching fibre. The preforms examined were both carbon fibre unidirectional and woven fabrics. Non-stitched and stitched quasi-isotropic fibrous preforms with Kevlar or T-900 carbon stitching as the fibres were examined. Three significantly different resin systems were used with the purpose to create differing laminates. In addition, an integrated investigation of thermal, rheological and mechanical characterisation was conducted to better understand the matrix dominant properties in non-stitched and stitched composites. Authors found cracking in the stitching region in all stitched laminates during processing. This was found to be related to the heterogeneity of the fibrous preform structure, thermal expansion and contraction of the carbon stitching reinforcement, and thermal shrinkage of the matrix resin during the autoclave process. Kevlar stitching was found to cause more severe cracking than carbon stitched composites and should be avoided or modified. For non-stitched composites, most of the surface cracks found during thermal cycling were negligible and limited to surface layers. Surface cracks of T-900 stitched composites were found to be more pronounced than non-stitched composites suggesting that the stitching fibre played an important role in initiating surface cracks. After initiation surface cracks further propagated during thermal cycling. Micro-cracking in stitched composites was found to be caused and affected by the heterogeneity, anisotropy, and elasticity of the fibre bed as well as viscosity of the resin. Specifically, the authors noted that micro-cracking exhibited in RSS-1623 stitched composites resulted from the inherently slow cure process of the RSS-1623, which results in only a partially cross-linked material after a two-hour isothermal autoclave process; non-uniform thickness caused by the stitching fibre which is an inherent textile property of the stitched fibrous preform; use of a metal plate during autoclave cure creating stress concentration in the centre of the fibrous preform between the stitching fibre; and lower glass transition temperature than cure process temperature which caused the matrix to

be in a rubbery state, building a large residual stress without any resistance against high pressure supplied by the autoclave.

In 1995, Lazarus described the history of resin infusion in the boat building industry.[37] He confirms Seemann's claims that large boat hulls (13-18 m) can be infused in one hour.[27] They also comment that it takes two men ten days to prepare the lay-up. The lengthy preparation time is taken up by the need to ensure accurate placement of all reinforcement layers before injecting the resin. The core used in SCRIMP is usually a foam which has to be scored with a grid pattern to provide channels so that the resin can spread over the laminate area and infuse the fabric. The fabric layers are tacked together using aerosol contact adhesive so that they stay in position before they are stabilised by the vacuum bag.

3.8. Preform permeability and process modelling

With the advent of advanced textile preforms, it has become imperative to understand and characterise the influence of preform permeability on the infiltration behaviour. During the infiltration phase of the RFI process, there exists two regions. Within the textile preform: a saturated region and a dry region. For a dry fibre bed, the saturation in the region infiltrated by the resin depends on infiltration capillary number, which is the ratio of viscous forces to surface tension force. Thus it is necessary to evaluate the permeability of both regions within the preform to fully comprehend resin infiltration during resin infusion.

In 1996, Ranganathan et al. proposed a generalised model for the transverse fluid permeability in unidirectional fibrous media.[38] They developed a predictive semi-analytical solution for flow across arrays of aligned cylinders with elliptical cross-sections modelling the fibre mats. The shape of the tow, its porosity, and the packing configuration were found to influence the transverse permeability of such an array significantly. Predicted results of the permeability from that model were compared with numerical results obtained from finite element calculations and gave a good agreement.

In 1997, Hammond and Loos investigated the effects of fluid type and viscosity on the permeability of both saturated and dry preforms.[39] Fluids used were water, corn oil, and an epoxy resin; Epon-815. Preforms tested included style 162 E-glass, a plain weave E-glass fabric, and IM7/8HS, an eight-harness satin carbon fabric. Two methods were used to measure the permeability of the textile preforms. The first, known as the steady-state method, measures the permeability of a saturated preform under constant flow rate conditions. The second, referred to as the advancing front method, measures the permeability of a dry preform to an advancing fluid. Results from the two methods showed that fluid viscosity had now significant influence on the two fabrics. Steady-state and advancing front permeabilities for the warp direction of the two fabrics were similar. In addition, advancing front permeability values were found to be similar for different fluids over a wide range of values of the capillary number. Contact angle measurements indicated that Epon-815 wets both fibres better than the corn oil. In

addition Hammond and Loos showed that E-glass has lower contact angles with both fluids.

In the same year Lai et al. determined the permeabilities of saturated and unsaturated fabrics composed of carbon and glass fibres by using 1 - dimensional and 2 - dimensional (radial flow) experiments.[40] The carbon fabric is a typical one used in fabrication of aerospace grade polymer matrix composites and the glass fabric is a 3 - dimensional woven fabric that was proposed as a standard reference material for permeability characterisation. The authors obtained a good comparison between the measured permeability using constant flow rate or constant inlet pressure, and 1 - dimensional flow experiments with both saturated and unsaturated preforms. It was shown that consistent permeability values can be determined with high accuracy for preforms of various architectural complexity.

3.9. Key Areas for further development.

Development of the RFI process has been component specific. Most examples manufactured using the process have been of low fibre content and so the limits of the technology have not been identified. For the technology to progress, parameters such as maximum achievable fibre content, flow rates (linked to fabric permeability and resin viscosity) must be understood and their relationship with vacuum levels, reinforcement/resin combinations and laminate quality need to be defined.

3.9.1. Fibre content.

Two modes of fabric compression exist with RFI which ultimately determine the fibre volume fraction. These are:

i. The initial compression of the dry reinforcement;
ii. A further compaction which becomes possible once the reinforcement has become lubricated by the flowing resin.

Much work has been carried out in both areas of fabric compression but most consider only the compression either between metal platens (RTM or pultrusion [41,42]) or vacuum bagging and pre-preg processes.[20,43] No data for the dry or wet compression of a fibre tack between a smooth rigid tool face and a vacuum bag has been identified. This is an area of research which has not been considered in this thesis.

Fabric relaxation, characterised by Kim et al.[44] and Pearce and Summerscales [45 below] might be a method by which higher fibre volume fractions could be achieved for lower consolidation pressures.[82 below] In RTM with completely rigid moulds the fibre content is defined by the tool cavity. In most commercial tooling, fibre lubrication effects may be observed as a relaxation of the reaction force on the mould. In RFI a further compaction may again occur upon lubrication such that a "wet" fibre volume fraction may exist which is higher than the "dry" value.

3.9.2. Porosity / permeability.

Much work has been conducted in this area with respect to the RTM process and the behaviour of fluids in permeable media is well documented. The resin flow rate through a reinforcement fabric is proportional to the pressure gradient and inversely proportional to the resin viscosity (Darcy's equation). The constant of proportionality is known as the permeability. Permeability is a complex function of the reinforcement architecture (Carman-Kozeny equation) and the wetted surface presented to the fluid (Blake's hydraulic radius). Permeability typically decreases with increasing fibre content (reduced porosity) and increases with an increasing clustering of the fibres.

The permeability of a particular lay-up and the resin distribution method will partly determine process times and void content. Preliminary studies of the process-property-microstructure relationship have been reported by Griffin and co-workers.[46 below47 below] If higher fibre volume fractions are to be achieved, the mechanism for resin infiltration into the fibre stack must be understood and optimised to reduce dry areas and voids. The permeability of the reinforcement is vital for the development of the mathematical simulation, and a number of tests will be performed to calculate the permeability of the woven materials used in the RFI process.

3.9.3. Void formation and component quality.

It has been shown that the use of vacuum has led to a reduction in the void content with a resultant improvement in laminate shear strength.[48 below] The void development and composite quality in RFI processed laminates will be dependent on the resin distribution method and can be determined by quantitative microscopy [49] and mechanical testing.[50] Furthermore various mechanisms of void formation will be studied and modelled analytically. These results will be included into the optimisation stages of the mathematical model to minimise voids in the final product. In particular the homogeneous nucleation of bubbles, i.e. voids by cavitation will be studied.

4. Material systems

4.1. Introduction

The material system was to be selected and developed within a number of boundaries. The two primary constraints were:

(a) A maximum temperature of 150°C.

This demand has been placed in keeping with the requirement that the process be simple and cheap i.e. not make use of expensive, heavy duty equipment. The search for an appropriate dry resin film should then tend towards thermosetting based polymer based materials rather than thermoplastics. While thermoplastic resin systems do exist with low melting points, they are not suitable for many structural applications, as the safe operating temperature is too low.

(b) Exclusion of Autoclave for the process.

The resin infusion process is to be conducted under vacuum only, with no external pressure, as is the case with autoclave processing. This constraint also is in keeping with the need to devise a system that is uncomplicated and cheap.

In addition there are a number of secondary constraints which affected the search and selection of the material system. These are requirements to produce a product that has improved quality, and ease of manufacture is also vital. Furthermore, the process should be suitable for making intricate parts in a one-stage process without the need for secondary bonding processes. The financial impact of the process is important in order for both the process and the end product to be cost effective.

4.2. The resin film

The ideal film would be one that is a thermosetting material, which exists as a dry film at room temperature with no cross-linked polymer chains. Upon heating, this film should melt, seep through the fibre material, thereby wetting it, and at some elevated specified temperature, cure by means of cross-linking.

The ideal temperature range for curing of the resin film should lie between 100°C and 150°C with a low melting point to ensure complete wetting out before the cure begins. Furthermore, compacting and wetting should occur purely under a vacuum, which means that no external pressure should be necessary to ensure total saturation of the preform.

4.3. Reinforcement

For resin film infusion to be a useful process, it should be compatible with all the standard fibre reinforcement materials currently used in polymer reinforced composites. For testing purposes, a choice between carbon fibre, glass fibre and Kevlar had to be made as the standard. Based on cost and availability and the number of experiments to be conducted, woven glass fibre fabric, which is relatively cheap, was selected. Furthermore, once the resin film infusion technique is optimised using woven glass cloth, other fibre materials can be used including the more expensive carbon fibre and Kevlar, The physical wetting out process should not vary significantly between the materials, although the bonding between the resin and fibres may vary. An RTM specific glass mat, with "channels" to allow resin flow, Injectex, was suggested and used in the preliminary studies. The results were unsatisfactory, and after consultation with Mr H le Grange at Kentron, it was agreed that the resin channels in the Injectex encouraged flow parallel to the surface of the mat, rather than through the preform, and this material was rejected as unsuitable for RFI. A plain weave glass mat, GFHL 1113/390/125 glass was then chosen as the standard reinforcement material for all testing.

4.4. Vacuum bag selection

The polythene vacuum bag used for room temperature vacuum bag composites moulding was found to melt at the elevated temperatures around 120'C. This bagging material was successful in the early experiments of the material selection process as vacuum bagging was conducted outside the oven, i.e. the tests consisted of heating the lay-up in an oven and then removing and vacuum bagging. A heat resistant vacuum bag (Capran 524) was then selected which allows vacuum bagging to be conducted within the oven at elevated temperatures. The regular black "tacky tape" sealant tape also proved unsuitable and HT200/16 sealant tape was purchased.

4.5. Miscellaneous

A number of problems were encountered during the experimentation phase of this research. In particular, the film adhesives tended to bond to the mould surfaces. Various release agents were tested including, Ram wax, and silicone spray lubricant. After consultation with Mr. H le Grange from Kentron and A.M.T. a Frekote product, 55NC was procured and used. A high temperature Halar perforated release ply (Halar WP3) was purchased and proved capable of handling both the elevated temperatures and the film adhesives. The breather material used was a standard cloth breather ply.

4.6. Discussion

The results of the physical testing on the various resin systems suggest that a material system based on the Redux thermosetting film adhesive range manufactured by Hexcel is suitable for RFI processes. A number of areas of concern should be noted and investigated further.

4.6.1. Control of the heating and cooling

Following discussions with Mr S Farrukh from Hexcel Europe, the following stepping rates have been suggested, for Redux film adhesives:

Stage #1	0°C to 80°C	3°C/min.
Stage #2	80°C to 120°C	1°C/min.

The Redux material is very sensitive to these stepping rates, and an accurate programmable controller will be necessary to ensure good wetting of the sample and low void formation. It was also suggested that these stepping rates have an effect on the surface finish of the final component. This has not been proven experimentally, and surface finish is discussed further below.

4.6.2. Use of breather ply

The breather ply is traditionally used to absorb excessive resin from wet lay-up systems, and to "spread" the vacuum throughout the tooling. As the lay-up is dry and precise amounts of resin can be calculated and placed in the mould, the breather ply is only performing the second task. Various embossed vacuum bag materials are available which would allow the breather ply to be dispensed with. This would have the effect of improving the surface finish on the non-mould surface. Similarly the results suggest that a better surface finish would be achieved by using a non-perforated release film.

4.6.3. Release agent

The elevated temperatures required by the RFI process mean that an effective high temperature release agent will be necessary. Studies have found that these are expensive, and Frekote 55NC has proven to be the most suitable. The Frekote product has proven itself very effective when used with the Redux system on a wide range of surfaces, both metallic and porous ceramics.

4.6.4. Seepage and dwell times

Attempts to produce a relationship between the dwell time (at 80°C) and the saturation of the preform have proven inconclusive. It was hoped that these tests would produce data, which could be incorporated into the mathematical model. This would give a link between the number and thickness of the layers of woven material in the preform and the required dwell time to ensure total wetting out of the product. Later tests which are discussed in section 5.4.2, suggest that the saturation occurs prior to the dwell temperature being reached, and hence the dwell time has a negligible effect.

4.6.5. Handling Considerations

It should be noted that as the Redux is removed from a freezer prior to use, its properties change significantly. The Redux becomes excessively adhesive with rising temperature and its handling also becomes more difficult. To overcome this, the polythene backing sheet (protecting the Redux film) has to be removed at the earliest opportunity, that is when it is a few degrees below room temperature. Handling at too low a temperature causes cracking and leaves the film vulnerable to condensing water vapour. Through experience methods for handling the Redux were developed, for example finding an edge and jerking the polythene free from the Redux, proved to be the easiest method of removing the backing sheet.

5. Physical testing and results

5.1. Introduction

The physical testing consisted of many components, initially the testing focussed on testing various resin films, including thermoplastics and thermosets, as well as refining the RFI technique and tooling. Once the material system had been decided, testing focussed on identifying the key process parameters. This was basically performed at a qualitative level. These parameters were then varied with in a strict range and under identical lay-up and material systems. The samples manufactured during this phase were subjected to a mechanical testing regime, of bend tests, impact and tensile tests to failure. In addition the surface finish was rated. These results identified a basic optimum process for RFI.

5.2. Materials system testing

An initial step towards finding a dry resin film was to experiment and find out whether dry plastic films will melt, seep through and wet a dry fibre lay-up and be compacted under a vacuum as is the case with the wet resin hand lay-up technique.

The initial investigation involved observing the behaviour of thermoplastic film adhesives in the temperature range specified in the introduction. After experiments with thermoplastic films (see below), it was concluded that they are unsuitable. One such experiment conducted (see Experiment 2, Appendix B) used a thermoplastic adhesive film named Xiro V587-1. From our observation we can conclude that this film was not suitable - within its bonding temperature range which is 85^0C -105^0C it did not melt sufficiently to seep through and wet the fibres.

However several other Xiro dry adhesive films were purchased (see Xiro specification sheets in Appendix D) and tested. The following dry adhesive films were tested, Haroco, 65g/m^2 and XAF 2061, 30g/m^2. Firstly, the use of Haroco, 65g/m^2 (see experiment 3a, appendix B) was ruled out as within its bonding temperature range, the film did not become sufficiently liquid to seep through and wet the fibre material. A further experiment (see Experiment 3b, Appendix B) using the same film but at a higher temperature was performed. It seemed as if the film melted sufficiently to seep through and bond the fibre material together. However, only slight wetting of the fibre material was visible because only a single layer of this very thin adhesive film was used. Therefore, the matrix volume was small. Thus several more experiments using Haroco were carried out to try and obtain the desired results. A further experiment using Haroco (55g/ m$^{2)}$ was conducted but yielded similar results as above (see Appendix B) and hence Haroco was eliminated as a potential dry resin film.

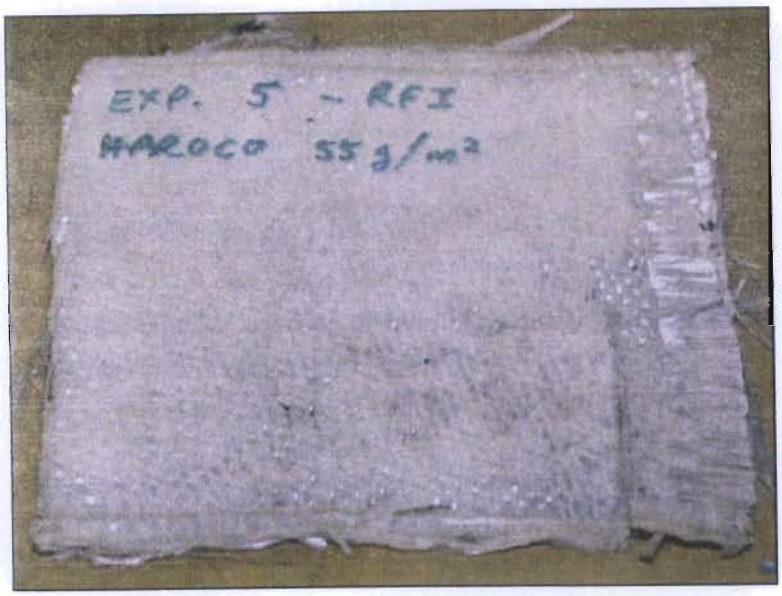

Figure 11 Top surface of Haroco Thermoplastic film RFI experiment.

Figure 12 Bottom surface of Haroco experiment, no wetting out of the material is visible.

With the use of XAF 2061, 30g/m^2 (see Experiment 4, appendix B), a similar result was obtained as that with using Xiro V587-1 dry adhesive film. That is, the film did not melt sufficiently to seep through and bond to the glass fibres. Advanced Materials Technologies (AMT) were requested to assist us in the search of a thermosetting dry resin film. They suggested the Hexcel range of film adhesives and managed to obtain a thermosetting film adhesive called Redux 312.

The first experiment conducted using Redux 312 yielded encouraging results (see Experiment R1, Appendix A). A high degree of fibre wetting took place with the resin seeping through parts of the lay-up. Despite the failure of the vacuum pump mechanism encountered during the experiment, the resin film melted and soaked through the fibrous lap-up under gravity. The final product contained a large amount of air spaces or voids. These tests were then conducted using Redux 312, 312L and 335J suggesting that this is indeed a suitable resin film, meeting the predetermined specifications. Not only are the processing characteristics desirable, but the fact that the Redux films have a small volatile content and negligible emissions falls directly in line with the requirement of a non-hazardous material system

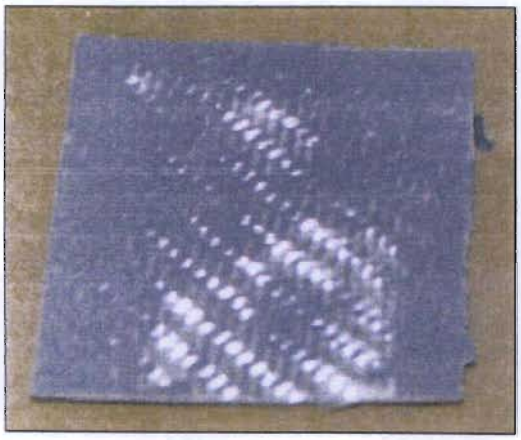

Figure 13 Early flat sample made from Redux 312.

Further testing using the Redux 312 and 335 films has proven successful. Testing has continued using these films, particularly studying the effects of lay-up, reinforcement fibre angle, dwell times and temperatures. In addition a series of tests to manufacture tensile test specimens has been undertaken. These samples were then tested to failure to check the strength properties as various process parameters were varied.

Figure 14 Complex 3-D sample manufactured using Redux 335.

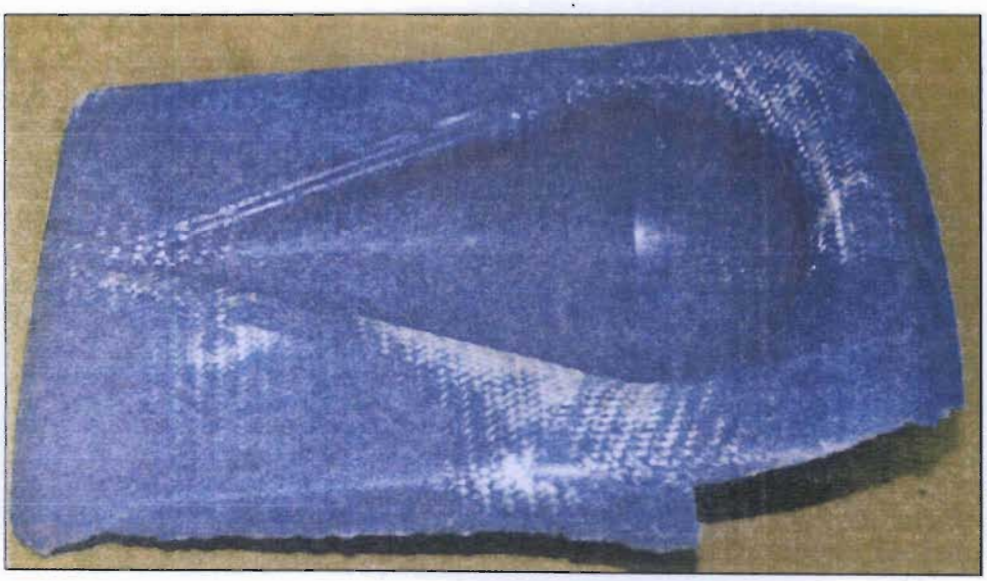

Figure 15 The bottom surface of the complex 3-D sample. The resin dry areas (white) are a result of a leak in the mould which allowed a continuous stream of air to be drawn into the component by the vacuum.

5.3. Equipment

In order to guarantee consistency and repeatability for all testing, the same equipment was utilised throughout the testing process. It should be noted that in many cases this was not identical to the equipment which would be used for full scale production and manufacture using the RFI process. This was in order to keep the project within the scope of work which could easily be performed at an academic institution, and to keep the costs manageable.

5.3.1. Oven

The exclusion of an autoclave and the small sizes of samples being manufactured, required the use of a small, highly controllable oven for the RFI process. The oven shown in Figure 16 below was originally designed and used for the manufacture of Photoelastic stress measurement samples. It has a forced air heating system which circulates the air in the oven over the samples and the heating elements. The elements are separate from the actual "oven chamber", ensuring fast responses to the controller.

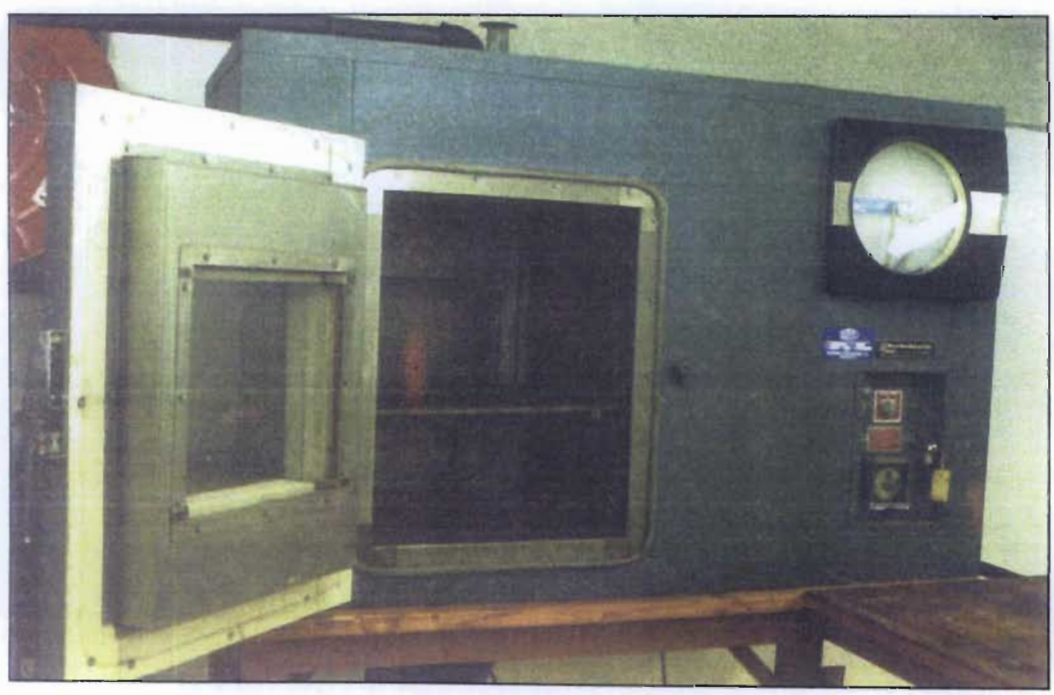

Figure 16 Photoelastic oven used for all RFI testing. (Shown with old cam type controller)

The oven was initially used with the cam type controller shown in the photograph, however this was replaced by a PLC controller (a REX P-300 16 stage programmable controller) for ease of use and the ability to program more complex heating and cooling cycles. (This is visible in the second photograph of the oven in the top right corner.)

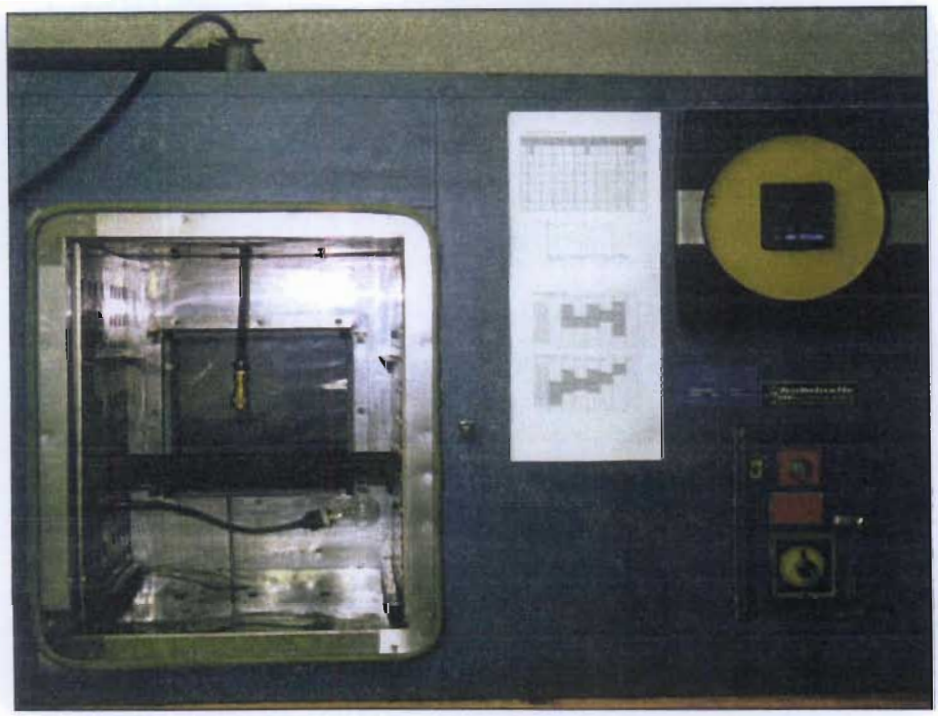

Figure 17 Photograph of oven and oven chamber.

The oven is fitted with two "chimneys", one of which was connected to the chimney system of the building to ensure that any volatiles produced are vented safely away (Black pipe visible at the top of the photographs). The second chimney is left open and is used as an access point for any pipes or sensors which need to be inserted into the oven, such as the vacuum pump pipe and thermocouples used as backup monitors during sample manufacture. Other than regular maintenance, and the fitting of a PLC controller, no changes were made to the oven during the two years of the testing program. The light visible in the second photograph was added to allow video footage to be taken of the resin flow tests. The heat given off by the bulb did not noticeably effect the heating rates, although it was switched off when the samples were cooling.

5.3.2. Vacuum pump

The vacuum pump shown below was used for all the RFI tests, which is a Speedivac high vacuum pump. The pump is able to draw a maximum vacuum of greater than –90kPa, and maintain it for long time periods. A standard vacuum gauge is used in conjunction with a brass gate valve to allow a range of pressures. By adjusting the amount of air entering via the valve, a range of pressures from 0 to –90kPa can be obtained. It should be noted however that if a vacuum of less than –40kPa is chosen, the system is not very stable and fluctuations are noticeable on the gauge. This falls well outside the range used for composites manufacture, and no problems were encountered with unstable pressures.

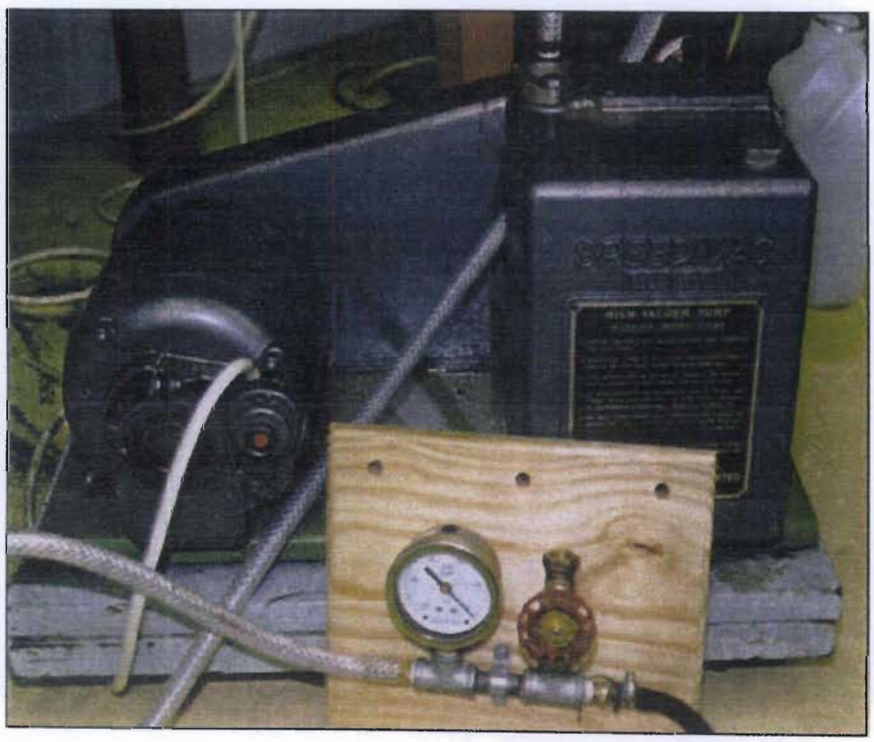

Figure 18 Speedivac High Vacuum pump with gauge and pressure control valve.

5.3.3. Mould design

The testing regime required the manufacture of a large number of samples with consistent and regular sizes and shapes. For the bend tests and impact samples, flat panels were manufactured using a polished stainless steel plate as the mould surface. The samples were then rough cut from these panels using a band saw before being machined to the required sizes, shapes and tolerances using a milling machine. The tensile test specimens were more complex and required special moulds to be

manufactured. Initially the moulds were constructed using "fast cast tooling" techniques, such as the Atlas M130 mould shown below in Figure 19.

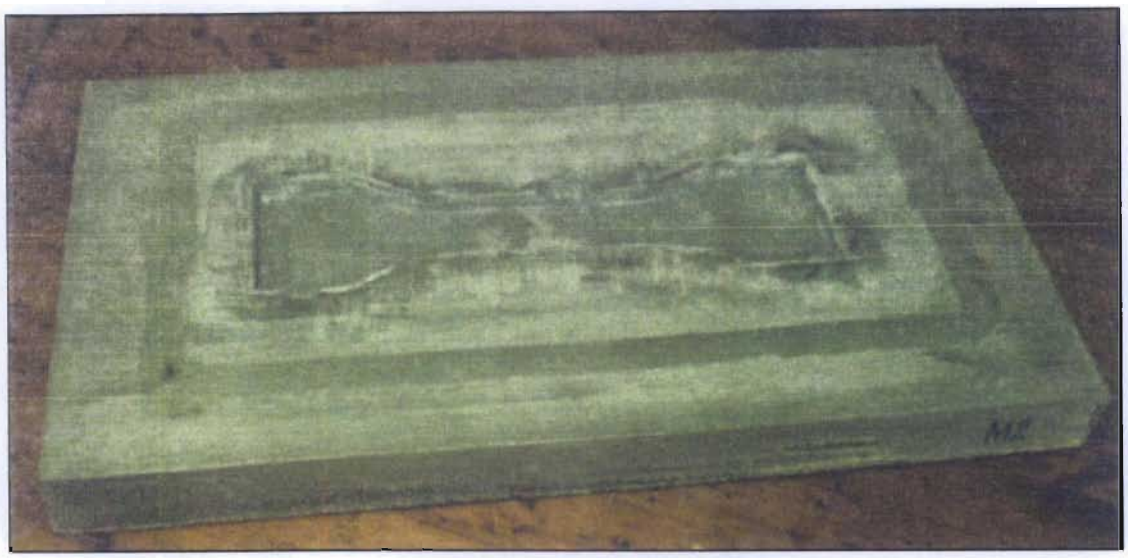

Figure 19 Atlas M130 Tensile test mould

This mould used a standard steel tensile test specimen, with one change, a 3° draft angle was machined to allow removal of the pattern from the cured mould and to facilitate the removal of the RFI moulded pieces.

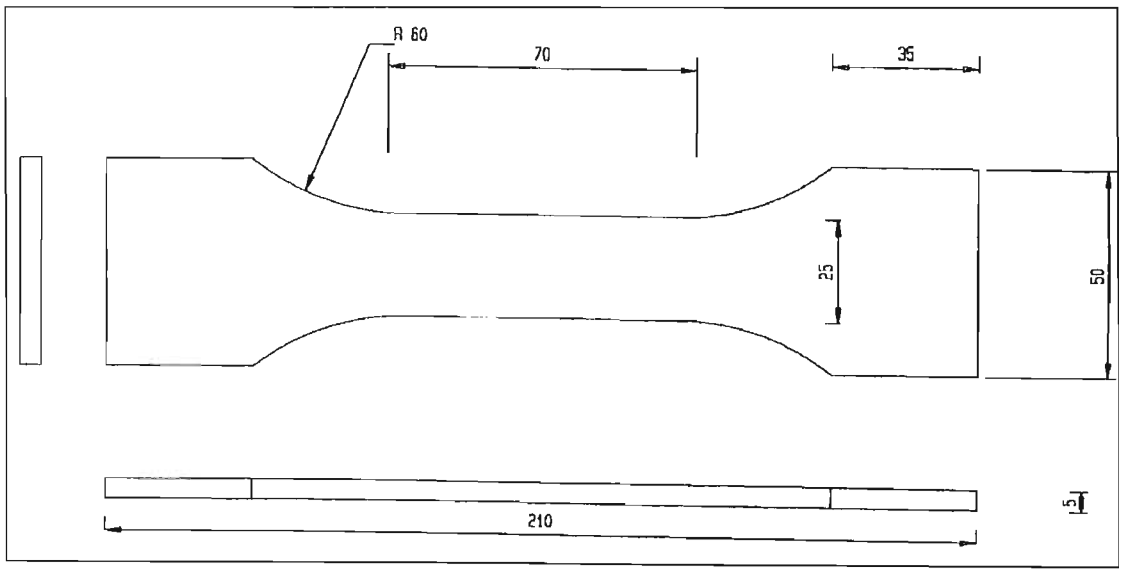

Figure 20 Pattern used for Atlas M130 tensile test specimen mould

The Atlas M130 moulds were replaced by a steel split mould before the process parameter testing phase was started. This was necessary for a number of reasons: Firstly the Redux resin system was bonding to the mould surface regardless of the release agent used. This was giving poor surface finishes and causing damage to the mould surface. Secondly the steel mould is split along the longitudinal centre line. This ensures easy removal of the component, and removed the need for a draft angle.

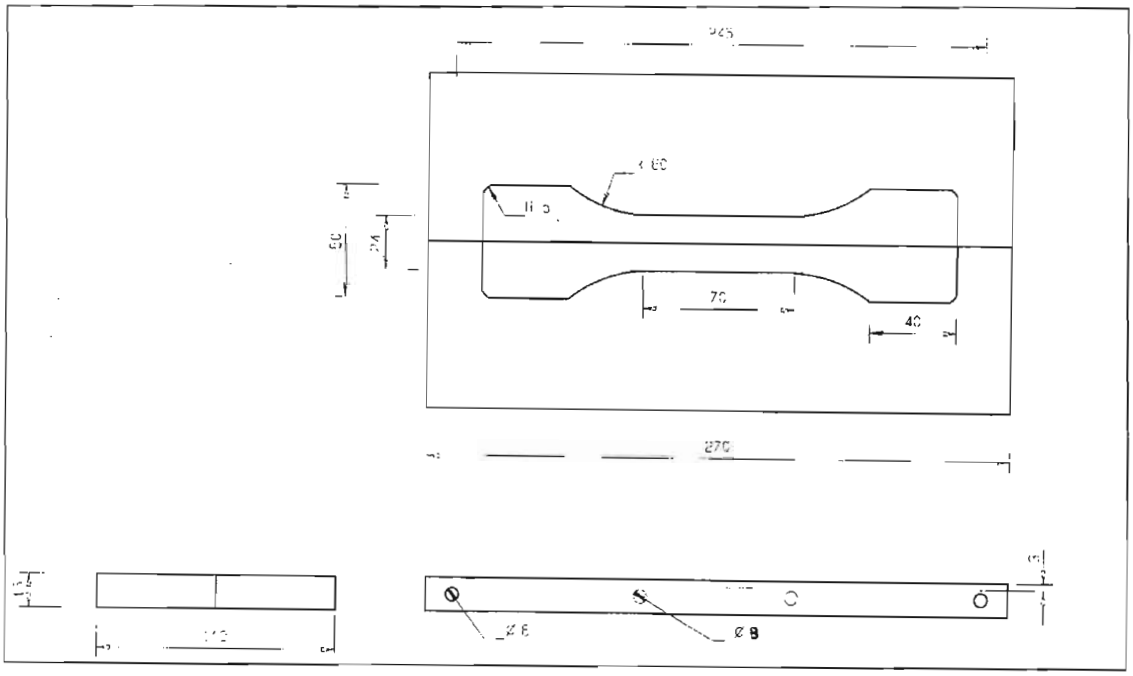

Figure 21 Steel split mould for manufacture of tensile specimens.

5.3.4. Mechanical test equipment

Figure 22 Instron testing machine (set up for tensile tests)

Figure 23 Instron testing machine (set up or bend tests)

The Tensile and bend tests were performed using an Instron Universal testing machine. The Instron 1195 Universal Testing Machine consists of two separate sections, namely the drive unit, with the load cell and moving cross head, enclosed in a rigid frame and the control unit (Figure 24). The control unit includes the readouts for the loads, and a printer. The above photographs (Figure 22 and Figure 23) show the Instron 1195 drive unit. Right at the top, the load cell is clearly visible, the moving cross beam is also identifiable. The crossbeam is driven up or down by two lead screws which are mounted in the sides of the frame. The motor and gearbox, which are hidden in the base of the frame, drive these lead screws as controlled by the operator. The grips are mounted as shown for tensile tests, (Figure 22) with the lower grip fastened to the crossbeam (which would be driven down for tensile tests), and the top grip is connected to the load cell by an extension piece and universal joint.

In order to perform a standard three point bend test, the grips are removed, along with the universal joint. In their place, at the top, a rounded "blunt knife edge" fitting is inserted, the lower fitting consists of two rollers mounted equidistant from the centre

line in a slot. Obviously the crossbeam is driven up to provide the compression for the bending test. The load cell is also re-calibrated to read compression forces as positive.

Figure 24 Instron universal testing machine control unit.

The control unit of the Instron 1195 machine is divided into two halves, the left half containing all the manual controls and readouts, with the right half containing a personal computer which is designed to allow computer control and recording of the data. The tests performed for the RFI work were all controlled manually.

5.3.5. Materials

Once the materials testing phase was completed, a standard materials system was developed for all testing, consisting of the following:

- Resin Film: Redux 312 (weight per unit area of 150 g/m^2)
- Fibreglass: E-glass GFHL 1037/600/125 (Satin weave)
  E Glass (Unidirectional cloth)
- Vacuum bag: Capran 524 High temperature vacuum bag.
- Sealant tape: HT 200/16 Sealant tape.

- Release ply: Halar WP 3 Perforated release ply.
- Breather / Bleeder cloth:
  Standard cloth breather ply.
- Release agent: Frekote 55NC.

The specifications for these materials can be found in Appendix F.

5.4. Process Parameters

For the determination of optimum process parameters physical testing was conducted in parallel with the development of the mathematical model. The testing consisted of the manufacture of specimens for mechanical testing. The process parameters were varied over a fixed range, and the samples strength tested as well as qualitatively appraised for other factors such as surface finish, wetting out of the preform and any visible voids. In addition a number of tests were performed to validate assumptions used in the mathematical modelling.

5.4.1. Lay-up

During the process of fibre composite manufacturing, it is usual to layer a number of layers of fibre reinforcement mat. This is necessary to give the necessary strength properties in the required directions. A number of experiments were performed to investigate if thicker laminates would be more difficult to manufacture and particularly if they would wet-out completely.

A number of samples were lay-up on the same plate, ranging from 1 layer of GFHL glass mat with one layer of resin film on top of it, to lay-ups consisting of 3 layers of mat underneath 3 layers of resin film. In addition, the orientation of the reinforcement layers was varied to give lay-ups with all the layers in the same orientation e.g. 0°/90° , while others were given 0°/90°, 45°/-45° stacking sequences. The samples were then vacuum bagged and placed in the oven, for a standard manufacturing cycle (80°C dwell for 30 minutes followed by 30 minutes at 120°C for cure). At the end of the cycle, the samples were removed and studied to determine what, if any, differences in the saturation could be determined. The samples were all totally wetted out by the resin and no discernible differences could be noted between them.

These results correlated with the layer dwell time / strength studies which suggest that complete saturation has taken place in less than 20 minutes and may occur before the dwell temperature is reached in the case of single layer reinforcement, single layer resin film laminates.

A similar series of tests were performed to study whether the ideal stacking sequence is an alternating lay-up of resin and reinforcement, or a single layer of dry film placed above a thick preform. Again no clear conclusions could be drawn from the tests, however the decision was made to use the alternating lay-up method. This was as a result of the available material system, Redux 312, which is only available (unless custom ordered from Hexcel) in the form of thin sheets with weights per unit area of 70 g/m^2 to 300 g/m^2. The most widely available weight was the 150 g/m^2, this film was thin and could easily be attached to the glass mat because it is sticky at room temperature. This had the added advantage of providing stability to the glass mat, especially if it was thin or a unidirectional weave.

5.4.2. Temperature Profile

In order to successfully manufacture a component using RFI, the temperature profile should be designed to firstly melt the dry film so that it saturates the reinforcement material, and once totally wetted out, cure and set. Figure 25 shows this idealised profile.

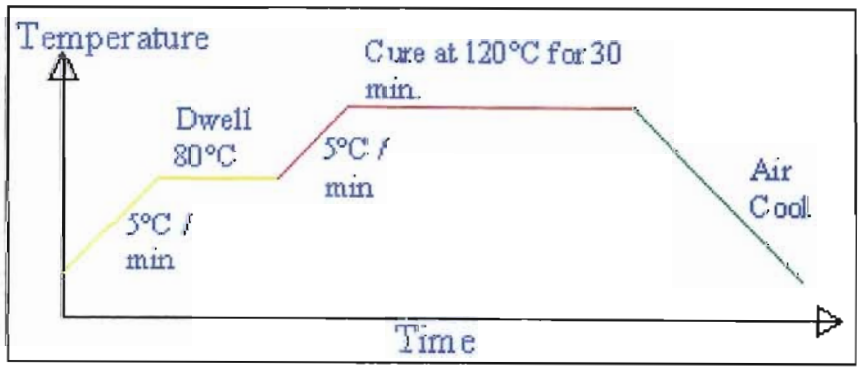

Figure 25 Idealised Temperature profile.

A number of experiments were performed to investigate the effects of varying both the dwell times and cure times, these results can be seen in the sections on the mechanical (strength) testing. Furthermore a series of tests was performed to verify the hypotheses related to the apparent complete wetting of the preform material prior to the dwell temperatures being reached. By placing a lay-up consisting of a single layer of woven mat and a single layer of resin film in a standard vacuum bag lay-up, but laid up on a

Pyrex glass plate rather than a stainless steel plate, in conjunction with a metal plate mirror and the glass window in the oven, the flow of the resin through the preform can easily be observed. The time taken and temperature reached for resin to initially appear and finally full saturation to be achieved was recorded to verify the assumptions made earlier. A video camera was used to record the tests for later study.

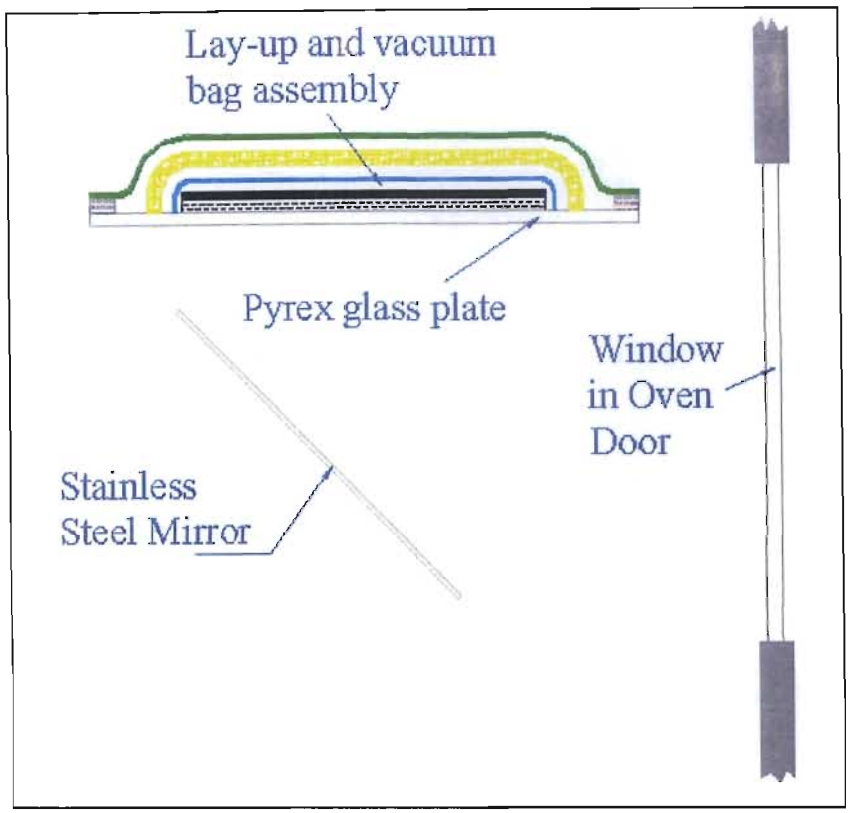

Figure 26 Schematic of experiment to study times and temperatures for saturation.

The tests were also repeated with two, three and four layers of woven mat, both in alternate lay-ups with the dry film, and with the layers of reinforcement underneath the layers of resin. These tests were performed using a unidirectional glass cloth rather than the regular woven mat, with stacking sequences ranging from all 0° to 0°/90°/45°/-45°.

Below are six figures which are captured from the video of the test. The first resin can be seen appearing against the glass plate after 4 minutes at the right hand end of the top left lay-up. This is even more visible after 7 minutes.

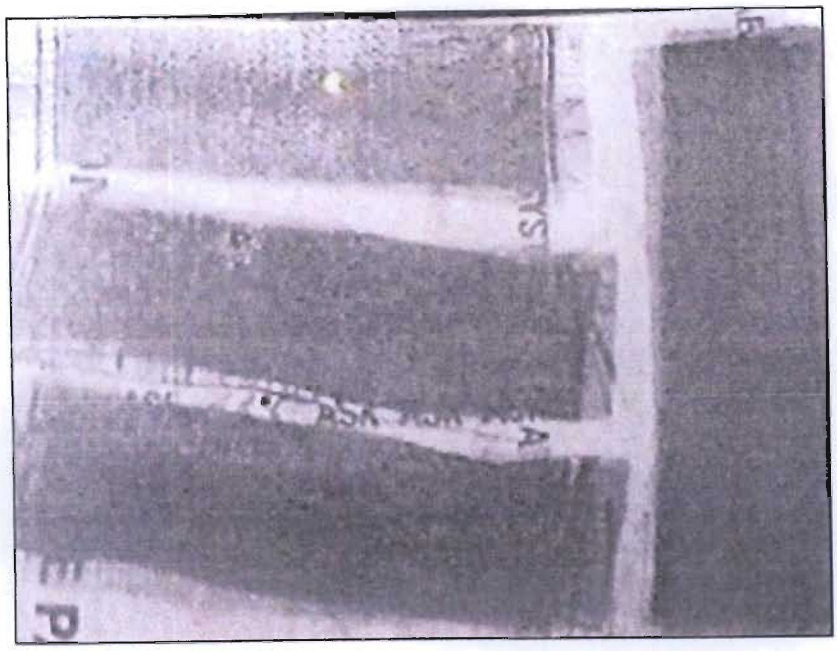

Figure 27 Video still of resin seepage test (4 minutes)

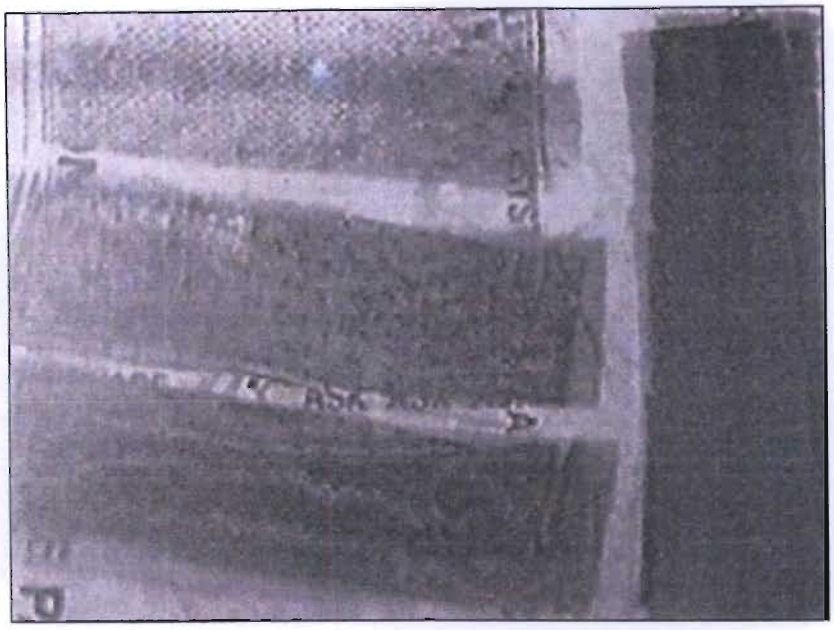

Figure 28 Video still of resin seepage (7 minutes)

As the test continues the temperature rises (2° C/min) and after 17 minutes, the samples are all nearly completely wetted out. By the time the dwell temperature is reached after 30 minutes, no change is visible (25 minute and 35 minute stills). The dwell temperature was maintained for another 30 minutes, but no change could be discerned. By this time the samples had begun albeit slowly to cure and resin flow was unlikely.

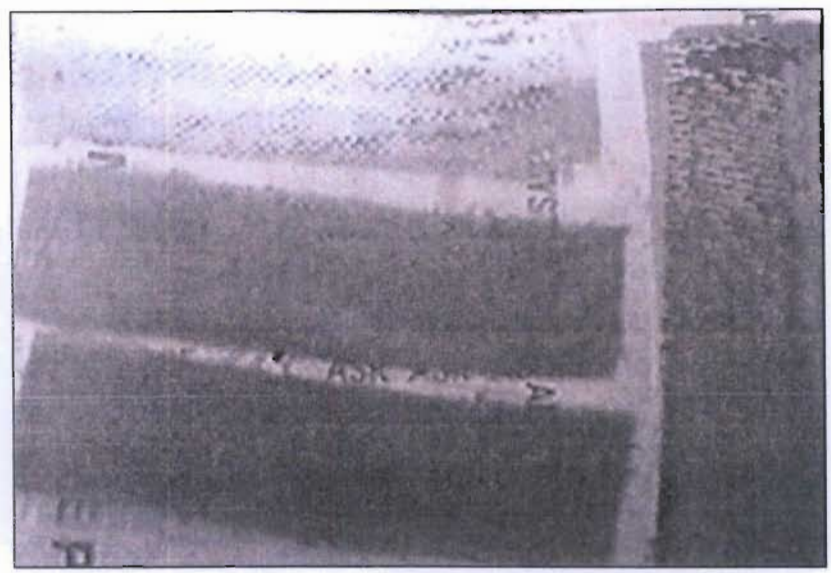

Figure 29 Video still of resin seepage (17 minutes)

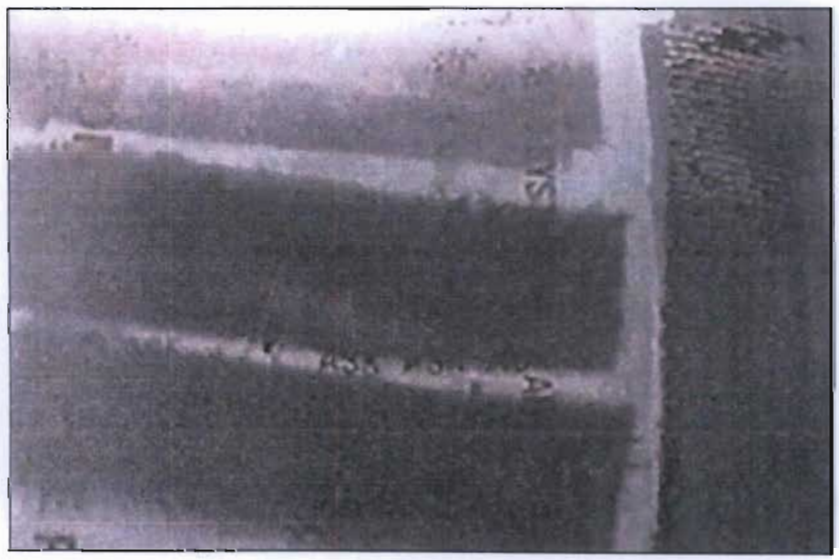

Figure 30 Video still of resin seepage (25 minutes)

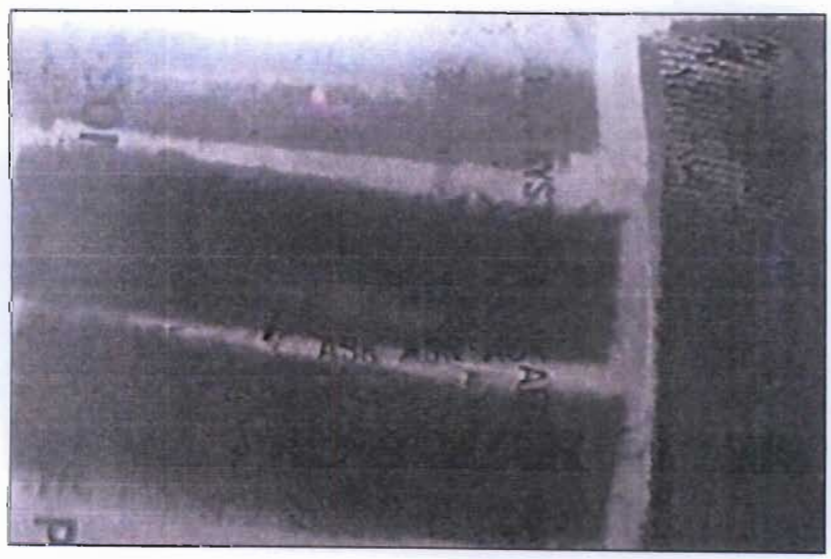

Figure 31 Video still of resin seepage (35 minutes)

5.5. Mechanical (Strength) Testing

5.5.1. Bend Testing

Method

The bend tests were performed using the Instron Universal testing machine described earlier. Flat plate samples were manufactured at a range of dwell and cure times. The bend test specimens cut from these plates consisted of simple rectangular pieces with a lay-up of 0°/90°. These samples were carefully measured and the moment of inertia was calculated using the equation for the moment of inertia of a rectangular cross-section

$$I_{rect} = \frac{b \bullet d^3}{12} \qquad (1)$$

The samples were all subjected to a standard three-point-bend test, with a roller separation of 40.54 mm. The 3rd support is placed at the mid-span point. This arrangement is clearly visible in Figure 32 below. The cross-head of the testing machine is driven up at a speed of 50 mm/min, this speed was chosen as it was not too fast to give inaccurate results, while still allowing a large number of samples to be tested. Five samples were cut from each plate and the stresses averaged to give a result for each test series.

As a result of the orthotropic nature of the samples manufactured for the testing, the basic stress strain equations cannot be used. Strains in the fibre directions are described as follows,

$$\sigma_1 = \frac{E_{11}\varepsilon_1}{1-\nu_{12}\nu_{21}} + \frac{\nu_{21}E_{11}\varepsilon_2}{1-\nu_{12}\nu_{21}} \qquad (2)$$

$$\sigma_2 = \frac{\nu_{12}E_{22}\varepsilon_1}{1-\nu_{12}\nu_{21}} + \frac{E_{22}\varepsilon_2}{1-\nu_{12}\nu_{21}}, \qquad (3)$$

$$\tau_{12} = G_{12}\gamma_{12} \qquad (4)$$

where E_{11} is the elastic modulus in the longitudinal direction, E_{22} is the elastic modulus in the transverse direction, G_{12} is the shear modulus, ν_{12} is the major Poisson's ratio and

v_{21} is the minor Poisson's ratio. When our loads are not in the fibre direction we transform the stresses and strains as follows,

$$\overline{\sigma}_{xy} = T^{-1}\overline{\sigma}_{12} \qquad (5)$$

$$\overline{\varepsilon}_{xy} = T^{-1}\overline{\varepsilon}_{12} \qquad (6)$$

where T is a transformation matrix made up of sine and cosine of the off axis angle. When dealing with many layers we use the plate curvatures to define the bending strains, with z being the co-ordinate of the layer in question measured from the laminate mid plane.

$$\overline{\varepsilon}_{xy} = \overline{\varepsilon}^{0} + z\overline{k} \qquad (7)$$

and hence the relevant plate constitutive equations are described as follows.

$$\begin{bmatrix} N \\ M \end{bmatrix} = \begin{bmatrix} AB \\ BD \end{bmatrix} \begin{bmatrix} \overline{\varepsilon}^{0} \\ \overline{k} \end{bmatrix} \qquad (8)$$

where $[N] = \begin{bmatrix} N_x \\ N_y \\ N_{xy} \end{bmatrix}$ is the vector of the loads, $[M] = \begin{bmatrix} M_x \\ M_y \\ M_{xy} \end{bmatrix}$ is the vector of the moments,

whereA, B and D are the transformation matrices.

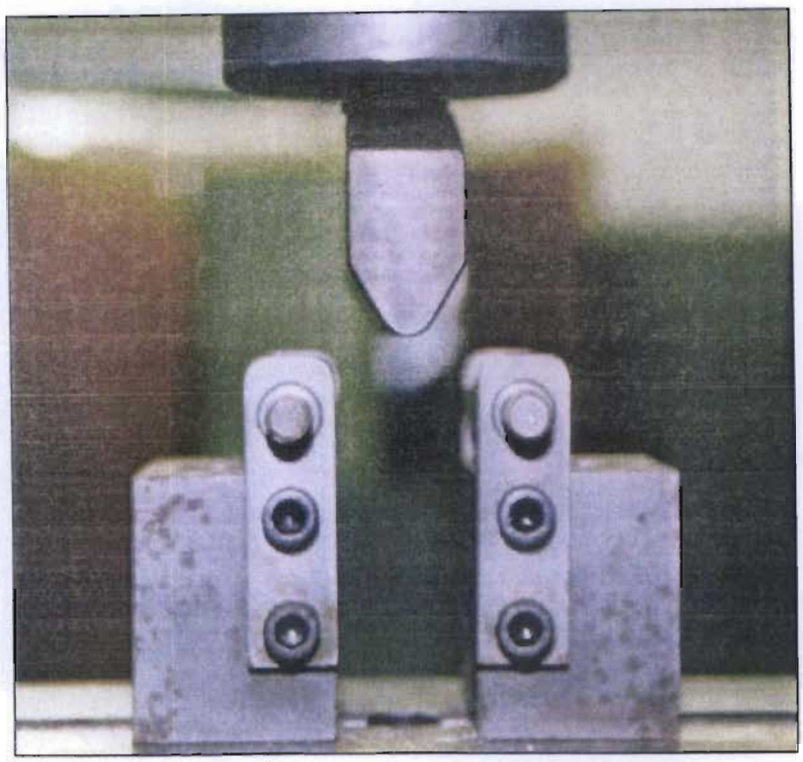

Figure 32 Bend Test fittings for Instron .

The samples are assumed to have failed once a fracture is seen or heard, this corresponded with an end the maximum recorded load in all the cases, i.e. although the specimen continued to support a load, it was far lower than the load at failure. A failed sample is shown below in Figure 33. As we were comparing samples which all had the same laminate construction a standard bend strength was calculated as follows.

$$\sigma_{bend} = \frac{M \bullet \bar{y}}{I_{rect}} \qquad (9)$$

where I_{rect} is the moment of inertia of the sample, $\bar{y}$ the distance from the neutral axis to the top or bottom surface and M is the bending moment at the midpoint of the beam

$$M = \frac{F \bullet L}{4} \qquad (10)$$

with F the load at failure and L the separation between the rollers. This allowed a simple and direct comparison of the effect of the process parameters to be made. It should be noted that as the beam has an unsymmetrical lay-up, the actual failure stress would be different for the top and bottom surface, and hence the results are not truly representative, but for comparison only.

Results

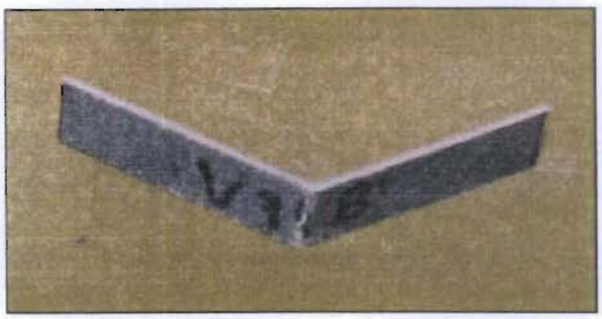

Figure 33 Bend test sample after testing to failure.

Twenty eight series of samples were manufactured, giving a total of 140 tests. The strength results, and averages were calculated and are presented below in Table 1. Graphs were plotted to show the relationships between the dwell and cure times and the corresponding strength of the product.

Series no.	Dwell time min.	Av. Failure Stress MPa
V11	15	212.8
V12	20	256.2
V13	25	534.6
V14	30	284.7
V15	35	209.5
V16	40	311.8
V17	45	183.9
V21	15	392.5
V22	20	249
V23	25	346
V24	30	291
V25	35	232.9
V26	40	421.7
V27	45	337.9

Series no.	Cure time min.	Av. Failure Stress MPa
V31	15	226.3
V32	20	304.5
V33	25	372.2
V34	30	268.1
V35	35	194.9
V36	40	145.5
V37	45	273.2
V41	15	179.7
V42	20	240.1
V43	25	183.6
V44	30	328.3
V45	35	353.7
V46	40	342.5
V47	45	316.8

Table 1 Failure stresses for the bend tests

Figure 34 shows the results for the series of dwell time varied samples which were manufactured under a –80kPa vacuum pressure. A 3rd order polynomial was fitted to the data, and clearly shows that a dwell time of approximately 25 minutes provided the highest strength.

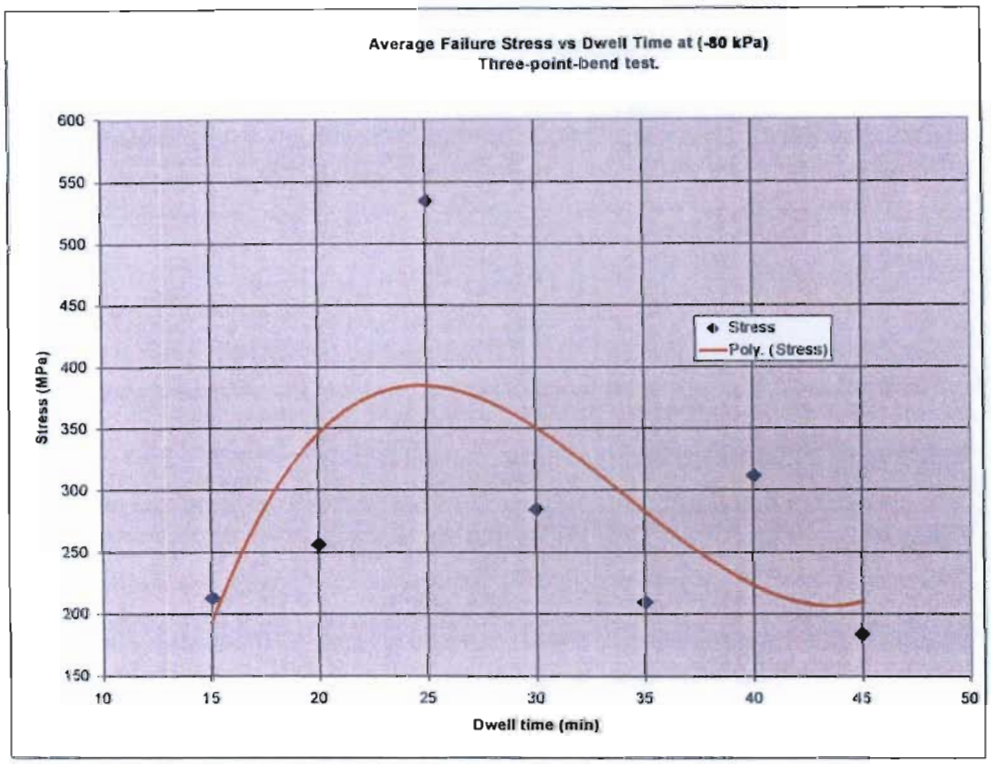

Figure 34 Graph of average failure stress vs. dwell time for bend test at -80 kPa vacuum.

When the data for the series of tests performed on the samples manufactured using a –90 kPa vacuum pressure are presented (Figure 35), no clear trend can be determined. This is most likely as a result of complete saturation occurring prior to the dwell temperature being reached. This assumption can be backed up by the results discussed above in Figure 34. The maximum point obtained at the 25 minute dwell time is significantly different to the average and may be the result of some factor other than the dwell time.

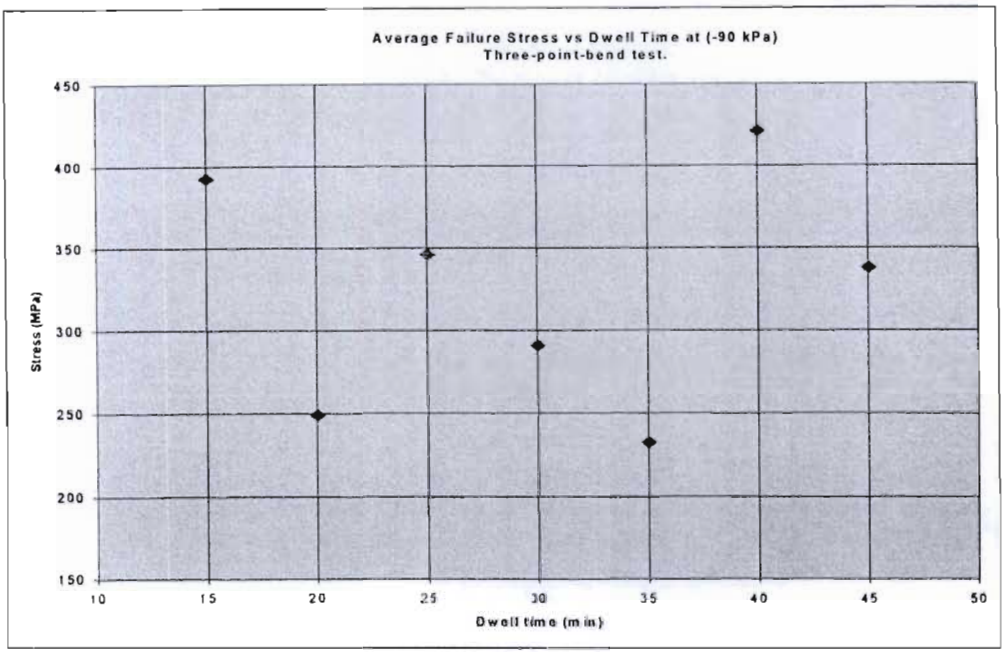

Figure 35 Plot of average failure stress vs. dwell time for bend tests at -90 kPa vacuum.

Similar plots (Figure 36 and Figure 37) have been generated for the varied cure samples. Unfortunately as with the dwell cycle tests, it is difficult to identify clear trends. However it does appear that the longer the cure, the stronger the component. This trend begins to fall off after around 40 to 45 minutes, and the strength appears to decrease. The most likely explanation is that residual stresses are damaging the component as a result of the long exposure to high temperatures.

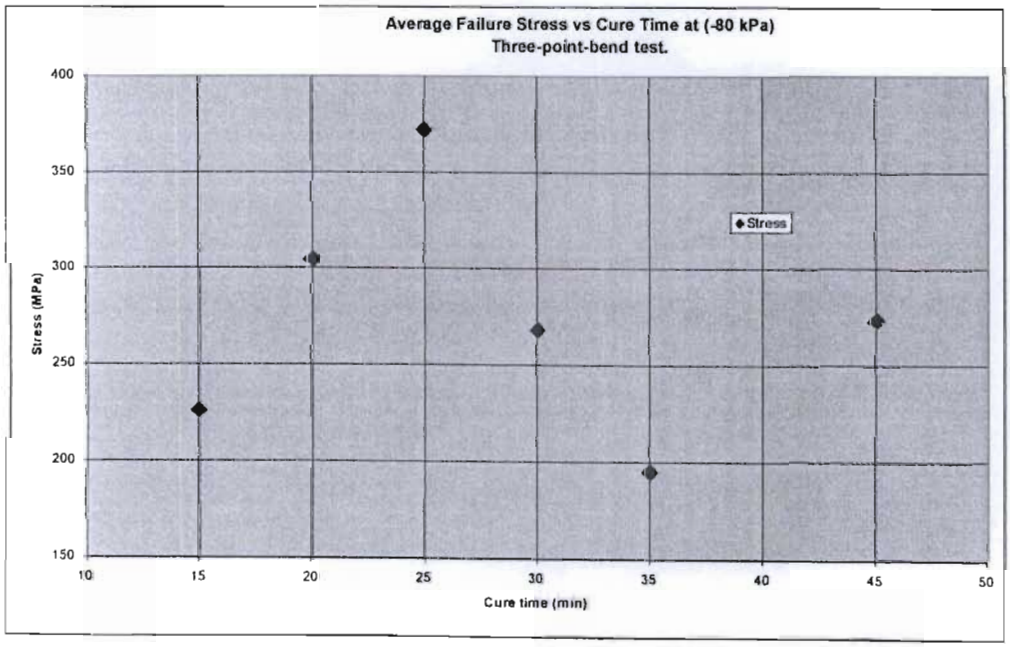

Figure 36 Plot of Average Failure stress vs. cure time for bend tests at -80kPa

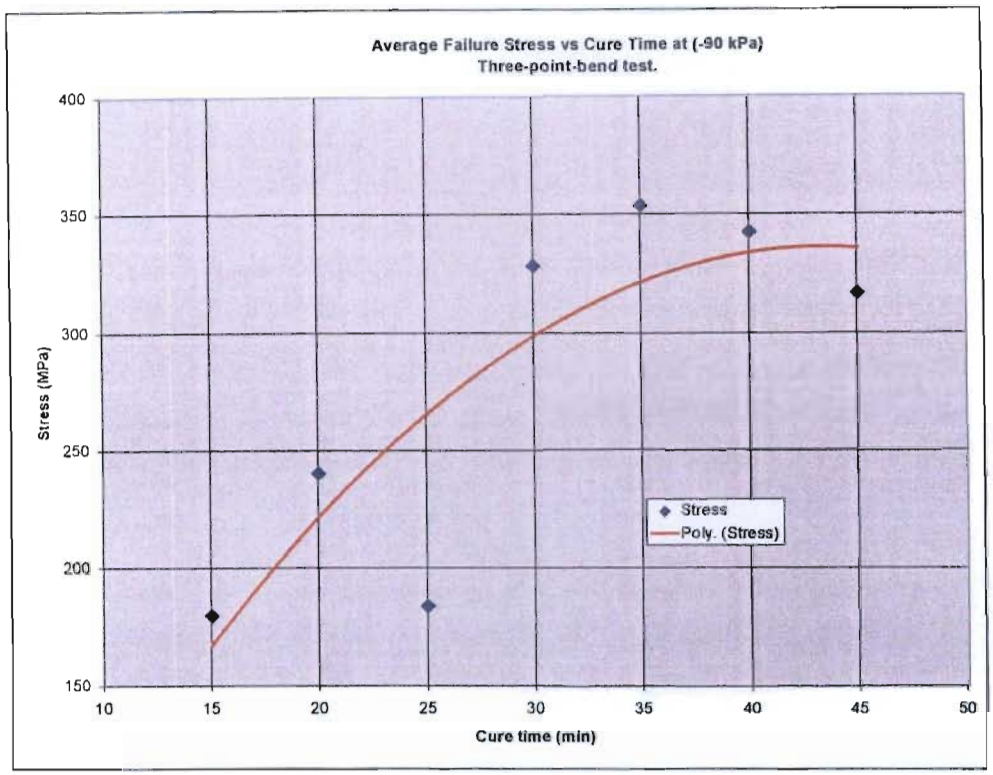

Figure 37 Graph of Average Failure stress for bend test vs. cure time at –90 kPa vacuum.

Although the data obtained from the bend tests is rather inconclusive, it does suggest that a dwell time of around 20 minutes should be utilised, however this may be reduced if very high vacuum pressures or thin components are to be manufactured. The ideal cure cycle should be in the region of 30 to 40 minutes and longer cures should be avoided as they seem to cause damage and reduce the strength.

5.5.2. Impact Testing

Method

The complexity of the failure process of composite materials under impact loading makes testing very difficult. The traditional Izod and Charpy tests give no indication of residual properties after impact.

Thus a low velocity impact of a few joules would be sufficient to get results which would allow comparison of the impact strengths against the process parameters. By using a mini double pendulum impact tester, for the impact testing of the resin film

infusion samples, differences could be determined between the samples. The double pendulum impact tester consists of three pendulums, two outer and one inner, the former being connected at their lower ends thus the two outer pendulums may be considered as one.

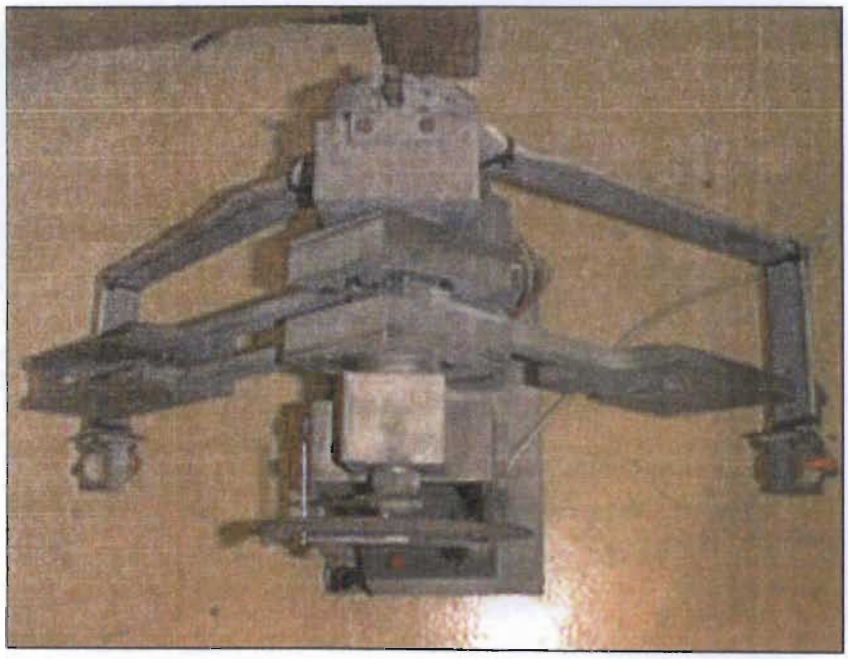

Figure 38 Photograph of double pendulum impact tester (top view)

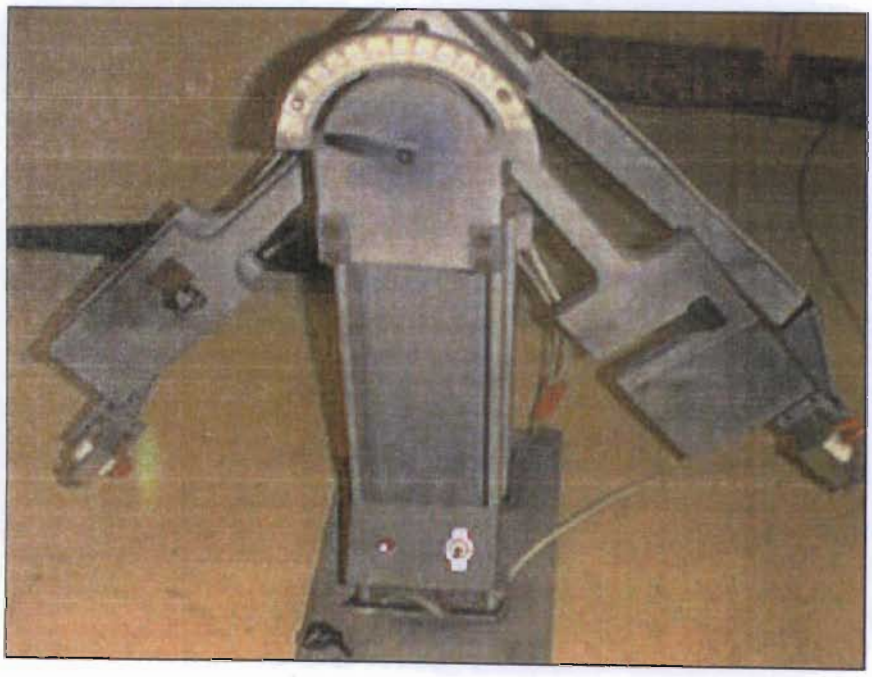

Figure 39 Photograph of double pendulum impact tester (front view)

A sample with dimensions 10 mm wide by 170 mm long is held in the outer pendulums. A solenoid releases both pendulums simultaneously and the resulting impact energy as the sample held by the outer pendulums is struck by the inner pendulum is read off a calibrated scale.

The calibrated scale allows different values of potential energy to be selected representing the height at which the two pendulums are released from. By choosing anyone of the seven pin positions a different potential energy impact is provided. For the RFI tests pin six was used and the impact energy value was read off from the gauge mounted to the tester frame. This gauge reading gives the height reached after the two pendulums are released, i.e. the potential energy lost during impact.

Using the table provided (Appendix G) the corresponding impact energy absorbed in joules was calculated.

Results

The results of the impact tests have been averaged to give the average impact energy for each series of samples, i.e. for each dwell and cure time. Graphs were then plotted of impact energy against dwell and cure times for the –80kPa (Figure 40 and Figure 42) and –90kPa samples (Figure 41). The results can be seen (sorted in descending order) in Table 2.

Sample no.	Average energy [J]	Sample. no.	Average energy [J]	Sample no.	Average energy [J]
V25	2.22	V17	1.46	V24	1.11
V23	2.15	V13	1.44	V31	1.11
V11	1.97	V32	1.38	V34	1.11
V22	1.93	V16	1.24	V44	1.11
V21	1.86	V27	1.24	V43	1.07
V36	1.74	V33	1.21	V45	1.07
V26	1.71	V14	1.18	V37	1.04
V15	1.61	V41	1.14	V42	1.04
V47	1.50	V46	1.14	V35	1.00
V12	1.49				

Table 2 Impact Energies for process parameter testing. (in descending order)

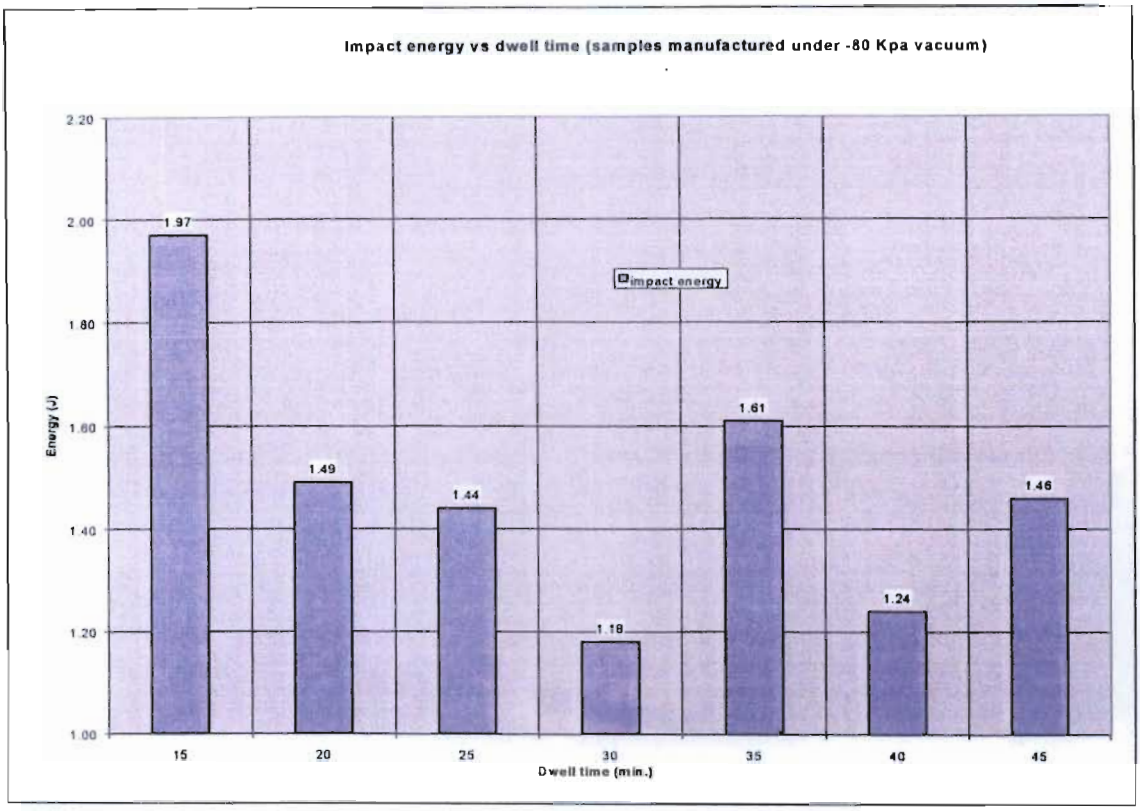

Figure 40 Graph of impact energy vs. dwell time for samples manufactured at -80kPa vacuum.

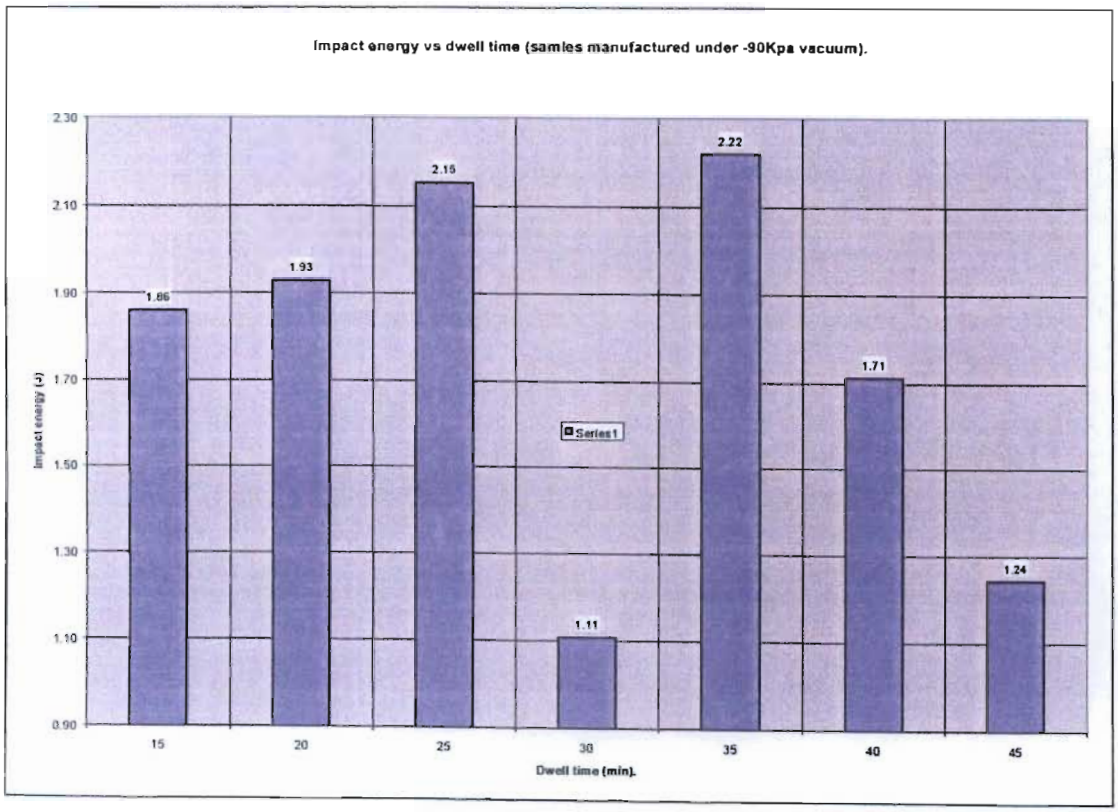

Figure 41 Graph of impact energy vs. dwell time for samples manufactured at -90kPa vacuum.

These impact tests were performed with the goal of comparing the effect of varying the process parameters, and the actual numbers obtained should not be compared to other materials or data. Unfortunately no clear trend can be discerned for the dwell time series tests. By not showing any clear trend it was consistent with the earlier results obtained for the bend tests, and further confirms the assumption that seepage and flow are complete before the dwell temperature is reached. It should be noted that the samples did not fail in the expected manner of metals for impact testing, i.e. a complete fracture, but rather the samples fracture and bend which causes them to be drawn through the "gate" of the impact tester. Composite fracture mechanics is a complex area which was not investigated as the impact tests were only used to compare the effect of process parameters.

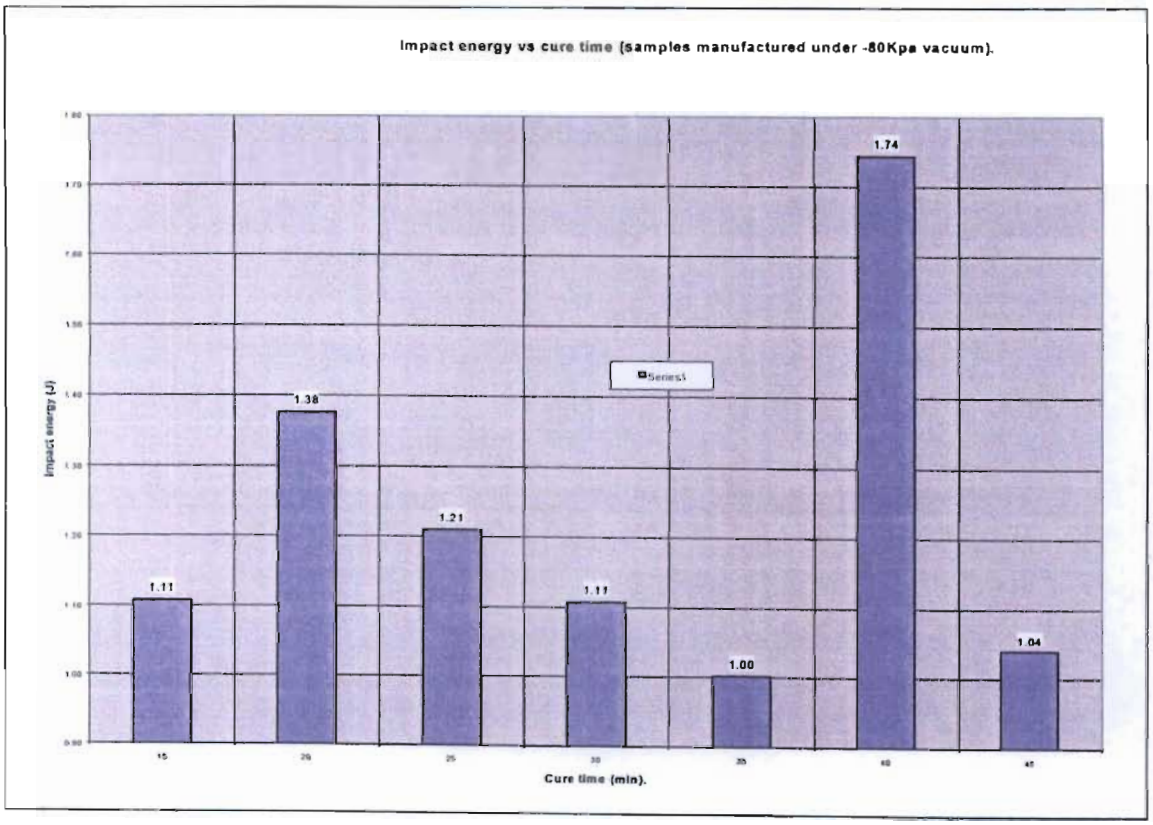

Figure 42 Graph of impact energy vs. cure time for samples manufactured at -80kPa vacuum.

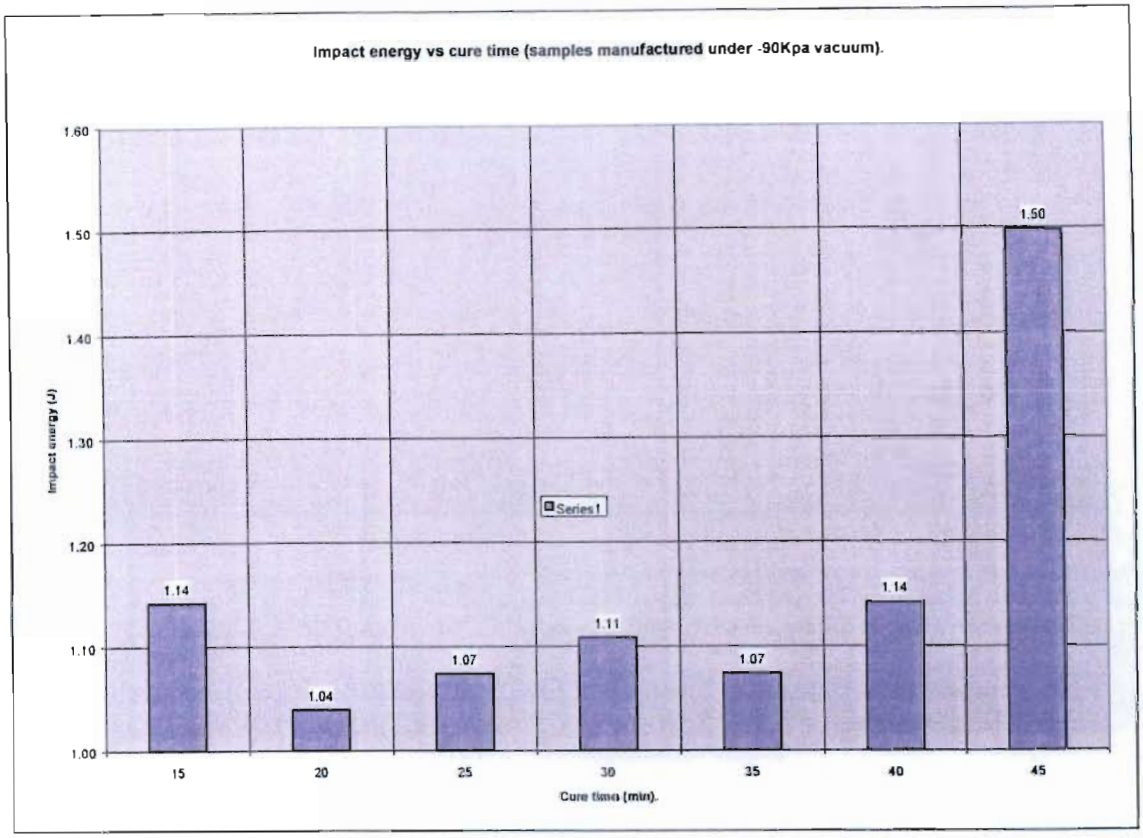

Figure 43 Graph of impact energy vs. cure time for samples manufactured at -90kPa vacuum.

Figure 42 and Figure 43 show the results for the cure time series. Again trends are not easy to determine, however both the –80 kPa and –90kPa vacuum series samples achieve their maximum impact energy absorption at the end of the range of dwell times. This is consistent with the theory that the longer the cure, the greater the cross linking and the harder (and more brittle) the matrix becomes. The failure mechanism in these impact tests was always a matrix fracture rather than a reinforcement fracture, hence as the matrix becomes stronger (more cross-linking) the higher the absorbed energy. The full set of impact test results can be found in appendix C.

5.5.3. Tensile Testing

Method

A series of tensile test specimens were manufactured using the steel split mould discussed earlier. These specimens were manufactured by choosing 6 best process parameters (heating cycles) from the bend samples. However they are thicker,

containing eight layers of plain weave glass mat in the following symmetrical stacking sequence, $(0°/90°, -45°/45°, 0°/90°, -45°/45°)_s$.

Figure 44 Tensile test specimen, made in steel split mould. (Top surface)

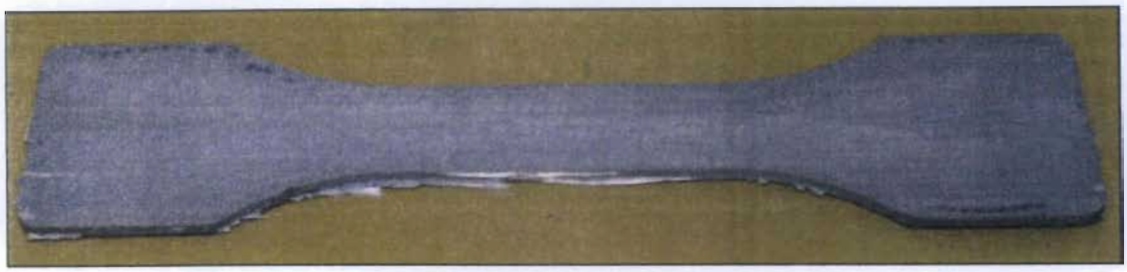

Figure 45 Tensile test specimen, made in steel split mould. (Bottom surface)

These samples were subjected to a standard tensile test to failure using the Instron universal testing machine. The ends of the samples were held in the jaws which clamp using a wedge type arrangement. (See Figure 22). The cross-head holding the lower jaws is driven down, while the upper jaws are connected to the load-cell by means of a universal joint. This helps remove any off-axis loading. Both the extension and load at failure are recorded and in conjunction with the cross-sectional dimensions (measured before the test) to determine the stress at failure. Again as was discussed earlier in the section on the bend tests, the orthotropic nature of the specimens requires a micro-mechanical approach. However as these tests were simply to compare the effect of various process parameters on the strength, a basic isotropic approach was used to simplify the calculations and provide easily compared data. Thus the failuer stress was calculated as follows,

$$\sigma_{tensile} = \frac{F}{A} \qquad (11)$$

where F is the failure load and A the cross-sectional area of the rectangular narrowed section. The strain at failure can also be calculated from the initial length L and the extension at failure ΔL

$$\varepsilon_{tensile} = \frac{\Delta L}{L} \tag{12}$$

Results

Table 3 shows the results for these tensile tests, along with the process parameters used in their manufacture.

Sample Series	Mean Tensile Stress	Mean Young's Modulus	Mean Strain	Dwell time / Cure time	Vacuum pressure.
	(MPa)	(MPa)		(min)	(-kPa)
T13	240.66	2910.64	0.0824	25/30	80
T26	214.10	2737.68	0.0781	40/30	90
T27	237.68	2771.96	0.0857	20/30	90
T31	193.88	2299.93	0.0843	20/15	90
T32	174.59	2284.52	0.0762	20/20	80
T33	243.86	2754.93	0.0886	20/25	80
T45	189.80	2254.00	0.0686	20/35	90

Table 3 Results of Tensile tests.

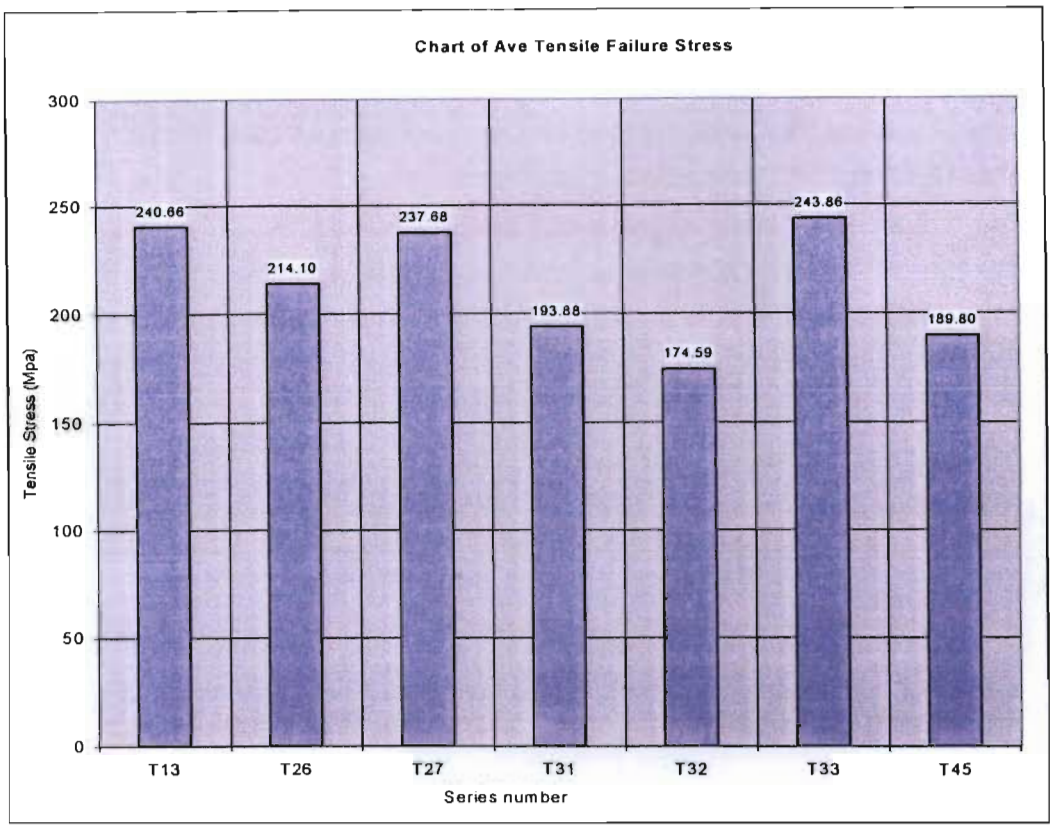

Figure 46 Chart of Ave. Failure Strength for tensile tests.

The six series of samples tested represent the process parameters, which produced the best impact and bend test results. Figure 46 shows the range of the tensile strengths of the various samples. The maximum strength was 243 MPa, from T33 which was manufactured using a –80 kPa vacuum and dwell of 20 minutes with a cure of 25 minutes. T13 and T27, which are very close to the maximum, represent series with dwell and cure times within 5 minutes of this result. The vacuum pressure applied was –80 kPa for T13, while T27 was –90kPa. No clear trend as to the effect of vacuum pressure can be identified, and this may be a result of the mould design, and the thick (compared to the bend and impact samples) laminate of the tensile specimens.

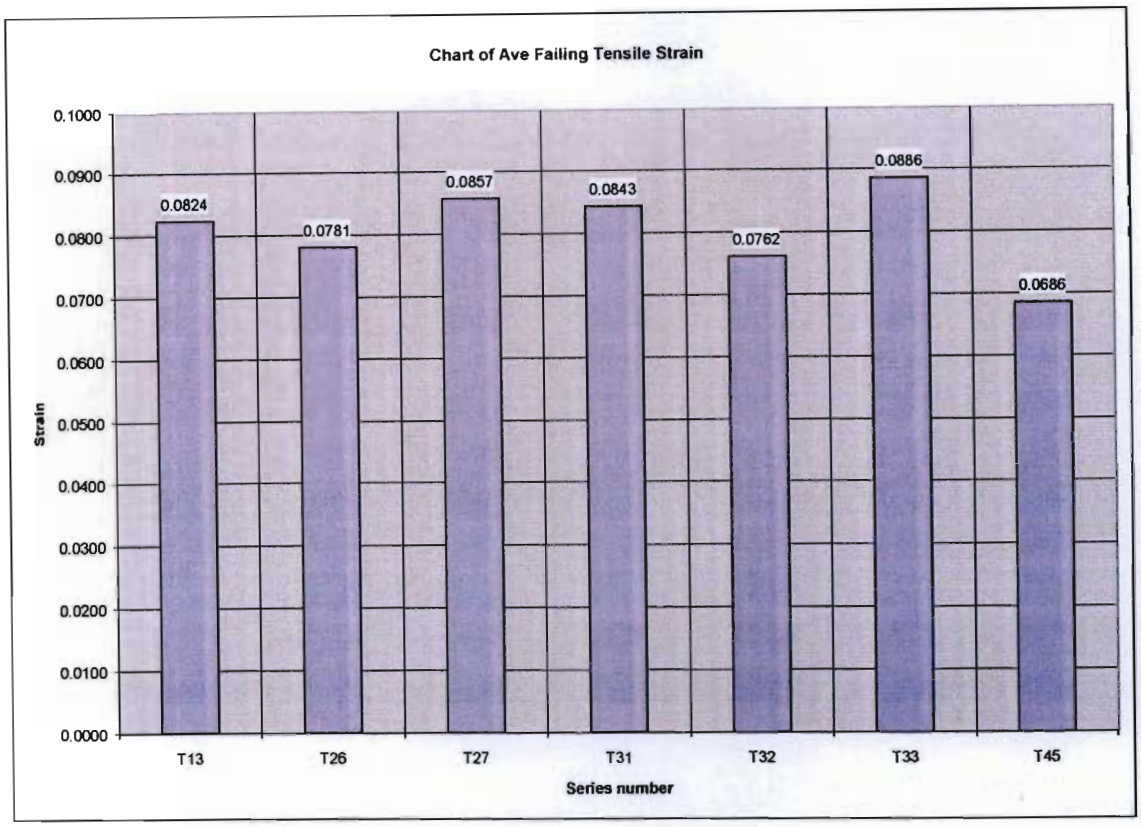

Figure 47 Chart of Ave Failure Strain for tensile tests

Figure 47 shows the strain data for the tensile tests, the results are all reasonably close and fairly low. This is consistent with the expected results for epoxy reinforced glass fibre which has low elongation. The results tend to mirror the strength data, i.e. lower strength samples had lower strain values.

The Young's modulus calculations are displayed in Figure 48, the calculations assume that the failure was brittle and the strain was linear up to the fracture point. T13 had the highest Young's modulus at 2.91 GPa, with T32 the lowest at 2.28GPa. Thus a component manufactured using the RFI process and Redux resin systems could expect to have an average tensile strength in the region of 200 MPa, and a Young's Modulus of approximately 2GPa.

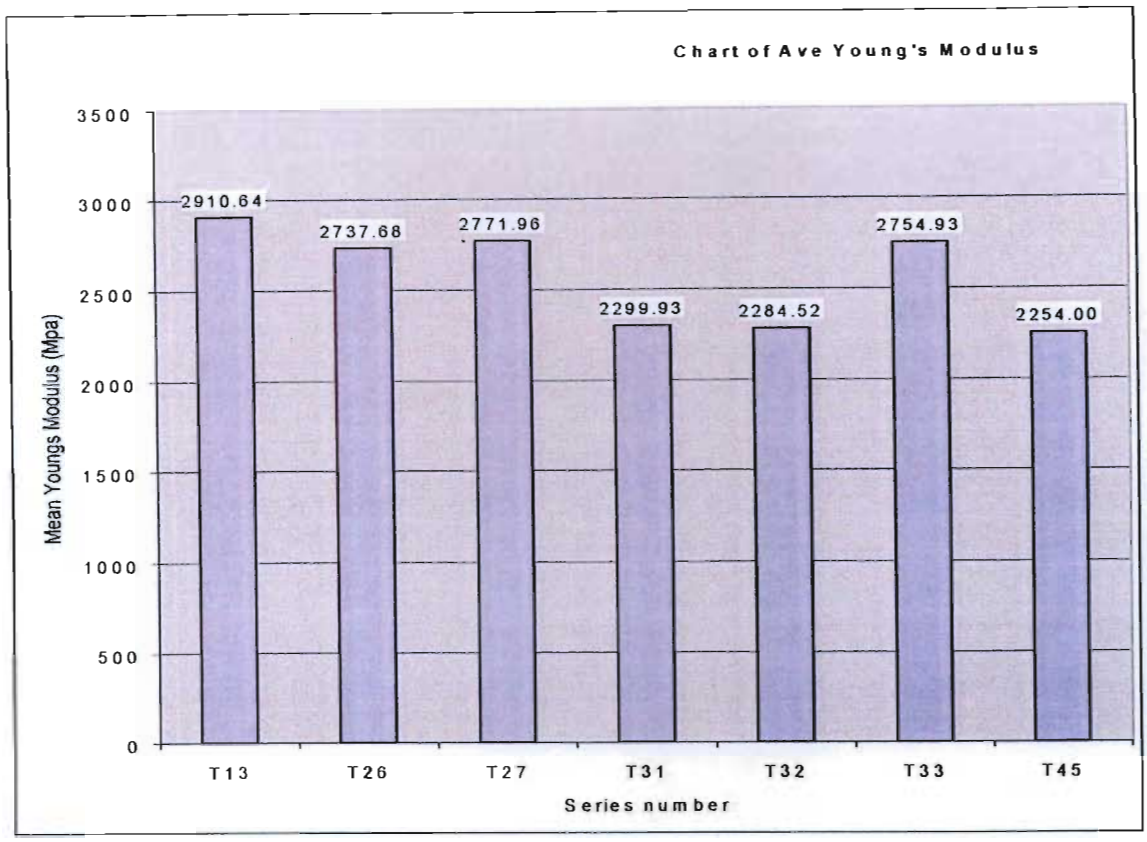

Figure 48 Chart of Ave Young's Modulus (from Tensile Tests)

5.5.4. Surface finish

Method

As each series plate sample was manufactured for the bend and impact tests, the surface finish was graded using a blind test method. Three students each studied the samples and gave them a rating out of 5 for surface finish. Five out of five represented a sample with a close to mirror finish while 0 would be a bad surface finish, e.g. glass cloth visible which has not been wetted out at all. The same polished stainless steel plate was used for the manufacture of all the samples and was cleaned and prepared in the same manner before sample manufacture. The results were then compared to the process parameters to see if dwell or cure time effect the surface finish.

Results

Figure 49, Figure 50, Figure 51 and Figure 52 show the surface finish grade against the dwell and cure times, with a best fit linear trend-line added. These trend lines are all reasonably level with the results ranging in the 2.5 to 4 out of 5 range. The series

manufactured with a –90kPa vacuum pressure tend to have a slightly better surface finish, which is most likely due to the higher compaction pressure. This will flatten the weave of the glass cloth improving the appearance.

Earlier in the experimental research, while the initial work to determine the suitability of Redux 312 was conducted it was determined that the surface finish was primarily dependent on the amount of resin film in the laminate. The dryer the lay-up the worse the surface finish. In addition, if the lay-up has a layer of dry resin film placed as the first layer (i.e. against the mould surface), it was found that a better surface finish resulted.

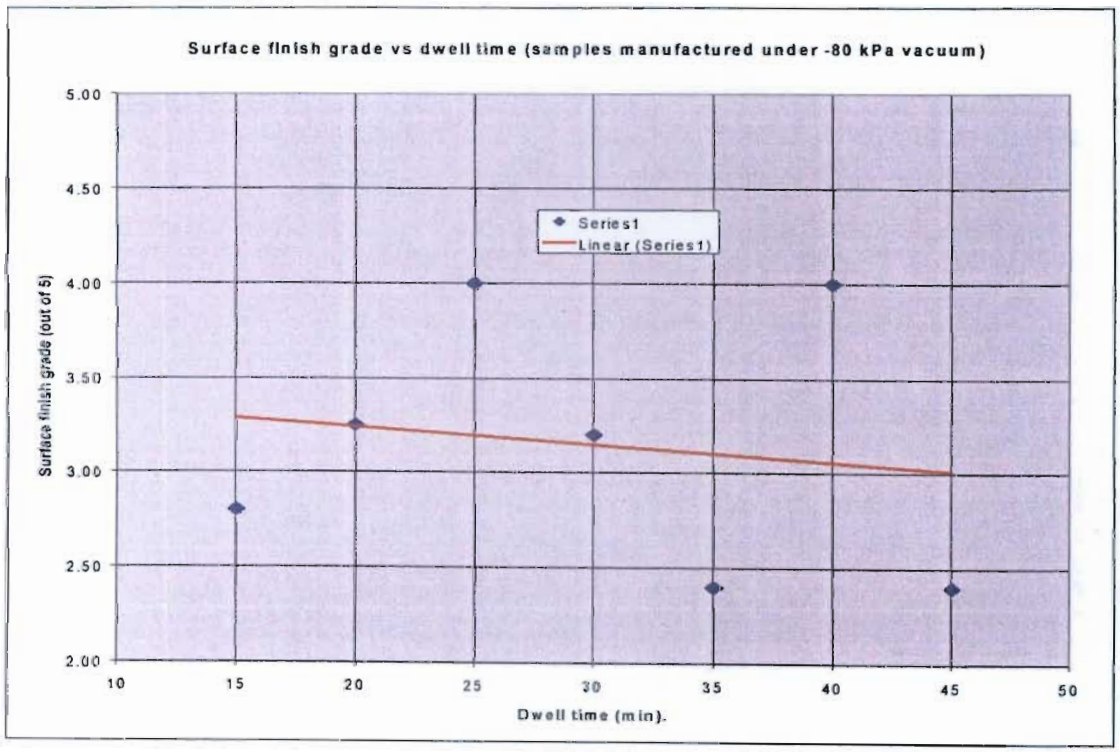

Figure 49 Graph of surface finish vs. dwell time (-80kPa vacuum)

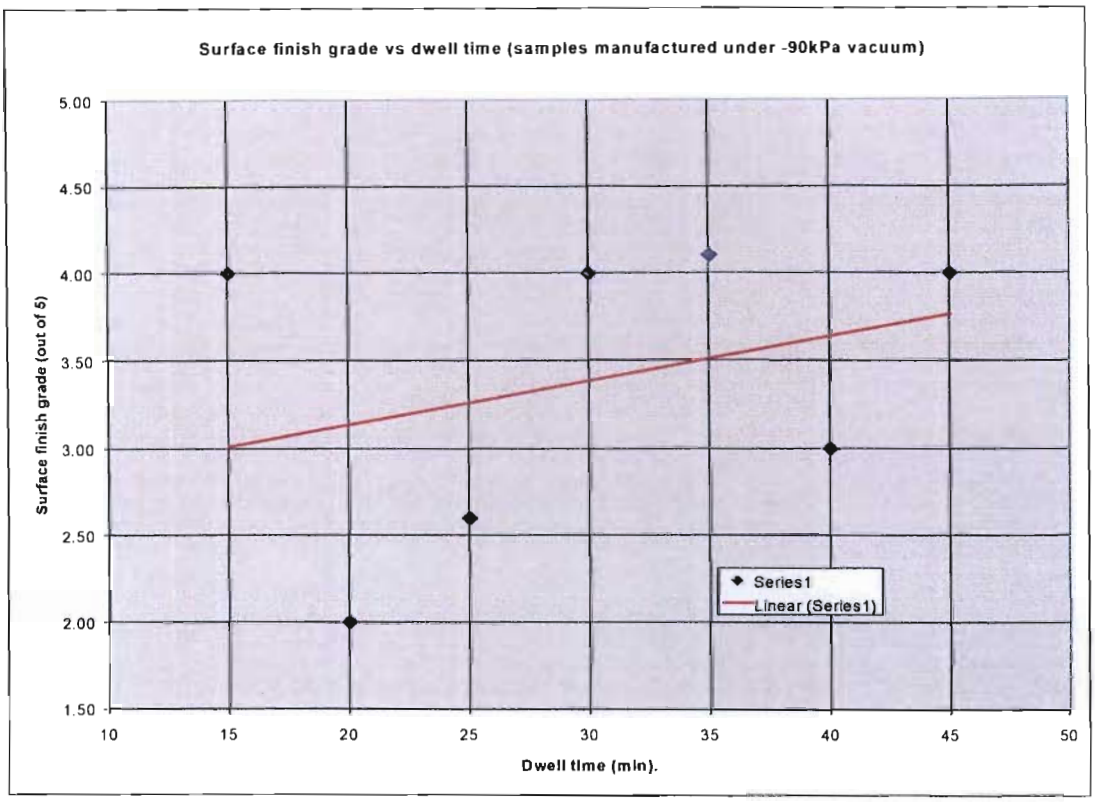

Figure 50 Graph of surface finish vs. dwell time (-90kPa vacuum)

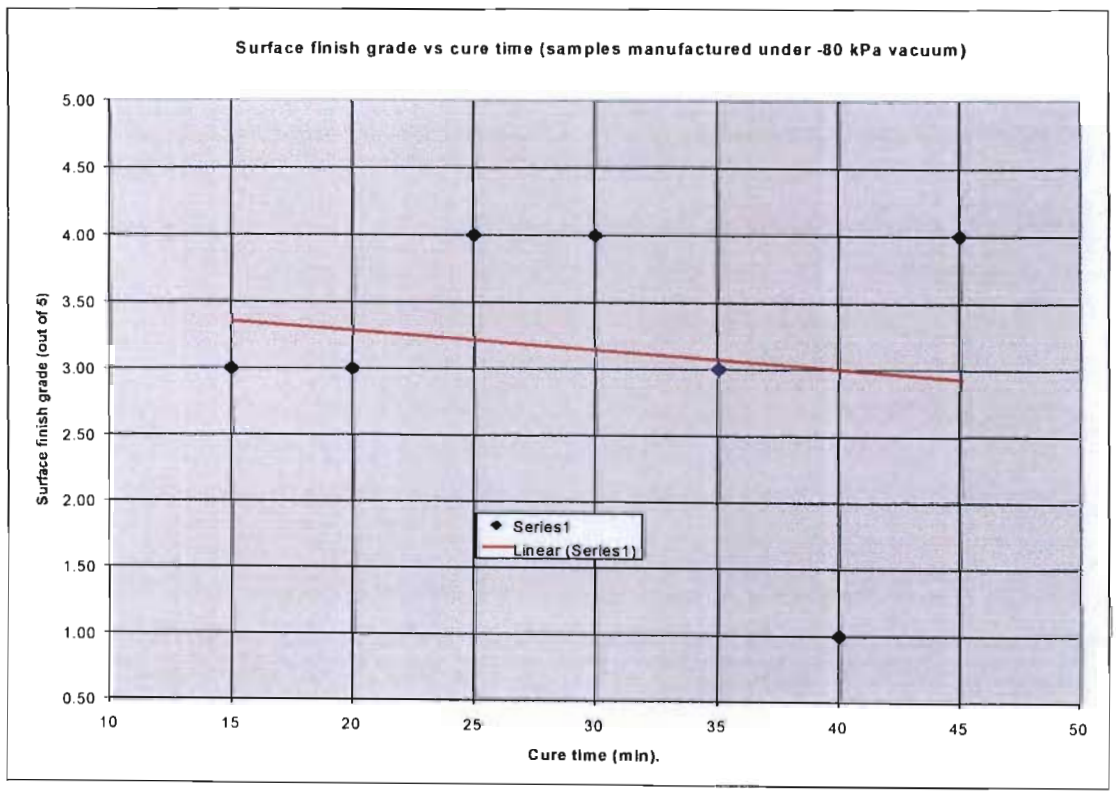

Figure 51 Graph of surface finish vs. cure time (-80kPa vacuum)

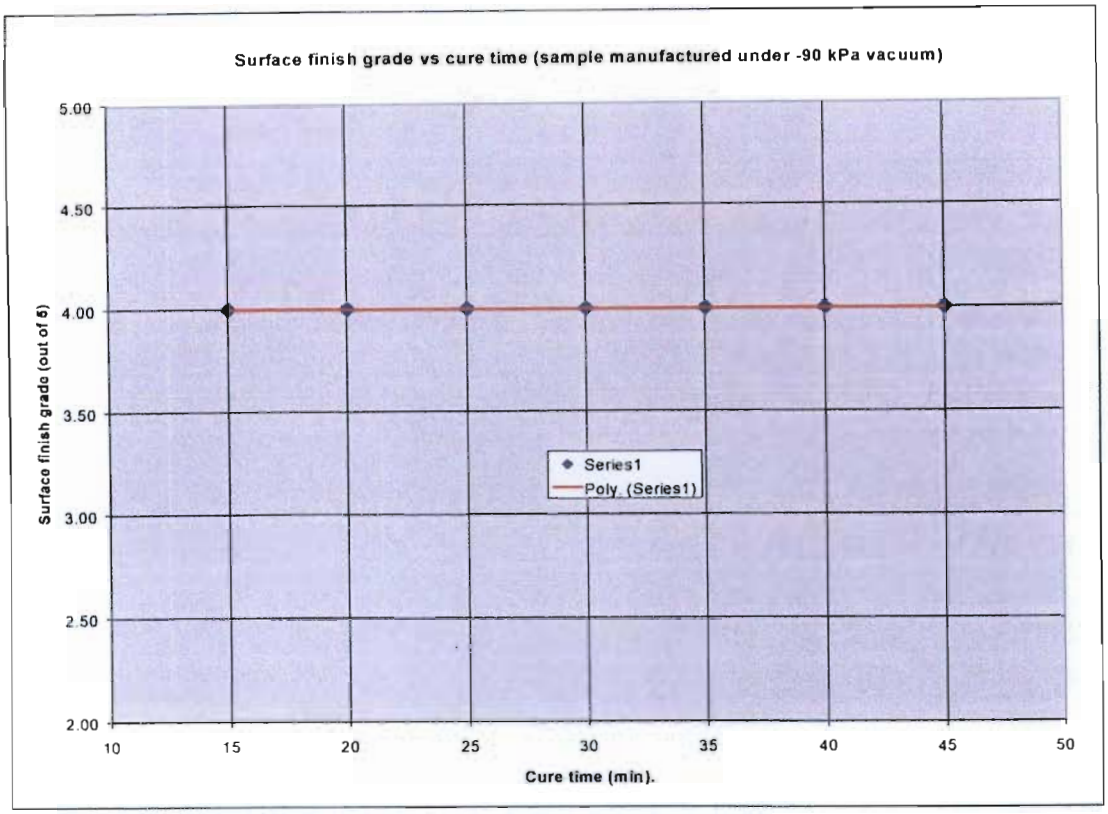

Figure 52 Graph of surface finish vs. cure time (-90kPa vacuum)

5.5.5. Burnout Tests.

A sample was cut from each of the plates used to make the bend and impact test specimens. These samples were sent to Dr Jim Huston at the CSIR for burnout tests, to determine the fibre volume fraction. Each sample was manufactured with the same ratios of masses of resin film and dry glass cloth. This means that the burnout tests will give an indication of the compaction and amount of resin, which is drawn out of the component into the bleeder cloth. Table 4 gives the results obtained by the CSIR, both in mass and volume fraction of glass.

Specimen	Mass fraction of Glass fibre	Volume Fraction of Glass
V11	0.633	0.480
V12	0.621	0.467
V13	0.657	0.506
V14	0.711	0.568
V15	0.683	0.536
V16	0.695	0.550
V17	0.687	0.540
V21	0.700	0.555
V22	0.712	0.570
V23	0.685	0.538
V24	0.698	0.553
V25	0.688	0.541
V26	0.552	0.397
V27	0.705	0.561
V31	0.691	0.545
V32	0.638	0.486
V33	0.673	0.524
V34	0.645	0.493
V35	0.692	0.546
V36	0.670	0.521
V37	0.665	0.515
V42F	0.651	0.500
V43D	0.702	0.558
V43F	0.669	0.520
V44F	0.692	0.546
V45	0.691	0.545
V46	0.684	0.537
V47	0.692	0.546

Table 4 Burnout test results.

Plotting the volume fraction results against the dwell times for the samples tested, gives us an indication of any trends which may exist. Figure 53 below shows the results for the series made under a vacuum of 80 kPa. The 2nd order polynomial trend line shows increasing volume fraction as the length of the dwell is increased. This is the expected result, as the longer the sample is held at the dwell temperature, the greater the compaction and the longer time available for excess resin to be "squeezed" out into the bleeder cloth.

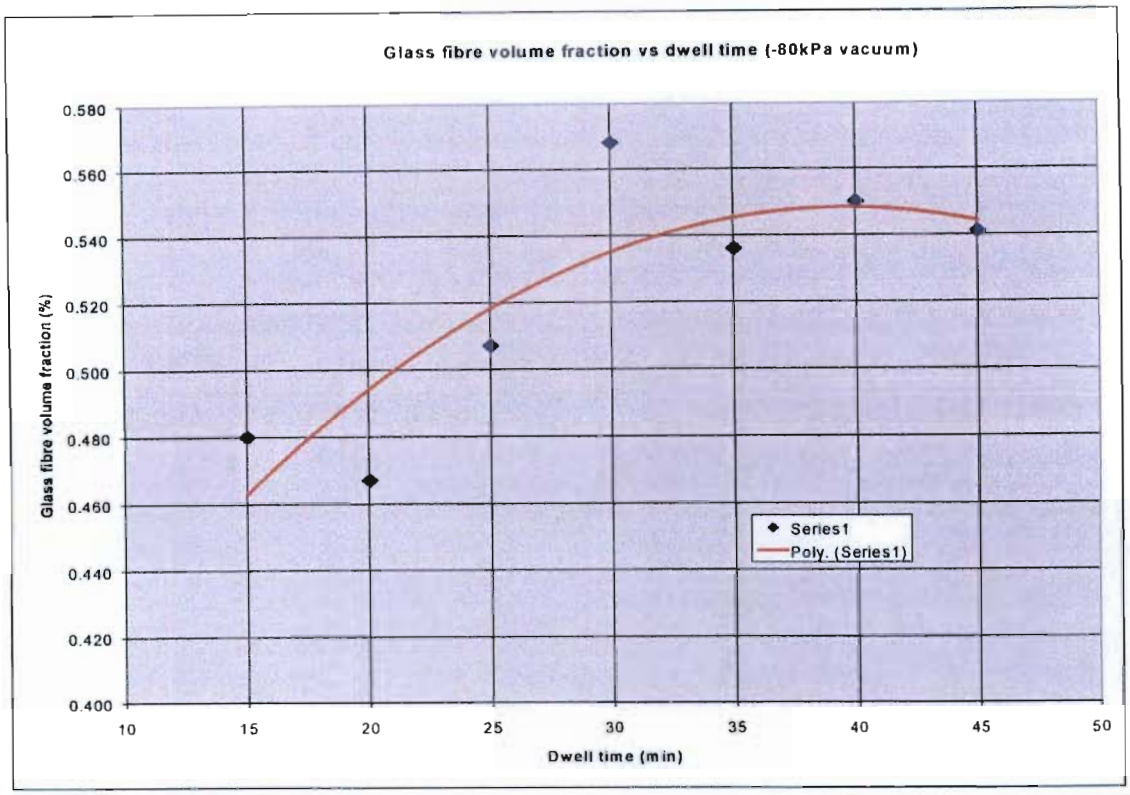

Figure 53 Graph of glass fibre volume fraction vs. dwell time (sample prepared at -80kPa vacuum)

The results for the sample manufactured with a –90kPa vacuum pressure are less clear (Figure 54). The result obtained for sample V26 is most likely an aberration as it does not fit into the trend for this series and is significantly below that of all the burnout tests. The most likely cause is that either the sample was cut from a part of the plate which had been badly laid up, or that a leak in the vacuum bag allowed a continuous stream of air in leading to voids. If this one point is ignored, then the results are fairly constant, around the 55% fibre volume ratio. This correlates with the assumption that most of the seepage (and in most cases full saturation) has occurred before the dwell temperature is reached and especially at higher vacuum pressures. This series had the best results (excluding V26) with sample V22 the best overall with a fibre volume ratio of 57%.

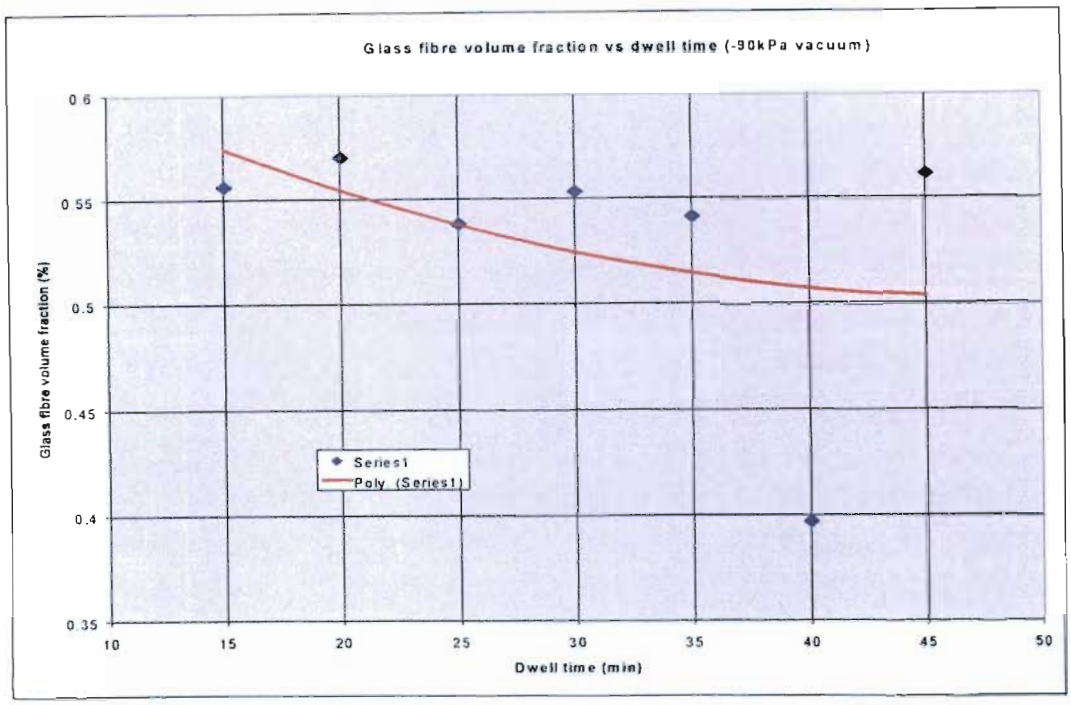

Figure 54 Graph of glass fibre volume fraction vs. dwell time (sample prepared at -90kPa vacuum)

The results from the cure varied samples are rather inconclusive (Figure 55 and Figure 56), the trend-lines suggest that at both –80kPa and –90kPa, the fibre volume drops around the 30 to 35 min cure cycle. It should be noted that these results are in a narrow range and probably within the range of experimental testing. This is particularly visible in the –90kPa graph (Figure 56) with the results all falling within the 53% to 55% range. These results tend to confirm the earlier assumption that the flow has ceased before the cure cycle is reached. This hypothesis is later used in the development of the mathematical model as it allows the model to be simplified as it is only necessary to focus on the ramp to the dwell and then to a lesser extent the dwell stage itself. It should be noted that these samples were all manufactured with single layers of glass mat layer alternatively with the dry Redux film, and this theory may not hold for thick or stitched composites.

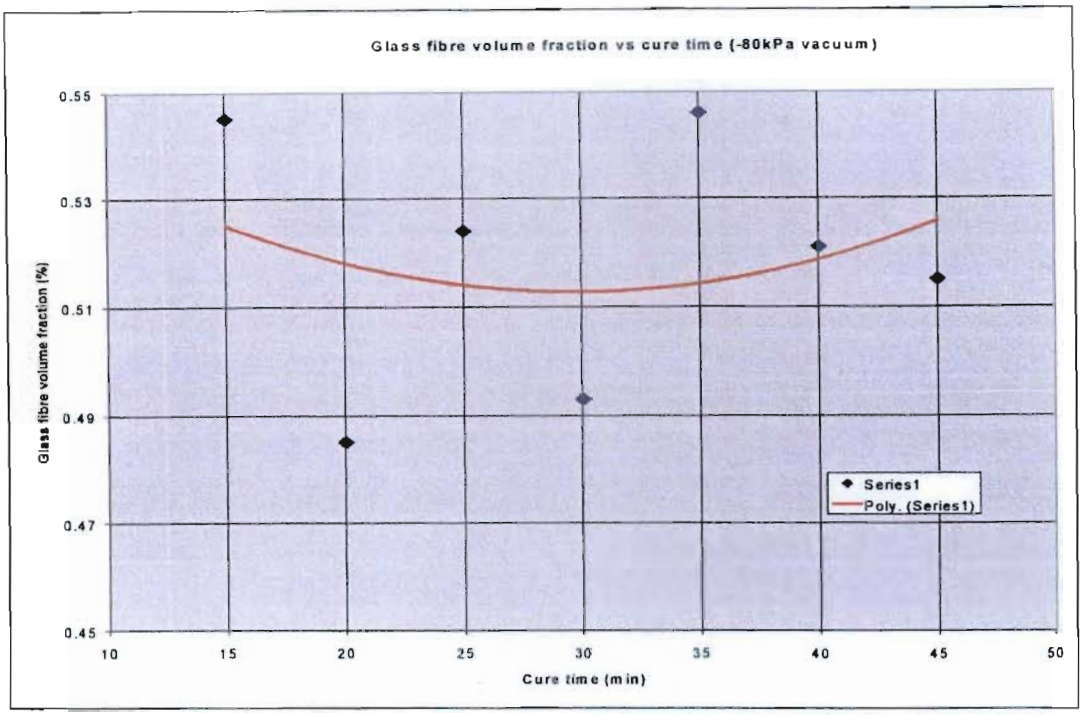

Figure 55 Graph of glass fibre volume fraction vs. cure time (sample prepared at -80kPa vacuum)

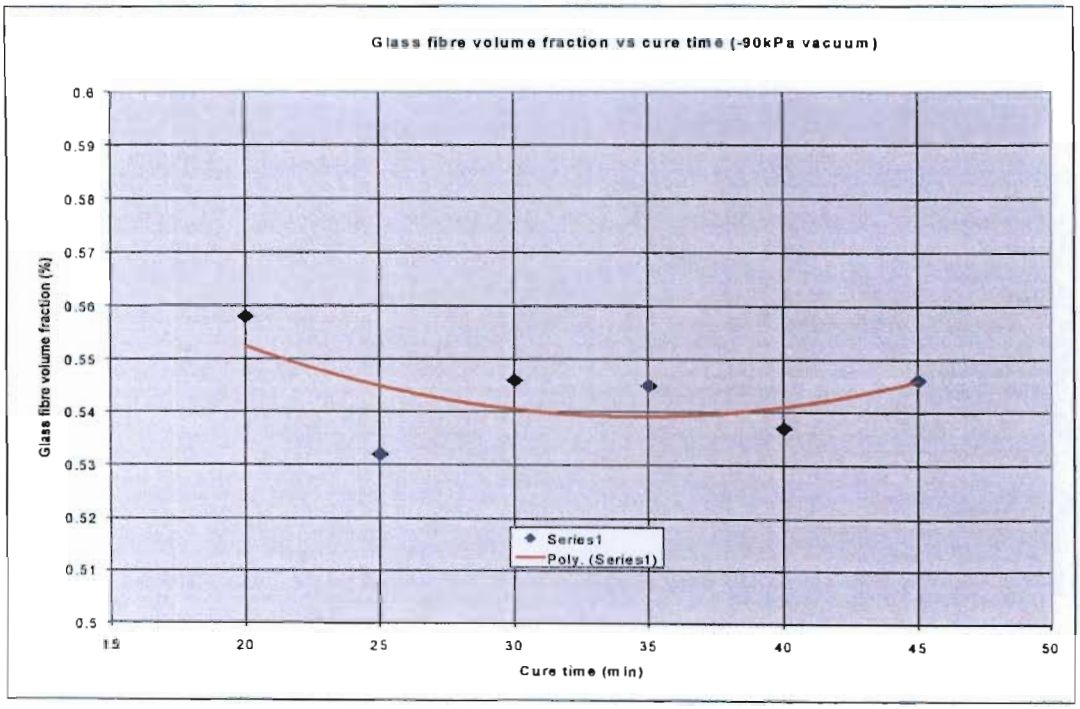

Figure 56 Graph of glass fibre volume fraction vs. cure time (sample prepared at -90kPa vacuum)

5.6. Permeability tests

Fibrous preforms are deformable and may therefore be modelled as anisotropic porous materials. The permeability would not only depend on direction, but on the amount of deformation or compression of the preform. The permeability of the fibrous preform may thus vary during processing due to the changing structure of the lay-up during resin flow. Such changes may be due to thermal expansion of the tooling, the advancing resin front and the applied vacuum pressure. The determination of the permeability is important, as it is a necessary input parameter for the mathematical model used to determine the optimum process parameters.

5.6.1. Measurement of permeability

Loos and MacRae[77] describe two techniques to measure permeability:

i. A steady state technique.

This measures the permeability of a fully saturated preform under constant flow rate conditions, and

ii. An advancing front technique

The permeability is determined by measuring the velocity of the advancing resin front into the dry preform.

Scheidegger[51] recommends the measurement of permeability using any form of Darcy's Law for isotropic permeability measurements. Darcy's Law is then solved for the permeability, knowing the geometry and fluid employed in the test system. The test systems are physically simple and the permeability of a range of materials have been determined. According to Wiggins et al.(1939) referenced in Scheidegger, the permeability range of fibreglass is 2.4×10^{-7} cm^2 to 5.1×10^{-7} cm^2. Permeabilities of any specific material may have a wide range. The value of the permeability measured is likely to be found within that range, clearly for anisotropic materials, permeability has to be measured in different directions.

An attempt was made to determine the steady state permeability of a two-layer laminate of dry glass fabric orientated at 0°/90°, using Darcy's Law. The apparatus used appears in Figure 57 below.

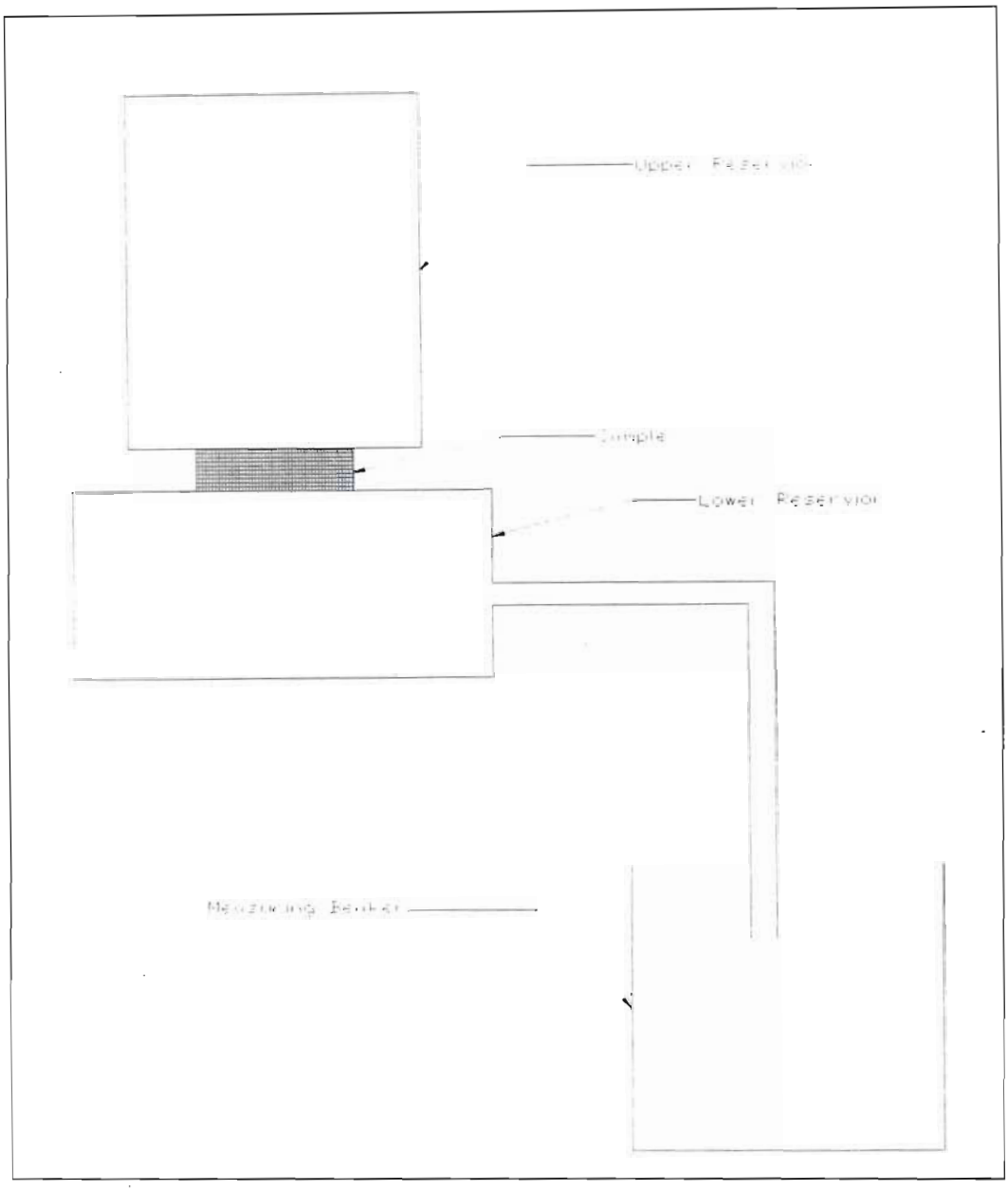

Figure 57 Apparatus used for measuring permeability of glass fibre mat.

5.6.2. Testing procedure

i. The fibre lay-up was wetted to remove air bubbles and then the thickness of the lay-up measured.

ii. The lay-up was placed below the upper reservoir

iii. The lower reservoir was filled with water until it began to overflow.

iv. The upper reservoir was then screwed onto the lower reservoir.

v. The upper reservoir was then filled with water until it began to overflow.

vi. Once all the air was removed by the flowing water, the flow rate of the water into the lower reservoir was measured by recording the time it takes to fill a volume of 200 ml.

vii. The procedure was repeated ten times.

5.6.3. Results of permeability tests

The pressure difference across the lay-up was calculated as follows,

$$\Delta P = \rho g h = 1226.3 \text{ Pa} \qquad (13)$$

where: is the density of water

g is gravitational acceleration

h is the height of water from the top of the upper reservoir to the exit pipe from the lower reservoir.

Using the area of a circle

$$A = \frac{\pi d^2}{4} \qquad (14)$$

the area across which the fluid flows was calculated to be:

$A = 1.017 \times 10^{-3} \text{ m}^2$.

The flow rate Q was calculated by dividing the volume of water (200 ml) by the time it took to fill the 200 ml. beaker. The flow rates of the water through the fibres were thus found to be in the range of 1.436×10^{-5} m^3/s to 1.466×10^{-5} m^3/s.

The values of the fibre lay-up thickness (Δz) varied between 0.95 mm and 1.08 mm.

The permeability of the lay-up was then calculated using Darcy's Law

$$Q = \frac{A}{\mu} k \frac{\Delta P}{\Delta z} \qquad (15)$$

where: k is the specific permeability and μ is the absolute viscosity

Re-arranging for k

$$k = \frac{Q\mu\Delta z}{A\Delta P} \qquad (16)$$

Substituting the values for the respective variables into the above equation yields a range of permeabilities from 1.015 xx10^{-11} m^2 to 1.26 x 10^{-11} m^2 with a mean value of 1.19 x 10^{-11} m^2.

Table 5 lists the steady state permeability for the samples tested.

Sample No.	Specific Permeability [m^2]
1	1.01497 × 10^{-11}
2	1.15101 × 10^{-11}
3	1.15751 × 10^{-11}
4	1.18621 × 10^{-11}
5	1.19728 × 10^{-11}
6	1.20593 × 10^{-11}
7	1.23994 × 10^{-11}
8	1.24625 × 10^{-11}
9	1.24991 × 10^{-11}
10	1.2596 × 10^{-11}

Table 5 Specific Permeability as measured for a 0°/ 90° lay-up of glass fibre

5.6.4. Discussion

Scheidegger[51] makes reference to the work done by Wiggins et al. in which the permeability of fibreglass was found to be in the range 2.4 x 10^{-11} m^2 to 5.1 x 10^{-11} m^2. The values obtained during testing are approximately half the minimum value of permeability obtained by Wiggins et al., however there is no reference to the lay-up of the fibres or the type of glass mat used.

Possible errors due to entrapped air were minimised by only recording the flow rate once all visible air bubbles had passed out of the woven material. Errors due to the deformation of the fibres while laying up the fibres were unfortunately unavoidable given the equipment available. The effect of change in permeability due to the relative movement of the fibres in the woven mat was not determined.

In conclusion, the mean permeability of the two unidirectional fibre lay-up orientated at 0°/90° was found to be 1.19×10^{-11} m^2 , assuming that the effect of fibre deformation was minimal.

6. Mathematical Model

6.1. Introduction

A mathematical model has been developed to simulate the flow of a viscous liquid (Resin) through a porous medium, (Woven reinforcement). This allows an understanding of the effect of various process parameters on the pressure distribution and resulting stresses. This model makes use of the Carman-Kozeny equation to define the permeability of the woven material, and a non-linear equation of filtration to determine the pressure distribution during the infusion process. In addition, the viscosity is assumed to be temperature and time dependent, and is defined by an exponential equation.

Void formation in resin during infusion and curing is a significant problem in most RFI processes. Voids can form by either a homogenous or heterogeneous nucleation process. Mathematical descriptions of both of these nucleation models have been developed to describe the void formation during the RFI moulding method.

6.2. Fracture of Liquids.

If a liquid is subjected to tension, i.e. a vacuum pressure, it is possible for bubbles to form homogeneously, by the process of cavitation. This is known as fracture of a liquid. During the vacuum infusion of resin, this process can lead to bubbles forming in the resin, which remain after curing, becoming voids in the final composite product. These voids adversely affect the mechanical properties of the product and the process should be optimised to minimise the formation of these bubbles. Fisher [11] showed that the rate of nucleation, I_V of these bubbles is given by the following equation

$$I_v = \frac{N_A kT}{V_M h} \exp\left[-\left(Q + \frac{16\pi\gamma_{LV}^3}{3(P - p_{vb})^2} \right) \Big/ kT \right] \qquad (17)$$

where N_A is Avagadro's number, k is Boltzman's constant, h is Planck's constant, V_M is the molar volume of the liquid, Q is the activation energy for transport across the liquid / vapour interface, T is the temperature in Kelvin, γ_{LV} is the liquid vapour interface energy, p_{vb} is the vapour pressure in the bubble and P is the stress in the liquid. This stress is equal in magnitude, but opposite in sign to the pressure, thus P is positive when the liquid is in tension, i.e. under a vacuum pressure. It can be seen from this equation that the nucleation rate is significantly dependent on P, allowing the fracture pressure to be well defined (see Figure 58). This equation can be simplified by noting that cavitation occurs at such high tensions that $P >> p_{vb}$, and hence the vapour pressure term can be neglected. In addition, the fracture pressure is not very dependent on Q, and this term can also be ignored. If a minimum detectable nucleation rate of $1 \times 10^6 m^{-3} s^{-1}$ is assumed, the fracture stress can be determined accurately as

$$P^* \approx \sqrt{\frac{16\pi\gamma_{LV}^3}{3kT \ln\left(10^{-6} N_A kT / V_M h\right)}} \qquad (18)$$

This can be further simplified by noting that the logarithmic term does not vary significantly between different liquids, giving us

$$P^*(GPa) = 19.8\gamma_{LV}^{3/2} / T^{1/2} \qquad (19)$$

where γ_{LV} is in Nm and T in Kelvin. This gives us the corresponding critical size of the radius for the bubbles, i.e. bubbles larger than r^* will grow, while smaller ones will shrink and collapse, where

$$r^* = \frac{2\gamma_{LV}}{P^*} \approx \sqrt{\frac{3kT\ln\left(10^{-6} N_A\, kT/V_M h\right)}{4\pi\gamma_{LV}}} \qquad (20)$$

Simplifying,

$$r^*(nm) = 0.16\sqrt{T/\gamma_{LV}} \qquad (21)$$

Using equation (13) the expected homogeneous nucleation can be calculated. Figure 58 shows the results for a temperature of 400K in an epoxy resin. Figure 59 shows the dependencies for P^* and r^* at typical RFI process temperatures. It can be clearly seen that cavitation is more likely to occur at higher temperatures. Q/k is a ratio of the activation energy for evaporation against Boltzman's constant. The lower the activation energy, the greater the chance of cavitation and homogeneous nucleation.

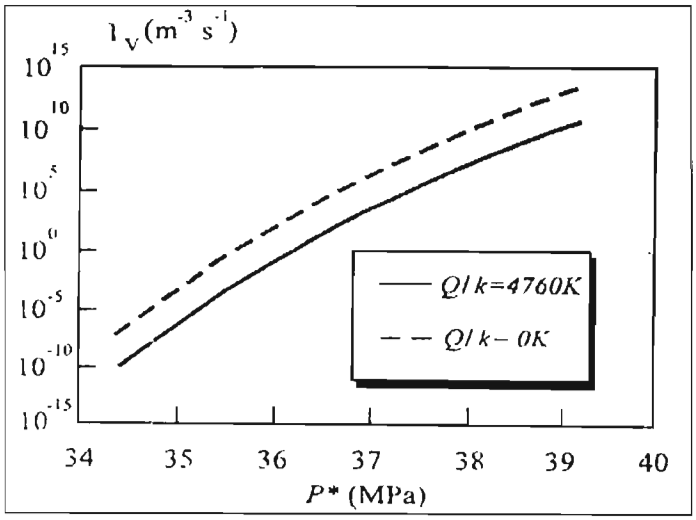

Figure 58 Homogeneous nucleation rate at T=400K for epoxy resin. (Using equation (10))

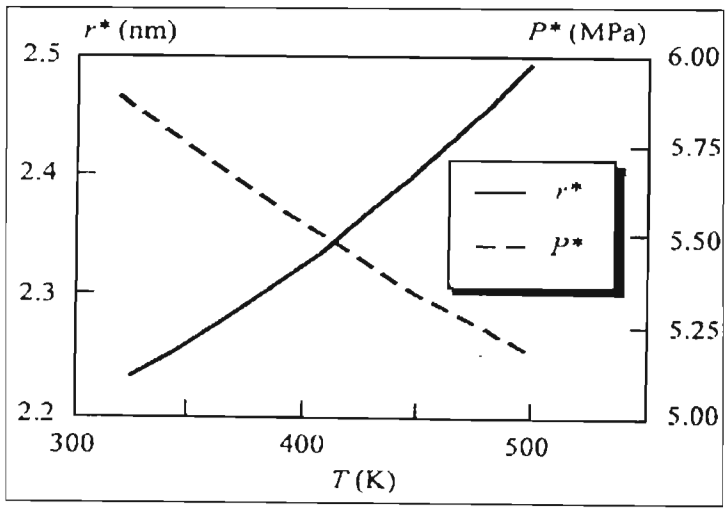

Figure 59 Effect of temperature on r^* and P^* for epoxy resin.

6.3. Pressure in the resin during the infusion process.

If we consider the resin infusion through individual pores of a rigid network, (see Figure 60), initially no resin flux is occurring (Figure 60a), the penetration is then initiated. This caused a reduction in the tension P of the liquid, which is governed according to the Gibbs-Thompson equation

$$P = -(RT/V_M)\ln(p_V/p_o) \qquad (22)$$

where R is the ideal gas constant, p_V is the partial pressure of the vapour, and p_0 is the partial pressure once equilibrium has been reached between the liquid and vapour phases.

If the contact angle θ between the resin and the pores of the network is less than 90°, fingering menisci start to form in the mouths of the pores. This is the initiation phase of the resin propagating through the network (See Figure 60b).

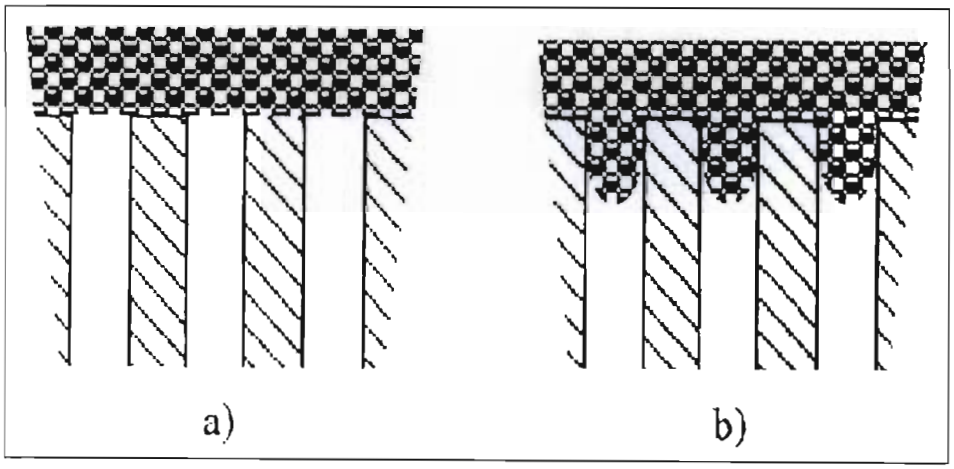

Figure 60 Schematic of a woven material with uniform pores: (a) before penetration of the liquid; (b) after fingering has started.

Laplace's equation links the radius of these menisci r_m to the tension P in the liquid resin

$$P = -2\gamma_{LV}/r_m \qquad (23)$$

The flow j_r of the resin through the woven preform material obeys Darcy's Law

$$j_r = \frac{D}{\eta}\nabla P \tag{24}$$

where D is the permeability of the woven material, η is the resin viscosity, and ∇P is the gradient of the pressure between the solid and liquid phases. This is modelled mathematically as a variation of Stephan's problem. In order to solve this as a moving boundary problem, we require an additional equation describing the resin flux. If we denote the position of the interface as h(t), we can use the following equation for the pressure gradient

$$\nabla P = -\frac{\eta\left(1 + C_S(0)P_C/K_W - C_S(0)\right)}{D}\frac{dh(t)}{dt} \tag{25}$$

where K_W is the bulk modulus of the woven material, $C_S(0)$ is the concentration of the solid phase at t=0, and P_C is the critical pressure at the resin front. These two equations can then be combined to give us an equation describing the pressure field in the resin

$$\frac{\partial P(h,t)}{\partial t} - \frac{K_L}{\eta K_W}\nabla\cdot\left(D\nabla P(h,t)\right) + \frac{D}{\eta}(\nabla P)^2 = 0 \tag{26}$$

It should be noted that the permeability D of the woven preform material will vary as the concentration of the solid C_S changes, this has been taken into account in equation (20). Furthermore it is assumed that the bulk modulus of the liquid is essentially less than that of the solid. The solution of this equation must satisfy the following boundary condition

$$\frac{D}{\eta}\nabla P(0,t) = j_{EXT} \tag{27}$$

where j_{EXT} is the external flux.

6.4. Method of Solution.

The numerical procedure used is a step process. The resin front is initially located on top of the woven reinforcement, and a boundary condition of constant pressure at a point is defined. A Flow Analysis Network technique is then used to calculate the free surface location at each time step. The free surface boundary conditions have to be reset after each time step to simulate the moving boundary, and the governing equations are solved using a Finite Element Method (FEM) to determine the new pressure values. The procedure is repeated, finding the pressure solutions, until the woven material is completely saturated. Figure 61 shows a flow chart of this procedure.

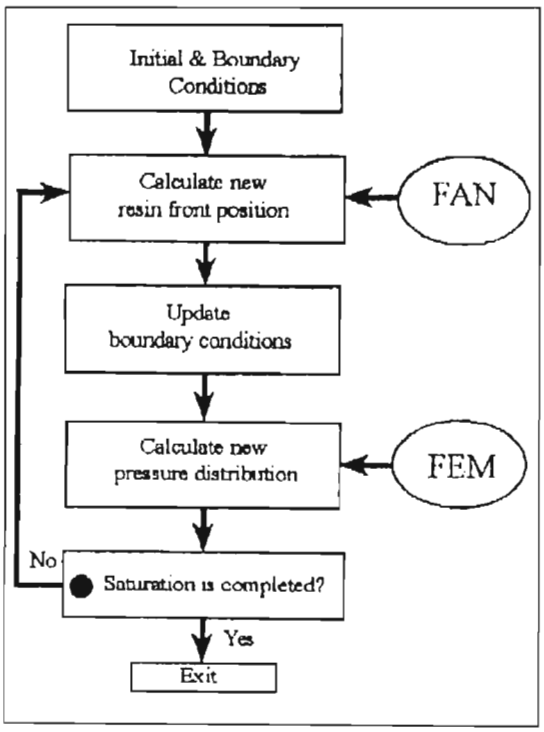

Figure 61 Flow chart of numerical algorithm

6.5. Numerical Results

6.5.1. Assumptions

A number of assumptions were made to simplify the development of the model, and its numerical analysis.

- The dwell and cure temperatures are functions of the material system. Hence the primary parameter requiring optimisation is the applied vacuum pressure. The dry resin film (REDUX 312 from HEXCEL) has a minimum viscosity at approximately 80°C, and cross-linking should not begin below 90°C. The manufacturer recommends a cure cycle of 120°C for 30 minutes.

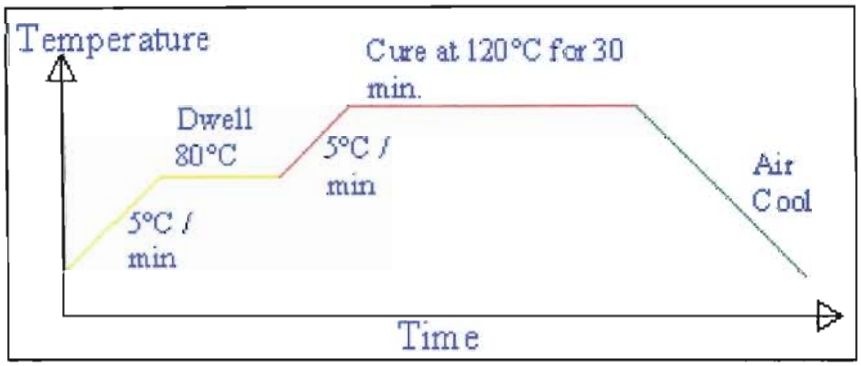

Figure 62 Schematic of the manufacturers recommended heating profile for REDUX 312 film adhesive

- Complete saturation has occurred before cure begins. As the lay-up consists of alternate layers of reinforcement material and dry resin, the resin will not have to travel a far distance to saturate the reinforcement, i.e. the maximum distance will be the thickness of one layer of reinforcement; approximately 0.5 mm. (See Figure 63). Initially the model was designed to handle only a single layer of resin above a single layer of reinforcement.

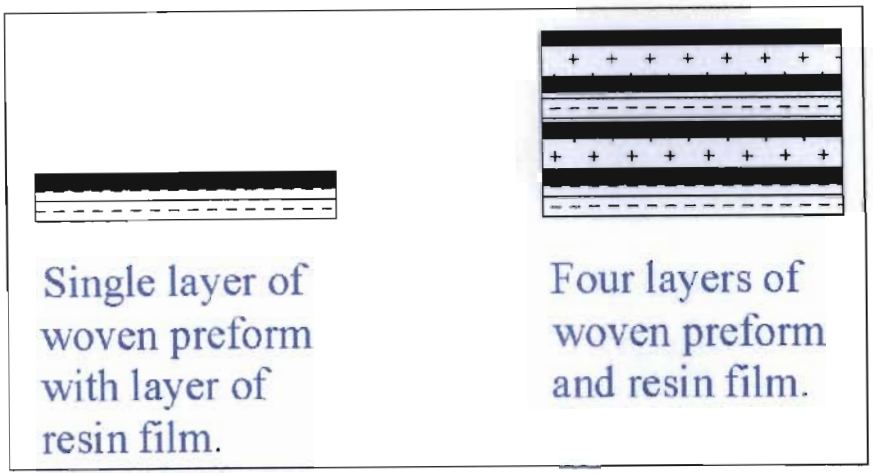

Figure 63 Lay-up for single and multi-layered components.

- Physical testing has suggested that this wetting out has occurred by the time the mould and component have reached the manufacturer's dwell temperature of 80°C. As a result, the model will not attempt to optimise the cure of the matrix material portion of the cycle, these parameters being set by the manufacturer, and assumed to not having an effect on the void formation. However as the heating is a two stage process, (as can be seen in Figure 62 above), the two stages can be considered separately.

- The flow of resin was initially studied in 1-D only, this was to simplify the formulation of the problem and can be justified for our case. If we assume that the lay-up of alternate layers of dry film and woven mat are used as described above then the mould geometry will not have a significant effect on the distances the resin will need to flow to saturate the preform material. In addition the thickness of the woven materials used does not vary significantly in any planar direction. It should be noted that this will not be the case if very "thick" preform materials or "stitched" woven preforms are used.

- By modelling the process in only one dimension (through the thickness), we ignore the edge effects on the component. Many mould designs, which are used in the RFI process, constrain the edges of the preform, and hence no flow should occur out of the reinforcement. Furthermore residual stresses are negligible once one considers a distance of more than the thickness of one layer from the edge.

As the viscosity of the resin is temperature dependent, the following relationship was used

$$\eta(T) = \eta_0 \exp\left(\frac{\varsigma}{T} + \kappa\alpha\right) \tag{28}$$

where μ, ς, and κ are experimentally determined constants; α denotes the degree of cure and T the absolute temperature at which the infusion process occurs. For the initial research, the data obtained by Kang et al.[52] was used: α=0.2, κ=26.89, and ς=1034.

This initial dependency was replaced once the rheology data for Redux 312 was obtained from Hexcel. The data was plotted and a 4th-order polynomial was fitted (see Appendix F)

$$\log_{10}(\eta(T)) = 0.002(T^4) - 0.8292(T^3) + 127.51(T^2) - 8810.2(T) + 231512 \tag{29}$$

Despite the fact that the data given only applied to the 70°C to 125°C range, using this equation, it was possible to extrapolate the viscosity readings to lower temperatures. The results are shown in Figure 64 where 1 Poise is equal to 0.1 Pa.s.

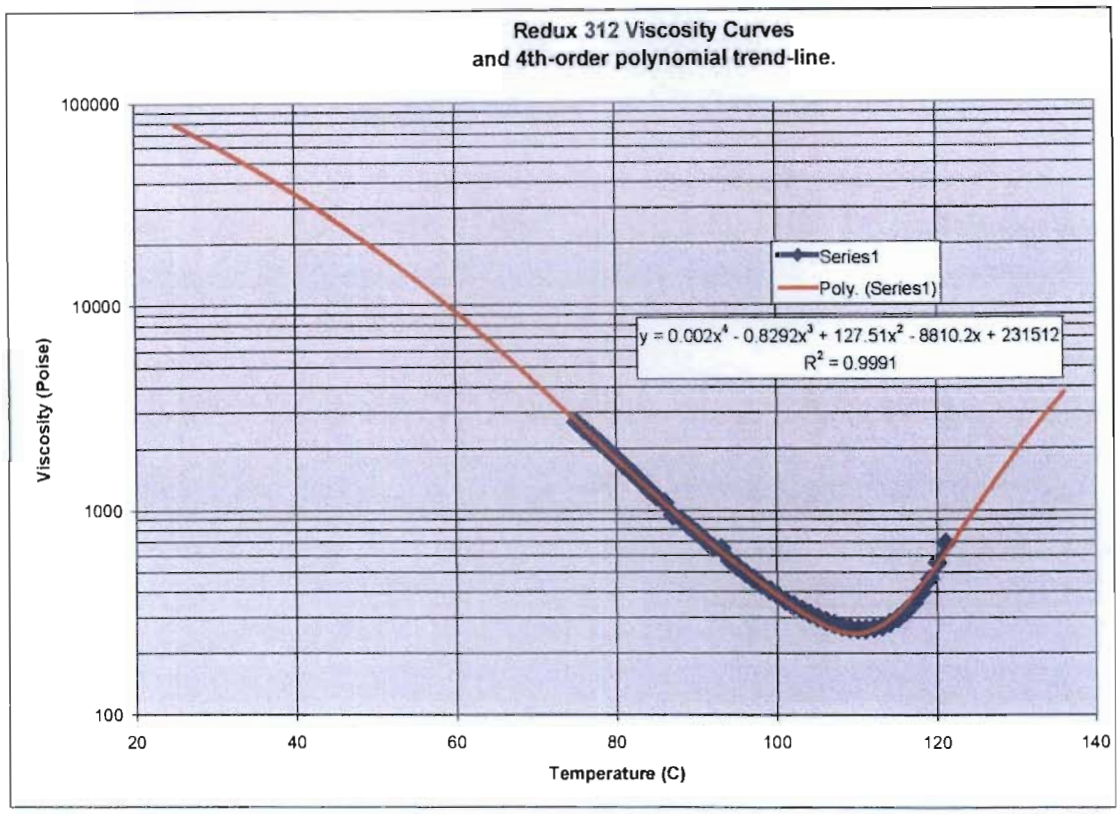

Figure 64 Graph of viscosity for Redux 312, with a 4th-order polynomial trend-line (projected back to 30C and forward to 135C)

At the preliminary stage in the research, external pressure was not considered. This simplified the analysis, however it was taken into account in later analyses by the use of superposition. The following mechanical properties were used:

Initial viscosity:	$\eta_0 = 1.0 \times 10^4$ Pa.s
Critical pressure:	$P_C = 280$ MPa
Compressibility modulus of resin:	$K_L = 130$ MPa
Initial volume fraction of fibres:	$C_s(0) = 0.5$
Permeability of the woven material:	$D = 1.19 \times 10^{-11}$ m^2.
Bulk modulus of the woven preform:	$K_W = 4.2$ GPa
Poisson's ratio of woven material:	$\nu = 0.25$

6.5.2. Simulation.

The viscosity of the resin will obviously vary with time, and hence is described in the following method:

$$T = 2t + 30° \tag{30}$$

and hence equation (22) becomes:

$$\eta(t) = 10\text{^}[\ 0.002\ (2t + 30°)^4 - 0.8292\ (2t + 30°)^3 + 127.51\ (2t + 30°)^2$$
$$- 8810.2\ (2t + 30°) + 231512]\ \text{Poise} \qquad (31)$$

This was done in order not to introduce another variable and was simple to do, as the dry resin film used in the process requires a smooth linear increase in temperature. A rate of 2°C / min was chosen here, but it can easily be varied within the program.

The Darcy's law equations can be described in the following format

$$\frac{\partial}{\partial x}(P) = -j\frac{\eta}{D} \qquad (32)$$

for the 1- D case and

$$\frac{\partial}{\partial x}\left[-\frac{\partial}{\partial x}(P)\bullet\frac{D}{\eta} - \frac{\partial}{\partial y}(P)\bullet\frac{D}{\eta}\right] + \frac{\partial}{\partial y}\left[-\frac{\partial}{\partial x}(P)\bullet\frac{D}{\eta} - \frac{\partial}{\partial y}(P)\bullet\frac{D}{\eta}\right] = 0 \qquad (33)$$

for the 2-D case.

These equations can then be solved for a region defined by the necessary boundary conditions. In the 1-D case, a triangular region is described, the base representing time from 0 to t_f. The vertical axis represents the thickness of the reinforcement to be infused. (see Figures 65, 66 and 67, and Appendix E, Flux2.pde).

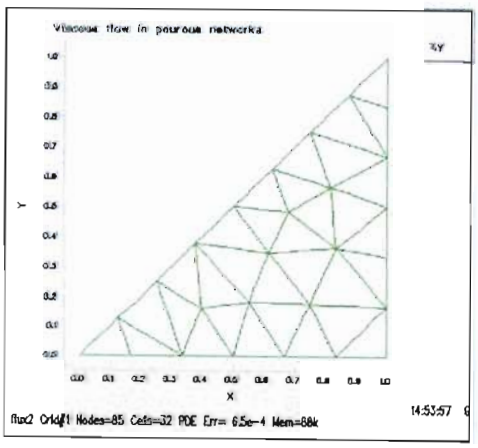

Figure 65 Plot of mesh for 1-D case

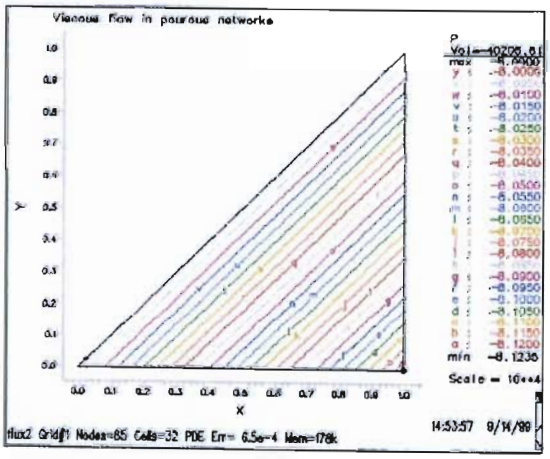

Figure 66 Plot of pressure field for 1-D case

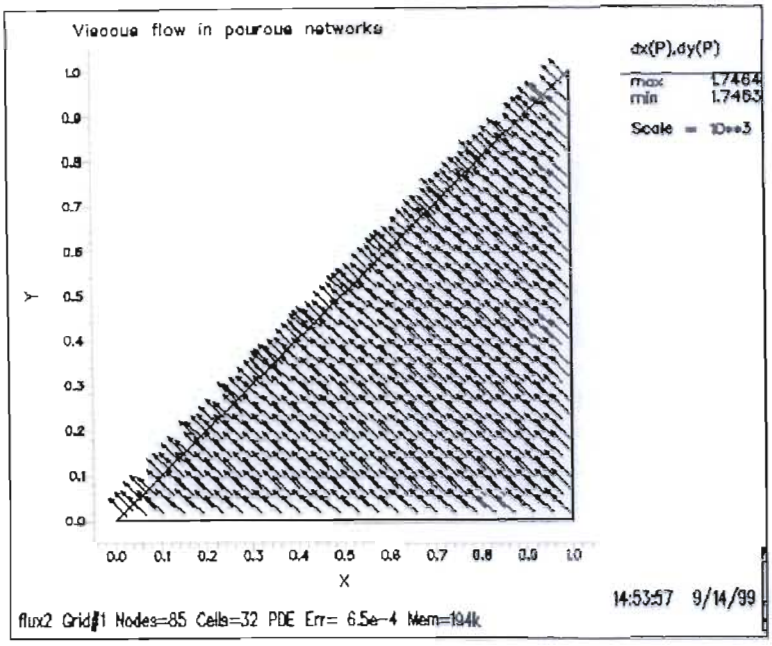

Figure 67 Vector plot of pressure field for 1-D case

In the case of the 2-D simulation, two differing regions were described. Initially a single layer of reinforcement under a layer of resin was modelled (Figure 68, 69 and 70, and Appendix E flux4.pde) and later the case of reinforcement layers on either side of a single layer of resin, i.e. resin flowing into both reinforcement layers (Figure 71, 72, 73, 74, and 75and Appendix E flux6.pde). The 2-D case is solved in a step-wise fashion and hence each plot represents the flow conditions at a given instant in time.

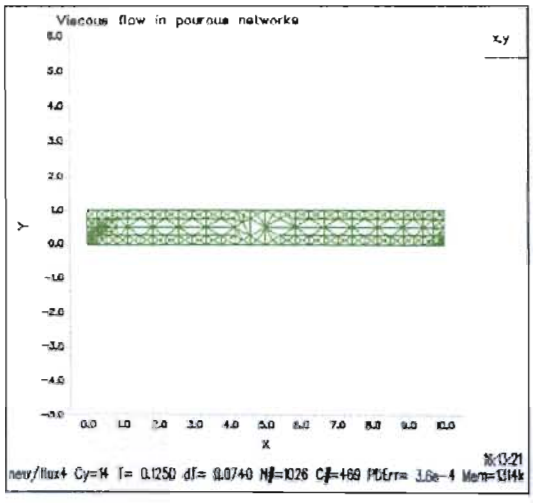

Figure 68 Plot of mesh for first 2-D case

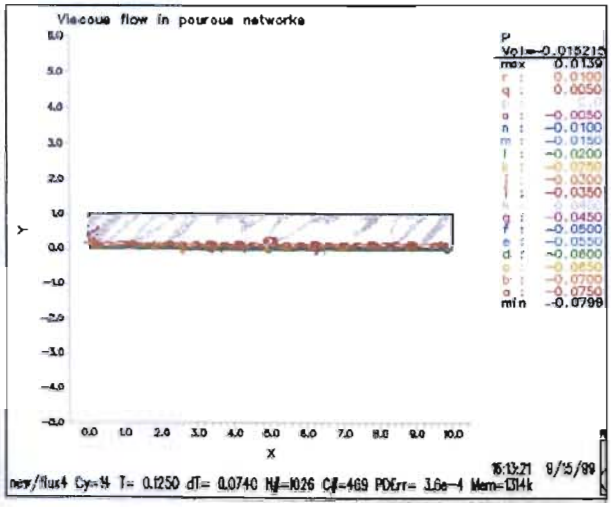

Figure 69 Plot of pressure field in preform at $t=t_f/8$

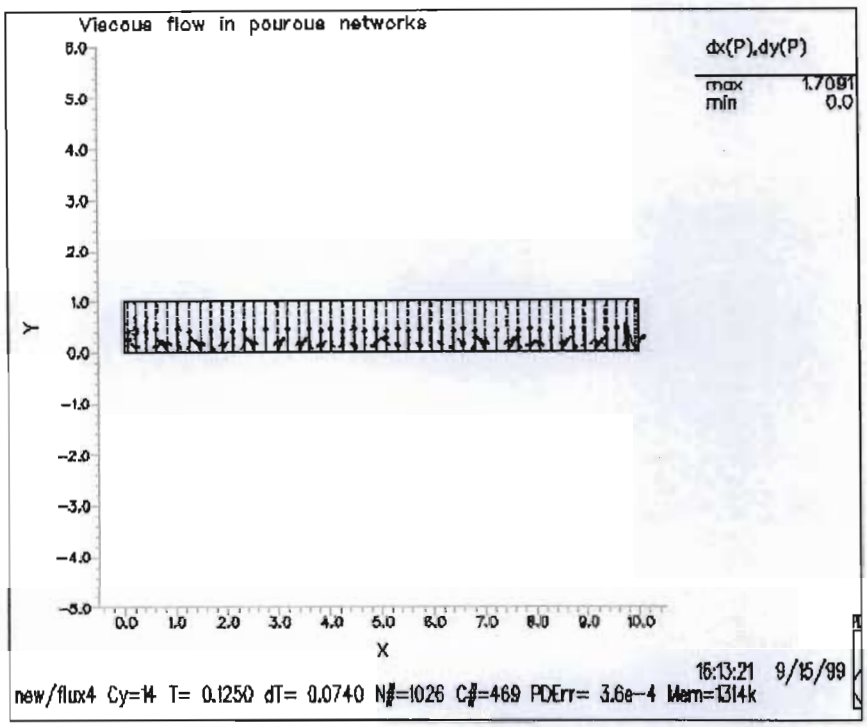

Figure 70 Vector plot of pressure field for first 2-D case at $t=t_f/8$

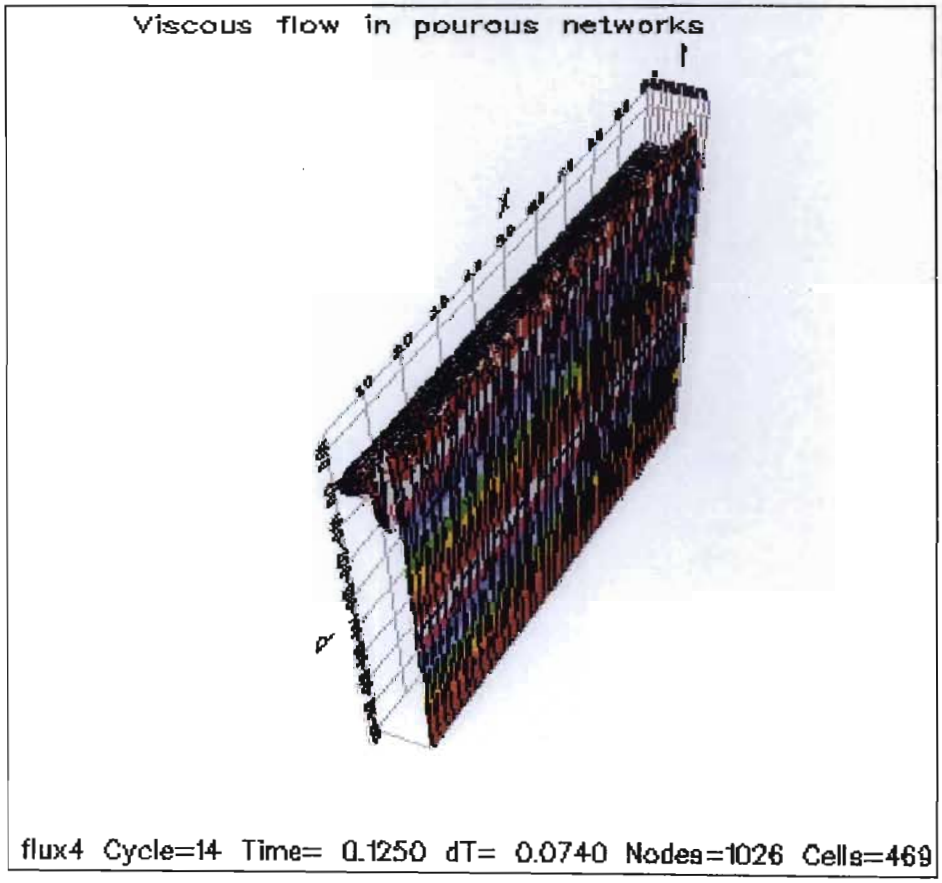

Figure 71 Surface plot of pressure field for first 2-D case at $t=t_f/8$

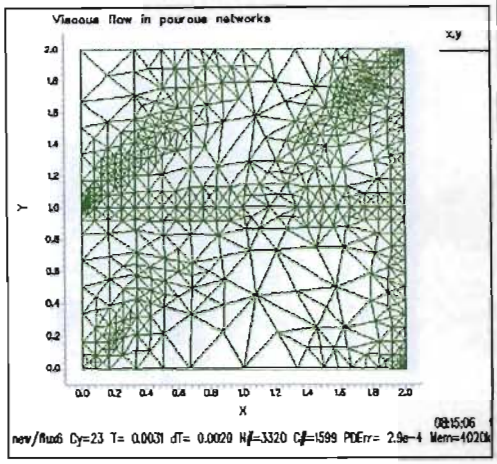

Figure 72 Plot of mesh for second case 2-D model

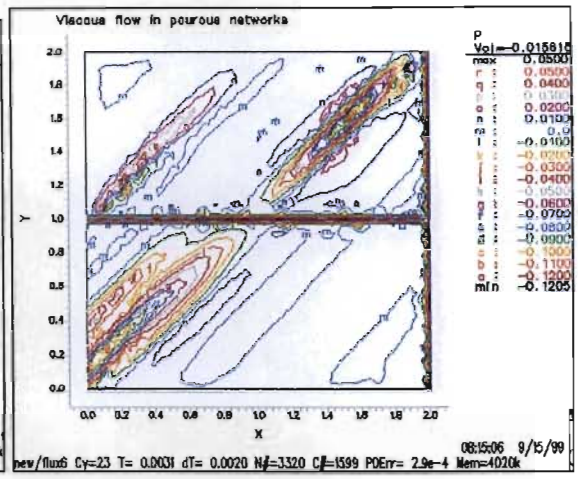

Figure 73 Plot of pressure field in preform at t=tf/12

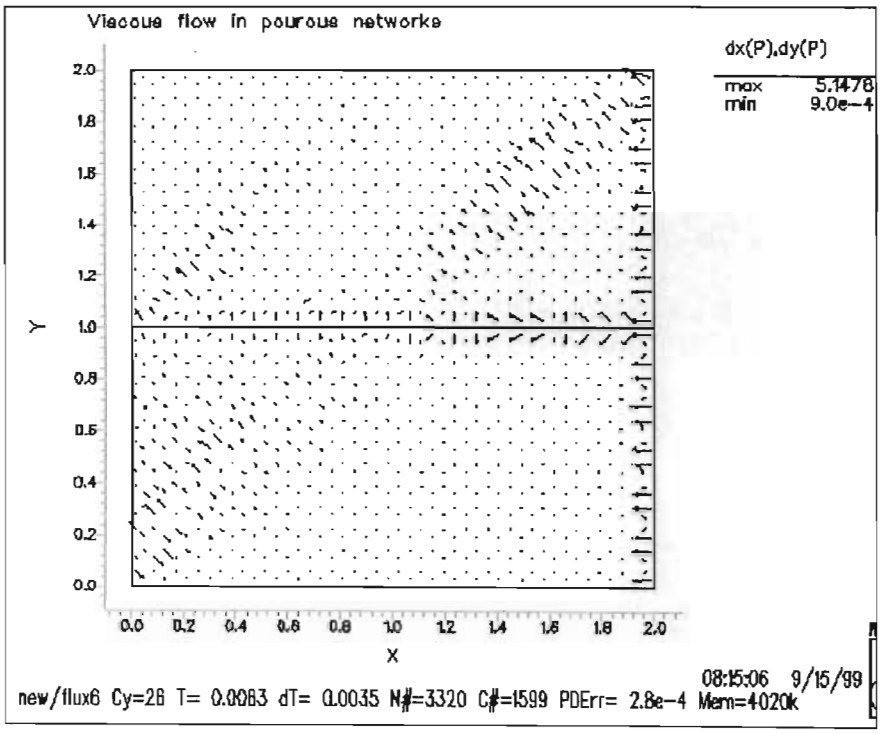

Figure 74 Vector plot of pressure field for second 2-D case at t=3tf/12

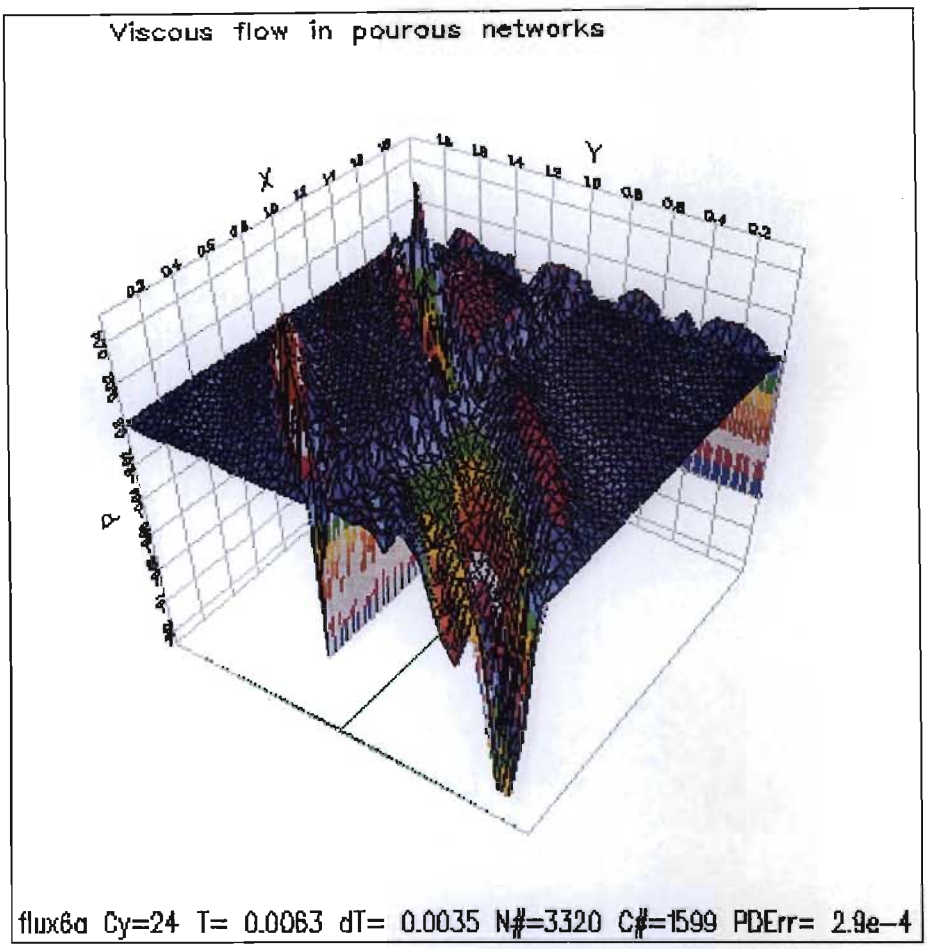

Figure 75 Surface plot of pressure field for second 2-D case at t=3tf/12

6.5.3. Results

The pressure distribution along the plate thickness at different times and for various temperatures is shown in Figure 76. The times are relative to t_f which is the time at which the preform is completely saturated.

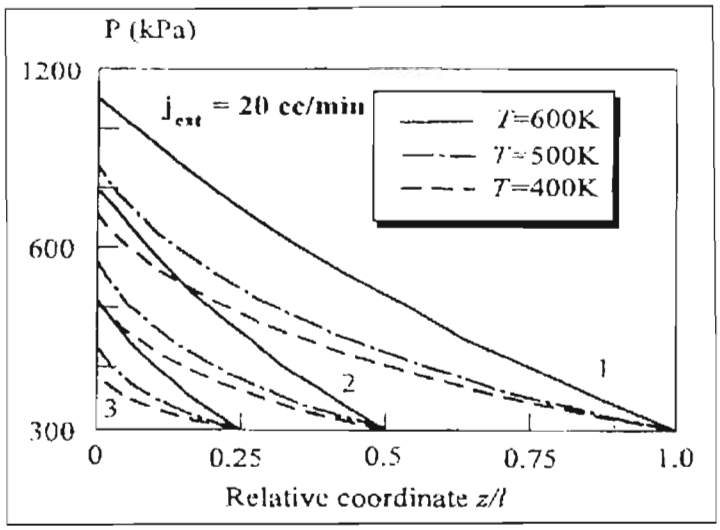

Figure 76 Pressure distribution through the preform thickness 1:t=t_f, 2:t=0.5t_f, 3:t=0.25t_f

The resin film infusion process uses heat to melt and cure the resin, these elevated temperatures, have two effects; firstly, the pressure in the resin drops as a result of the lowered viscosity, and secondly, the cavitation pressure P^* is reduced as the resin gains more molecular energy. The first effect is beneficial, whereas the second is detrimental to void creation. In order to optimise the temperature process, a minimax problem will have to be solved. This optimum profile will need to minimise the working vacuum pressure P and maximise the cavitation pressure P^*. There are two significant parameters in this problem, the pressure field, and thickness of the saturated zone. By choosing to maximise the relation P^*/P, the optimum profile can be determined. This profile is shown below in Figure 77 (A value of $\gamma_{LV} = 3 \times 10^{-2}$ Nm for the liquid vapour interface energy was used).

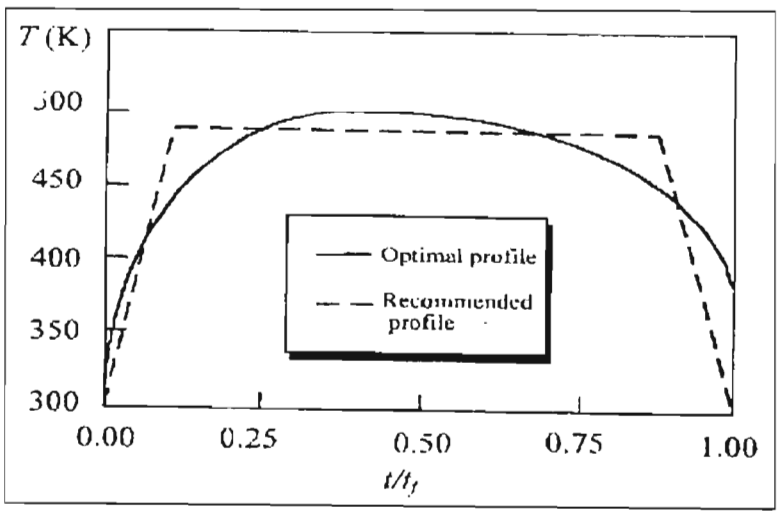

Figure 77 Optimum temperature profile for epoxy resin RFI process

-

The results above do not take the cure of the resin material into account, and clearly a complex curve such as this would not be practical. The dotted line reflects a simplified process, which could be programmed into an oven controller. This profile indicates a profile, which should minimise the void formation during the RFI manufacturing process. This will ensure a component without defects, which could affect the strength properties.

7. Conclusions

Resin Film Infusion Moulding is a relatively new process, and there is not much data on the optimum process parameters. The flow of the resin during this method is similar to that used in vacuum infusion moulding and RTM. Literature in these fields was studied in order to provide a starting point for this research, including the material systems, mathematical modelling of flow, and environmental concerns. The literature survey highlighted the need to accurately model this flow, so that the processes by which the preform is wetted out could be identified and studied. The main factors affecting product quality were identified as void formation and resin dry areas. Thus careful attention was given to the modelling of the flow of resin through the fibrous preform and the mechanisms of void formation. These studies produced a basis for the later work on mathematical modelling.

The requirements for a suitable material system for use in RFI processes were determined, including maximum temperatures and excluding expensive capital equipment costs such as autoclaves. From these requirements a number of resin systems were identified and tested, using a simple vacuum bag process in an oven. From these test results the Redux series of film adhesives was identified as suitable for RFI based manufacturing. Further testing and sample manufacture have identified other components of a material system. These included high temperature release plies manufactured by Halar, mould release agents from Frekote which prevent bonding between the Redux film adhesive and mould surfaces at the elevated temperatures, Capran high temperature vacuum bag materials, sealant tapes and breather plies.

A physical testing regime was undertaken with the aim of firstly identifying and secondly optimising the process parameters. This included manufacturing simple flat plate samples for mechanical bend and impact strength testing using a variety of heating cycles and vacuum pressures. In particular the dwell and cure times were studied along with vacuum pressure. A standard tensile test specimen mould suitable for RFI manufacture was developed and samples were manufactured according to the same process parameters used for the flat plates. These test pieces were then tested to determine their tensile strengths and to compare them to the thin flat samples tested for bend and impact strength. Furthermore the samples were all studied and graded according to their surface finish quality. The results suggest that for maximum strength, a minimum cure time of 30 minutes be required to ensure complete cross-linking of the

matrix. The resin film melts and flows throughout the preform before the recommended dwell temperature of 80°C is reached. Thus the effect of dwell time is rather limited, however this may not hold for thick or stitched (3-D) preforms. The steady state permeability of the woven glass fibre cloth used for all testing was also experimentally determined so that it could be incorporated into the mathematical model.

In conjunction with the experimental work, a mathematical model was developed. This uses Darcy's law of flow through a porous medium to simulate the flow of the resin as it melts from a dry film and soaks through the preform material. Using the PDEase software to solve the partial differential equations, the model was initially developed to solve a one-dimensional case of resin flowing through the thickness of the preform material. A 2-D step-wise version was then attempted which allows visual simulation of the flow, pressure field and the position of the flow front at various discrete intervals in time. The simulation gives an indication of the time needed to fully wet-out a component, and provides a visual picture of the expected flow patterns, and potential problem areas. This model was then coupled with a second model, which describes the homogeneous formation of voids in the resin under vacuum pressure. This model determines the critical radii of stable bubbles, and the pressures in the resin at which they occur. Thus the optimum temperature profile to minimise void formation, and hence maximise the strength and quality of an RFI manufactured component could be found.

The results obtained by the experimental and theoretical approaches provide a starting point which will be close to the optimum parameters required to successfully manufacture a component using an RFI process based on Redux film adhesives and utilising the modified vacuum bag method described in this research. This research was conducted utilising and modelling flat plate type components and the results may not hold for more complex geometries.

References

1. Palmer R J, Dow M B and Smith D L, *Development of stitching reinforcement for transport wing panels.* 1st NASA Advanced Composite Technology Conference, Part 2, 1991, pp 621-646.

2. Chen V, Hawley A, Klotzshe M, Markus A and Palmer R, *Composite technology for transport primary structures.* 1st NASA Advanced Composite Technology Conference, Part 1, 1991, pp 71-126.

3. Seferis J C and Ahn K J, *Pre-preg processing science and analysis*, 34-th Intl. SAMPE Symposium, 1989, pp 63-87.

4. Cano R J and Dow M B, *Evaluation of the mechanical properties and damage tolerance of five new toughened matrix composite materials.* 37th Intl. SAMPE Symposium, 1992, pp 1312-1324.

5. Dexter H B and Hasko G H, *Mechanical properties and damage tolerance of multi-axial warp-knit composites*. Composites Science and Technology, vol. 56, 1996, pp 367-380.

6. Loos A C and MacRae J D, *A process simulation model for the manufacture of a blade-stiffened panel by the resin film infusion panel.* Composites Science and Technology, vol. 56, 1996, pp 273-289.

7. Mijovic J, Kim J and Slaby J, *Cure kinetics of epoxy formulations of the type used in advanced composites.* Journal of Applied Polymer Science, vol. 29, 1984, pp 1449-1462.

8. Weideman M H, Loos A E, Dexter H B and Hasko GH, *An Infiltration / Cure Model for Manufacture of Fabric Composites by the Resin Infusion Process.* VPI-E-92-05, Virginia Polytechnic Institute, Blacksburg, 1992.

9. Groth-Marnat G, *Neuropsychological effects of styrene exposure: A review of current literature.* Journal of Perceptual and Motor Skills, vol. 77, 1993, pp 1139-1149.

10. White D M, Daniell W E, Maxwell J K and Townes B D, *Psychosis following styrene exposure: case report of neuropsychological sequelae.* Journal of Clinical and Experimental Neuropsychology, vol. 12, 1990, pp 798-806.

11. William C, Summerscales J and Grove S, *Resin Infusion Under Flexible Tooling (RIFT).* Composites Part A, vol. 27A, 1996, pp 517-524.

12. *Marco Method*, US Patent no. 2495640, 24 January 1950.

13. Group Lotus Car Ltd. *Vacuum moulding patent.* GB Patent No. 1432333, 30 March 1972.

14. Gotch T M, *Improved production process for manufacture of GRP on British Rail.* 11th Reinforced Plastics Conference, BPF RPG, Paper 4, 1978, pp 33-39.

15. Gotch T M, *Developments and potential of vacuum impregnation techniques for GRP manufacture.* 12th Reinforced Plastics Conference, BPF RPG, Paper 7, 1980, pp 25-31.

16. Gotch T M, *Low investment alternatives to hand lay GRP production.* Hands off GRP, 2nd Conference, 1985, pp 1/1 – 11/1.

17. Allen R, Best P F, and Short D, *Vacuum injection moulding of high volume fraction fibre composites.* 13th Reinforced Plastics Congress, BPF RPG, Paper 49, 1982, pp 207-209.

18. Le Comte, *A Method and apparatus for producing a thin walled article of synthetic resin, in particular a large sized vehicle.* US Patent No 4359437, 16 November 1982.

19. Editorial, *Injection moulding for large craft.* Ship and Boat International, January-February 1986, pp 43-44.

20. Tengler H, *Vakuum-Injektionsverfahren.* J. Kunststoffe, vol. 75, No. 2, 1985, pp 73-75.

21. Adams A A and Roberts J H, *A general outline of the main characteristics and prime uses of a vacuum injection moulding system.* Hands off GRP, 2nd Conference, 1985, pp 5/1-5/3.

22. Editorial, *30 years experience of composite cars at Lotus.* Reinforced Plastics, vol. 35, No. 2, pp 34-37.

23. Ciba-Geigy Publication, *Vacuum Injection Process.* Ciba-Geigy Aileron Publication No 28626 / d,f,e 880. 729/40, (Printed in Switzerland).

24. Thirion J M, Girardy H, and Waldvogel U, *New developments for producing high-performance composite components by the RTM process.* Composites (Paris), vol. 28, No. 3, 1988, pp 81-84.

25. Letterman L E, *Resin film infusion process and apparatus.* US patent No. 4622091, 11 November 1986.

26. Brittles P, *New developments in RTM.* 19th Intl. BPF Composites Congress, 1994, pp 11-26.

27. Höhfeld J, *Consolidation of thick, close, circular knitted glass fibre textiles with epoxy resin into flat panels, tubes and T-profiles.* 3rd Intl. Conference on Flow Processes in Composite Materials, 1994.

28. Marcus S A, *New developments in vacuum bag forming.* Journal of Advanced Materials Processes, Metal Progress, vol. 6, No. 87, 1987, pp 33-39.

29. Shepherd G, *Embossed vacuum bag methods for producing said bag and composite article produced using said bag.* World Patent No W092/13695, 10 February 1992.

30. Kohama K, Abe T, Okamoto H and Fukuda A, *A new vacuum and/or pressure forming system using a pre-preg sheet of thermoset FRP with a gel coat layer.* 48th. SPI Conference, Session 3-F, 1993, pp 1-6.

31. Boey F Y C, *Reusable vacuum bagging technique for autoclave curing of composites*. Experimental Techniques, 22 September 1989, pp 21-23.

32. Ahn K J, Seferis J C and Letterman L, *Autoclave resin infusion process: analysis and prediction of resin content.* SAMPE Quarterly, vol. 21, No. 2, 1990, pp 3-10.

33. Hayward J S and Harris B, *Processing factors affecting the quality of resin transfer moulded composites*. Plastics & Rubber Processing & Applications, vol. 11, No. 4, 1989, pp 191-198.

34. Hayward J S and Harris B, *The effect of vacuum assistance in resin transfer moulding.* Composites Manufacturing, vol. 1, No. 3, 1990, pp 161-166.

35. Lundström T S, Gebart B R and Lundemo C Y, *Void formation in RTM.* Journal of Reinforced Plastics and Composites, vol. 12, 1993, pp 1339-1349.

36. Lundström T S, *Measurement of void collapse during resin transfer moulding.* Composites Part A, vol. 28A, 1997, pp 201-214.

37. Boey F Y C, *Reducing the void content and its variability in polymeric fibre reinforced composite test specimen using a vacuum injection moulding process.* Polymer Testing, vol. 9, 1990, pp 363-367.

38. Boey F Y C and Liu C Y, *Vacuum injection moulding process for fibre reinforced composites.* Experimental Techniques, vol.2, March-April 1991, pp 48-50.

39. Seemann W H, *Vacuum-forming method and apparatus for vacuum forming fibre reinforced composites*. European Patent Application No. EP 0525263Al, 1 August 1991.

40. Seemann W H, *Vacuum-forming fibre reinforced resin composites.* UK Patent Application No. GB 2257938A, 25 July 1991.

41. Seemann W H, *Plastic transfer moulding techniques for the production of fibre reinforced plastic structures*. US Patent No. 4902215, 30 March 1989.

42. Pfund B, *Resin infusion in the US marine industry.* Reinforced Plastics, December 1994, pp 32-34.

43. Lazarus P, *Infusion.* Professional Boat Builder, vol. 30, 1994, pp 42-55.

44. Barnes F, *Composite reinforcement of steel structural members.* Proceedings Institute of Mechanical Engineers, London, 17 November 1994, pp 1-5.

45. Barnes F, *Composite reinforcement of steel structural members*. SAMPE UK Club presentation, 25 November 1994, pp 24-27.

46. Barnes F and Galbraith D, *The development of process methods for in-situ composite reinforcement of existing steel structures.* Proceedings of 16th Intl. SAMPE Conference, 1995, pp 293-304.

47. Shim S B, Ahn K, Seferis J C, Berg A J and Hudson W, *Flow and void characterisation of stitched structural composites using resin film infusion process.* Polymer Composites, vol. 15, 1994, pp 453-463.

48. Shim S B, Ahn K, Seferis J C, Berg A J and Hudson W, *Cracks and microcracks in stitched structural composites manufactured with resin film infusion process.* Journal of Advanced Materials, vol. 7, July 1995, pp 48-62.

49. Lazarus P, *Infusion.* Professional Boat Builder, vol. 31, 1995, pp 28-34.

50. Ranganathan S, Phelan Jr. F R, and Advani, S G, *A generalised model for the transverse fluid permeability in unidirectional fibrous media.* Polymer Composites, vol. 17, 1996, pp 222-230.

51. Hammond V H, Loos A C, *The effects of fluid type and viscosity on the steady- state and advancing front permeability behaviour of textile preforms.* Journal of Reinforced Plastics and Composites, vol. 16, 1997, pp 50-72.

52. Lai Y H, Khomami B and Kardos J L, *Accurate permeability characterization of preforms used in polymer matrix composite fabrication processes.* Polymer Composites, vol. 18, 1997, pp 368-377.

53. Gauvin R and Chibani M, *Modelization of the clamping force & mould filling in RTM*, 43rd Annual Conference, Composites Institute, The Society of the Plastic Industry, Session 22, 1988, pp 1-3.

54. Gutowski T G and Cai Z, *The consolidation of composites.* Proceedings of Manufacturing International'88, Vol. IV, 1988, pp 13-25.

55. Gutowski T G, Morigaki T and Zhong C, *The consolidation of laminate composites.* Composite Materials, vol. 21, 1987, pp 172-188.

56. Kim Y R, McCarthy S P and Fanucci J P, *Compressibility and relaxation of fibre reinforcements during composite processing.* Polymer Composites, vol. 12, 1991, pp 13-19.

57. Pearce N R L and Summerscales J, *The compressibility of a reinforcement fabric.* Composites Manufacturing, vol. 6, 1995, pp 15-21.

58. Griffin P R, Grove S M, Guild F J, Russell P and Summerscales J, *The effect of microstructure on flow promotion in resin transfer moulding reinforcement fabrics.* Journal of Microscopy, vol. 177, 1995, pp 207-217.

59. Summerscales J, Griffin P R, Grove S M and Guild FG, *Quantitative microstructural examination of RTM fabrics designed for enhanced flow.* Composite Structures, vol. 32, 1995, pp 519-529.

60. Judd N C and Wright W W, *Voids and their effects on the mechanical properties of composites - an appraisal.* SAMPE Journal, January-February 1978, pp 10-14.

61. Guild F G and Summerscales J, *Microstructural image analysis applied to fibre composite materials: A review.* Composites, vol. 24, 1993, pp 383-394.

62. Basford D M, Griffin PR, Grove SM and Summerscales J, *Research report: the relationship between mechanical performance and microstructure in composite fabricated with flow enhancing fibres.* Composites, vol. 26, 1995, pp 675-679.

63. Scheidegger A E, *The Physics of Flow Through Porous Media.* University of Toronto Press, 1960.

64. Kang M K, Lee W I, Kim TW, Kim B S and Jun E, *Numerical simulation of resin transfer mould filling process.* Proceedings of 10th Intl. Conference on Composite Materials, Whistler, Canada, vol. 3, August 1995, pp 253-260.

65. Loos AC, MacRae J D, Hood D, Kranbuehl D E and Dexter H B, *Resin Film Infusion (RFI) process simulation of complex shaped composite structures.* American Institute of Aeronautics and Astronautics Journal, 1996, pp 1828-1837.

66. Coulter J P, and Guçëri S I, *Resin Impregnation during Composit· s Manufacturing: Theory and Experimentation.* Composites Science and Technology, vol. 35, 1989, pp 317-330.

67. Coulter J P, and Guçëri S I, *Resin impregnation during the manufacture of composites materials subject to a prescribed injection rate.* Journal of Reinforced Plastics and Composites, vol. 7, 1988, pp 200-219.

68. Skartsis L, Khomami B and Kardos J L, *Polymeric flow through fibrous media.* Journal of Rheology, vol. 36, No. 4, 1992, pp 589-620.

69. Sevostianov I B, Verijenko V E, von Klemperer C J and Chevallereau B, *Mathematical model of stress formation during vacuum resin infusion process.* Composites Part B, vol. 30, 1999, pp 513-521.

70. Matthews F L and Rawlings R D, *Composite Materials: Engineering and Science.* Chapman and Hall, First ed., 1994.

71. Backstrom G, *Fields of Physics on the PC by Finite Element Analysis.* Studentlitteratur, Second ed., 1996.

72. Benham P P and Crawford R J, *Mechanics of Engineering Materials.* Longman Scientific and Technical, First ed., 1991.

73. Shim SB, Ahn K and Seferis J C, *Flow and void characterisation of stitched structural composites using resin film infusion process (RFIP).* Polymer Composites, vol. 15, No. 6, December 1994, pp 453-463.

74. Specifications sheets: *Special Flexible Films/Webs*, Xiro-Guttacoll, 1997.
Redux Film Adhesives, Hexcel, 1996.

75. Lundström T S, Gebart B R and Lundemo C Y, *Void formation in RTM.* Reinforced Plastics and Composites, vol. 12, 1993, pp 1339-1349.

76. Lundström T S, *Measurement of void collapse during resin transfer moulding.* Composites Part A, vol. 28A, 1997, pp 201-214.

77. Hayward J S and Harris B, *Effect of process variables on the quality of RTM moulding.* SAMPE Journal, vol. 26, 1990, pp 39-46.

78. Mahale A D, Prud'Homme R K and Rebenfeld L, *Quantitative measurement of voids formed during liquid impregnation of non-woven multi-filament glass*

networks using an optical visualisation technique. Polymer Engineering and Science, vol. 32, 1992, pp 319-326.

79. Lundström T S and Gebart B R, *Influence from process parameters on void formation in resin transfer moulding.* Polymer Composites, vol. 15, 1994, pp 25-33.

80. Patel N and Lee L J, *Effects of fibre mat architecture on void formation and removal in liquid composite moulding.* Polymer Composites, vol. 16, 1995, pp 386-389.

81. Crank J, *Free and Moving Boundary Problems.* Clarendon Press, Oxford, 1982.

82. Fisher J C, *Nucleation of vapour bubbles in liquid.* Journal of Applied Physics, vol. 19, 1948, pp 1062-1074.

83. Phelan Jr. F R, *Simulation of the injection process in resin transfer moulding.* Polymer Composites, vol. 18, 1997, pp 460-476.

Appendix A

REDUX Experiments

The following series of experiments were carried out in order to examine the behaviour of the chosen material system (i.e. Redux film adhesives) under various conditions.

Experiment R1 (R = Redux) **08-07-1998**

Aim: To attempt RFI using a dry thermosetting film (Redux 312L) and glass fibre fabric (GFHL 1113/390/125).

Apparatus: Oven (Model P-2301-M)
Speedivac vacuum pump (Serial # 5300)
Stainless steel backing plate

Consumables: Vacuum bag (Capran 524 heat stabilised nylon)
High temperature sealant tape
Breather ply
Release film (Halar E.C.T.F.E. fluoropolymer)

Materials: Redux 312 thermosetting film (300 g/m^2)
Glass fibre woven fabric (GFHL1113/390/125)

Procedure:

1. The Redux film was taken out of the refrigerator and allowed to reach room temperature after which the protective polythene was removed. Thereafter, the film was cut to the shape and size required.

2. A lay-up was constructed consisting of dry layers of fibre material interleaved with layers of Redux 312L film so as to give approximately 75:100 resin to fibre ratio (approximately 300g/m^2 resin: 400g/m^2 fibre). The lay-up was placed inside a vacuum bag and put into the oven at 90 degrees Celsius.

3. Time was allowed for the lay-up to reach 90 degrees Celsius during which time the vacuum was applied. This is the temperature at which proper resin flow is achieved (see Viscosity vs. Temperature graph in Appendix D)

4. The temperature was then raised to 120 degrees Celsius and was held there for approximately one hour to cure the resin (see Viscosity vs. Temperature graph in appendix D)

5. The oven was then allowed to cool down and then the lay-up was removed.

Results/Observations

When the lay-up was removed from the oven, it was observed that the vacuum hose was facing out of the vacuum bag which indicates that vacuum was not applied throughout the whole duration of the experiment. Whatever seepage had occurred, was due to the action of gravity alone.

The sample was analysed carefully and it was observed that the resin had seeped through right to the last layer of fibre but not completely since dry areas were visible at the bottom surface. The top surface of the sample was covered in excess resin. It was also observed that the sample had obtained a high degree of stiffness after resin cure.

The oven successfully met our requirements of keeping constant temperatures for the cycles required.

Conclusion:

The reason for not achieving complete seepage of the resin was probably due to the fact that vacuum was not applied during the resin flow stage. The temperature values of 90 degrees Celsius and 120 degrees Celsius to melt and cure the resin respectively, were successful for a first time effort and can be supported by the Viscosity vs. Temperature graph for Redux 312 (see Appendix F).

Experiment R4 **08-10-1998**

Aim: To find a relationship, if any, between the dwell time and seepage of resin through a glass fibre lay-up.

Apparatus:
Oven(Model P-2301-M)
Speedivac vacuum pump (Serial # 5300)
Stainless steel backing plate

Consumables:
Vacuum bag (Capran 524 heat stabilised nylon)
High temperature sealant tape
Breather ply
Release film (Halar E.C.T.F.E. fluoropolymer)
Frekote 55NC

Materials:
Redux 312 thermosetting film (300 g/m^2)
Glass fibre woven fabric (GFHL 1113/390/125)

Procedure:

Four identical samples each consisting of 1 layer of fibre and 1 layer of resin were prepared. At the same time, a stainless steel backing plate was prepared. The plate consisted of 4 square areas of similar dimensions to accommodate the lay-ups individually. Individual vacuum bags, breather plies and release films were cut for each lay-up. Each of these areas were inter-linked via small silicon pipes such that the vacuum could be shared

The surface of the four areas were coated with a release agent, Frekote 55 NC and thereafter placed into the oven and allowed to reach 80°C. Once the plate reached this temperature, the first lay-up was put into area 1 and closed off with a vacuum bag. The inter-linking pipe between sample1 and sample 2 was blocked thus providing the necessary vacuum for sample 1. The other three lay-ups were put in subsequently at 5-minute intervals while the plate was in the oven. After a total dwell time of 20 minutes, the plate temperature was raised to 120°C and held there for a cure time of 30 minutes.

Results/Observations:

In heating the stainless steel plate from 24.3°C to 80°C a stepping rate of 2.228°C/min was achieved. The stepping rate from 80°C to 120°C was 1.905°C/min.

On observing the 4 samples, they were found to be similar in terms of stiffness, top and bottom surface finishes and the wetting of the fibres were uniform in all. Furthermore, a pattern of seepage versus dwell time was not evident from sample to sample. Removal of the sample from the plate was quite easy because of the use of the release agent Frekote 55NC.

Conclusion:

No observable relationship between seepage and dwell time was achieved using one layer of resin with one layer of fibre. It was further deduced that the Frekote 55NC would provide a better bottom surface finish as well as provide quicker and easier removal of samples from the stainless steel backing plate and other backing surfaces.

Experiment R6 **12-10-1998**

Aim: To find a relationship, if any, between the dwell time and seepage of resin through a glass fibre lay-up.

Apparatus:
Oven(Model P-2301-M)
Speedivac vacuum pump (Serial # 5300)
Stainless steel backing plate

Consumables:
Vacuum bag (Capran 524 heat stabilised nylon)
High temperature sealant tape
Breather ply
Release film (Halar E.C.T.F.E. fluoropolymer)
Frekote 55NC

Materials:
Redux 312 thermosetting film (300 g/m^2)
Glass fibre woven fabric (GFHL 1113/390/125)

Procedure:

Similar to experiment R4 except that 2 layers of fibre were used for each layer of resin

Results/Observations:

In heating the stainless steel plate from 25.7°C to 80°C a stepping rate of 2.586°C/min was achieved. The stepping rate from 80°C to 120°C was 2.353°C/min. These stepping rates were unusually high.

Analysis of the 4 samples indicates that they share the same wetting characteristics on both the top and bottom surfaces. However, the bottom surfaces were much drier than those of the previous experiment (that is, 1 resin layer with 1 fibre layer). Close inspection of the bottom surfaces reveal the presence of many surface voids. The stiffness was the same from sample to sample. Also, a pattern of seepage versus dwell time was not evident from sample to sample.

Conclusion:

There was no observable relationship between seepage and dwell times when using 1 resin layer and 2 fibre layers.

Experiment R7 **14-10-1998**

Aim: To find a relationship, if any, between the dwell time and seepage of resin through a glass fibre lay-up.

Apparatus:
Oven(Model P-2301-M)
Speedivac vacuum pump (Serial # 5300)
Stainless steel backing plate

Consumables:
Vacuum bag (Capran 524 heat stabilised nylon)
High temperature sealant tape
Breather ply
Release film (Halar E.C.T.F.E. fluoropolymer)
Frekote 55NC

Materials:
Redux 312 thermosetting film (300 g/m^2)
Glass fibre woven fabric (GFHL 1113/390/125)

Procedure:

Similar to experiment R5 except that 3 layers of fibre were used with each layer of resin

Results/Observations:

In heating the stainless steel plate from 25.1°C to 80°C a stepping rate of 1.83C/min was achieved. The stepping rate from 80°C to 120°C was 1.33°C/min. These stepping rates were lower than those of experiment R6.

The top surfaces of all the samples are the same. However, on inspecting the bottom surfaces, they were found to be extremely dry as individual strands of fibre were visible. In terms of stiffness all the samples were more or less the same. But comparing the stiffness of the samples from experiment R6 to those of this experiment (R7), it was evident that the stiffness of these samples was greater than that of the samples of experiment R6.

Conclusion:

It can be stated that experiment R7 was the superposition of 1 fibre layer to the lay-up of experiment R6. Furthermore, a relationship between seepage and dwell time could not be deduced.

Experiment R8 **15-10-1998**

Aim: To find a relationship, if any, between the dwell time and seepage of resin through a glass fibre lay-up.

Apparatus:
Oven(Model P-2301-M)
Speedivac vacuum pump (Serial # 5300)
Stainless steel backing plate

Consumables:
Vacuum bag (Capran 524 heat stabilised nylon)
High temperature sealant tape
Breather ply
Release film (Halar E.C.T.F.E. fluoropolymer)
Frekote 55NC

Materials:
Redux 312L thermosetting film (150g/m^2)
Glass fibre woven fabric (GFHL 1113/390/125)

Procedure:

Similar to experiment R5 except that 8 layers of resin were used with 4 layers of fibre and all 8 layers of resin were placed on top of the 4 layers of fibre. Since the areal weight of Redux 312L is half that of Redux 312 twice the amount of resin layers to fibre layers had to be used to obtain a ratio of 1:1.125 between fibre to resin.

Results/Observations:

In heating the stainless steel plate from 25.8°C to 80°C a stepping rate of 2.36°C/min was achieved. The stepping rate from 80°C to 120°C was 2.22°C/min.

It was observed that resin had seeped through from the top to the bottom surface. The majority of the bottom surfaces were similar, however dry spots were observed. The samples possessed remarkable stiffness, which was consistent from sample to sample.

Conclusion:

The dry spots were not attributed to inconsistency in seepage but rather to problems during the vacuum bagging process. Furthermore, no observable relationship was achieved between seepage and dwell time.

Experiment R9 **30-10-1998**

Aim: To manufacture a composite tensile test piece using the Atlas M130 mould manufactured previously.

Apparatus:
Photoelastic oven (Model P-2301-M)
Speedivac vacuum pump (Serial # 5300)
Atlas M130 mould
Ram wax
Axson Heptane Demoulant release agent

Consumables:
Vacuum bag (Capran 524 heat stabilised nylon)
High temperature sealant tape
Breather ply
Release film (Halar E.C.T.F.E. fluoropolymer)

Materials:
Redux 312 thermosetting film (300 g/m^2)
Glass fibre woven fabric (GFHL 1113/390/125)

Procedure:

The Redux film adhesive and glass mat were cut in the shape of the tensile test piece. Eight layers of each were obtained and placed in the mould cavity. Release film, breather ply and the vacuum bag were added, as per a normal lay-up. The lay-up was placed in the oven and heated to a dwell of 80°C and a cure temperature of 120°C (both or 30 minutes) with the mould temperature being monitored.

Results/Observations:

The test piece was found to be stuck to the mould and had to be knocked out causing the mould to chip on surfaces where the Redux was stuck to the mould. The test piece sample had reasonable stiffness. There was excess resin build-up on top surface with a reasonable surface finish. The bottom surface was dry especially where the edges of the Redux had torn in laying up. (In attempts to peel off the polythene backing sheet).

Conclusion:

It was discerned that because ram wax was used, the Redux bonded to the mould thereby chipping the edges of the mould cavity on release of the sample. Also, the lack of a draft angle aggravated the problem of release.

The curved upper edges of the sample can be attributed to:

(i) Layers being bigger than the cavity and therefore having to be forced in during the lay-up stage

(ii) An inadequate number of layers

(iii) The vacuum bag, which acts as a flexible tool, could not take the 90° edges and this in turn caused the resin to form a curved surface.

The bottom surface of the test piece was dry as part of the resin was stuck to the mould and the was inadequate seepage.

Experiment R10: **02-11-1998**

Aim: To produce an RFI sample using a complex metal mould and to test the characteristics of Redux 335J (150 g/m^2)

Apparatus:
Photoelastic oven (Model P-2301-M)
Speedivac vacuum pump (Serial # 5300)
Complex 3-D Metal mould

Consumables:
Vacuum bag (Capran 524 heat stabilised nylon)
High temperature sealant tape
Breather ply
Release film (Halar E.C.T.F.E. fluoropolymer)
Frekote 55NC

Materials:
Redux 335J thermosetting film (150 g/m^2, characteristic blue with perforations)
Glass fibre woven fabric (GFHL 1113/390/125)

Procedure:

A complex metal mould was obtained from Kentron which was previously used for drapeability studies. Four glass fibre layers were used with 12 layers of Redux so as to obtain a ratio by mass of 1g fibre to 1.125g resin. The glass and resin were in turn cut up into strategic shapes to fit the contours of the mould. The resin layers were interleaved with the fibre layers.

Since the mould has two sections, that is, one spherical and the other conical, the fibre together with the resin were first draped over the conical section and then over the spherical section. These lay-ups were pressed into the shape of the mould. Thereafter, the normal procedure of vacuum bagging was implemented. Once this was done, the entire assembly was placed into the oven.

In order to accelerate the heating up of the mould from 24.9°C to 80°C, the oven was set to 125°C. The stepping rate of the oven was calculated to be 1.196°C/min up to 125°C

and that of the mould was 0.63°C/min up to 80°C in the same space of time. Once the mould reached 80°C, the oven temperature controller was reset to 80°C and 30 minutes dwell time was allowed for seepage. This was done because since the oven was still hotter than the mould, the mould had the potential to heat up further and this was undesirable. In order to counteract this problem, the oven door was opened to release some heat.

After 30 minutes of dwell time, the oven controller was set to 160°C to again accelerate the heating up of the mould to 120°C but when the mould reached 110°C, the oven controller was brought back to 120°C to prevent overheating. The stepping rate achieved for this stage was 0.4°C/min.

On reaching 120°C, 30 minutes were allowed for the resin to cure.

Results/Observations:

The unusually slow heating up rates were due to the fact that the mould was large which therefore prolonged the time to heat up.

Larger dry areas were observed on the bottom surface of the sample. It was also observed that there was a concentration of resin in certain areas forming an asymmetrical distribution of resin. Also, the breather ply was well soaked with resin.

The top surface had a far better surface finish than the bottom although few dry spots were visible on the perimeter of the sample shape. The sample provided great stiffness and the desired shape was achieved.

Conclusion:

The asymmetrical distribution of resin on the bottom surface could be attributed to uneven heating of the mould or due to the mould not sitting flat in the oven. It can be argued that the breather ply served to remove excess resin. This suggests that the vacuum pump should have been switched off during the cure cycle. It was also noted

that the Redux 335J has better peel characteristics than Redux 312 and Redux 312L, and hence is easier to lay up, but retains similar seeping characteristics.

The results of using a complex mould were found to be quite satisfactory and acceptable in producing an intricate sample. One major downfall of using a mould of this sort is that it takes a long time to complete the cycle which in this case was found to be over seven hours.

Experiment R12 **10-11-1998**

Aim: To produce a tensile test piece using Redux 335J.

Apparatus:
Photoelastic oven (Model P-2301-M)
Speedivac vacuum pump (Serial # 5300)
Atlas M130 mould (exp. R11)

Consumables:
Vacuum bag (Capran 524 heat stabilised nylon)
High temperature sealant tape
Breather ply
Release film (Halar E.C.T.F.E. fluoropolymer)
Frekote 55NC
Cured silicon rubber sheet

Materials:
Redux 335J thermosetting film (150 g/m^2, characteristic blue with perforations)
GFHL glass fibre woven fabric (1113/390/125)

Procedure

The procedure follows that of experiment R9 except that a layer of cured silicon rubber was placed between the release film and breather ply to try and produce a better surface finish. Also, Frekote 55NC, a release agent more effective than Ram wax was applied onto the moulding cavity to facilitate easier removal of sample from the mould cavity. In this experiment 12 layers of glass fibre and 36 layers of resin were used, again to give as close a ratio of 1:1 as possible (actual ratio of glass to resin 1:1.125 by mass). To prevent the curling of the edges as experienced in experiment R9, not only were more layers used but the first 5 layers were cut smaller than the rest so that they fit more loosely without edges becoming curved. The remaining 7 layers were then placed on top.

Observations/Results

Heating of the mould from 82.2°C to 120°C produced a stepping rate of 0.59°C/min. Even though it was a struggle at first to remove the sample, chiselling away the excess

resin from the sides of the sample exposed an edge enabling the sample to be levered upwards. From this point, the sample slid out effortlessly. However small parts of the mould did chip because of the Redux sticking to the mould - these could later be patched. It is noted that this damage was a lot less severe when compared to experiment R9. The top surface finish was very good despite being slightly scratched by the removal process. The bottom surface was well wetted but a large amount of bubbles were visible (Redux 335J, is more translucent than 313). The sides of the sample were not completely wetted and surface voids were present. Since the layer of cured silicon rubber was used above the release film, no resin was able to seep through to the breather ply as in previous experiments.

Conclusion

A better surface finish was achieved proving the effectiveness of the layer of cured silicon rubber. A much flatter and uniform top surface was achieved. The increase in number of layers contributed significantly to the sample's stiffness. The cause of the entrapped air bubbles is unknown however a probable cause is that Redux 335J is a perforated resin film. This may have caused air to be trapped in the perforations, which could not escape during the infusion process.

Experiment R13 **13-11-1998**

Aim: To produce a tensile test piece from the Atlas M130 mould using Redux 312L.

Apparatus:
Photoelastic oven (Model P-2301-M)
Speedivac vacuum pump (Serial # 5300)
Atlas M130 mould (exp. R11)

Consumables:
Vacuum bag (Capran 524 heat stabilised nylon)
High temperature sealant tape
Breather ply
Release film (Halar E.C.T.F.E. fluoropolymer)
Frekote 55NC
Cured silicon rubber

Materials:
Redux 312L thermosetting film (150 g/m^2)
GFHL glass fibre woven fabric (1113/390/125)

Procedure

The mould was first patched using a small quantity of Atlas M130 mixture. The procedure followed from the previous experiment (R12) except that 10 layers of fibre and 30 layers of resin were used (interleaved) to again give a ratio of 1:1.125 by mass.

Observations/Results

The stepping rate achieved for heating from 25°C to 80°C was 0.466°C/min. and that for heating from 80°C to 120°C was 0.476°C/min. The test piece was removed in a similar fashion as that of experiment R10. The stiffness was appreciable but not as good as the tensile test piece produced with Redux 335J (experiment R12). The top surface of the sample was extremely smooth but is uniformly spotted due to the perforated release film through some resin passed. The bottom surface was well wetted for the most part except that some areas revealed large surface voids.

Conclusion

Since Redux 312L is very opaque no observation of internal voids was possible as observed in the sample made from Redux 335. The difference in stiffness between this sample and the previous one can be attributed to two factors: (1) the number of layers were fewer here, and (2) the matrix materials were different (i.e. 312L versus 335J).

Appendix B

Dry resin film testing.

Tests performed to find a suitable dry resin film for the RFI process.

Experiment 1

Aim: To attempt RFI using a dry thermoplastic adhesive film (Xiro VS-87) and Injectex glass fibre fabric.

Apparatus:
Gallenkamp oven (Serial # 126115)
Speedivac vacuum pump (Serial # 5300)
Stainless steel backing plate
Stainless steel work surface

Materials:
Xiro VS-87 dry adhesive film
Injectex glass fibre woven fabric
Masonite pieces for insulation

Consumables:
Vacuum bagging plastic
Tacky tape
Breather ply
Release film

Method:

1. The dry film and fibre fabric was cut into squares approximately 10cm by 10cm, with the dry film having a few millimetres of overlap.

2. The lay-up was placed in the oven on a stainless steel plate. The oven temperature was set to 100°C. The thermocouple reading showed 80°C, this was attributed to the fact that the oven door has to be kept slightly open for the thermocouple wire).

3. The temperature was continually monitored and the oven controller adjusted to increase the temperature.

4. Once the adhesive film was observed to have softened, the lay-up was removed and compacted by vacuum bagging.

5. Vacuum was applied for approximately 15 min until the lay-up was observed to be close to room temperature and the thermoplastic had set.

6. Lay-up was put back in the oven at a setting of140 'C. Thermocouple read 117 'C

7. After approximately another 15 min the lay-up was removed and again vacuum bagged.

8. Vacuum removed on cooling,

Observations:

After the first heating and vacuum bagging process, the adhesive film was found not to have bonded to the glass fibres (i.e. no 'wetting' was observed) - the film easily peeled off the woven glass cloth.

After further heating and subsequent vacuum bagging, the bonding only improved marginally - the film still peeled of due to very poor bonding.
Further heating was not undertaken as this would bring the lay-up close to the upper Limit temperature imposed by the process specifications.

Conclusion:

The film (Xiro V587-1) proved unsuitable for use in RFI. It has thus been eliminated from our list of possible dry resin films. A film with a much lower melting temperature would prove to be more effective. This is the subject of the following two experiments.

Experiment 2

Aim: To attempt RFI using a dry thermoplastic adhesive film (Haroco, 65g/m^2, see appendix F) and Injectex glass fibre fabric.

Apparatus:
Gallenkamp oven (Serial # 126115)
Speedivac vacuum pump (Serial # 5300)
Stainless steel backing plate
Stainless steel work surface
Masonite pieces for insulation

Consumables:
Vacuum bagging plastic
Tacky tape
Breather ply
Release film

Materials:
Haroco, 65g/m^2 dry adhesive film
Injectex glass fibre woven fabric

Method:

- The experiment consisted of two parts (2a & 2b):

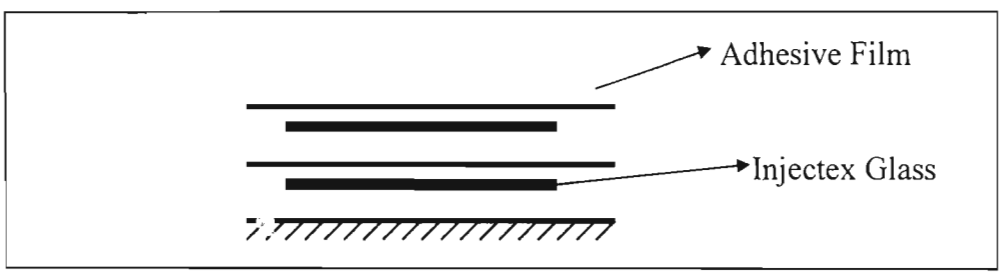

Figure 78 Exploded View of Lay-up

Experiment 2a

1. The lay-up was placed in the oven at 91 'C for approximately 45min.
2. Then the sample was vacuum bagged until it was cool.

Experiment 2b

1. The lay-up was placed in the oven at 112 'C for approximately 15min.
2. Then the sample was vacuum bagged, again, until cool.

Results/Observations

1. In the first part (2a) bonding was observed with no seepage through the fibres. It was then decided to increase the temperature to get a higher degree of wetting and seepage (2b).

2. In part two (2b) the film bonded to the fibres and appeared to have seeped through to some degree. However the edges of the top layer of film had shrunk.

Conclusion:

More experiments with Haroco, $65g/m^2$ need to be done with the following modifications: (1) Use larger sheets that completely overlap the fibre fabric pieces and (2) Use multiple layers of film (or alternatively, obtain a thicker film).

Experiment 3

Aim: Attempt RFI using XAF 2061, 30g/m^2 (see Appendix F)

Apparatus: As for previous experiment

Consumables: As for previous experiment

Materials: XAF 2061 perforated dry adhesive film
Injectex glass fibre fabric

Method:

1. The lay-up consisted of a layer of glass fibre, then film then glass and finally film on top.

2. The lay-up was heated in the oven at 112 'C for approximately 15min.

3. Then it was removed and vacuum bagged until cool.

Observations:

No bonding between the film and fibre at all and no seepage through the fibre. The film also shrank on some corners reducing coverage of the fibre.

Conclusion:

The result was unsatisfactory. The film was eliminated as a possibility.

Experiment 4

Aim: To attempt RFI using Haroco (55g/m2) and GFIIL 1037/600/125 glass fibre fabric.

Materials: Haroco 55g/m2) dry thermoplastic adhesive film
GFIIL 1037/600/125 glass fibre fabric

Consumables: Polythene vacuum bag
Release film
Breather ply
Sealant tape ('tacky tape')

Equipment: Speedivac vacuum pump
Photoelastic oven
Fluke thermocouple meter

Procedure:

1. The film and fibre were cut into square pieces of approximately 10cm by 10cm, with the film layers slightly larger to cover the fibre completely.

2. The lay-up was prepared with alternating layers of thermoplastic film adhesive and glass mat on a stainless steel plate. Release film and breather ply was placed over the lay-up and then the entire assembly was placed in a vacuum bag.

3. The entire lay-up was then placed in the oven at 120°C.

4. This temperature was held for about 15 minutes.

5. The vacuum was applied and held for about 10 minutes, while the assembly was still in the oven at 120°C

6. The oven was then switched of and the lay-up was allowed to cool to room temperature. The vacuum was maintained during this phase.

Results :

1. The Haroco had melted but seeped only slightly through the fabric. Wetting of fibres was poor.

2. The panel produced lacked stiffness and was found to be flexible and elastic in nature.

3. The fibres were easily pulled apart from the film indicating poor bonding

Conclusion:

The results were unsatisfactory. Based on these and results obtained from previous experiments with the Haroco thermoplastic adhesive film, we conclude that it is an unsatisfactory film and has thus been eliminated from further testing.

Appendix C

Results of process parameter testing.

Experimental results.

Heating Cycles:

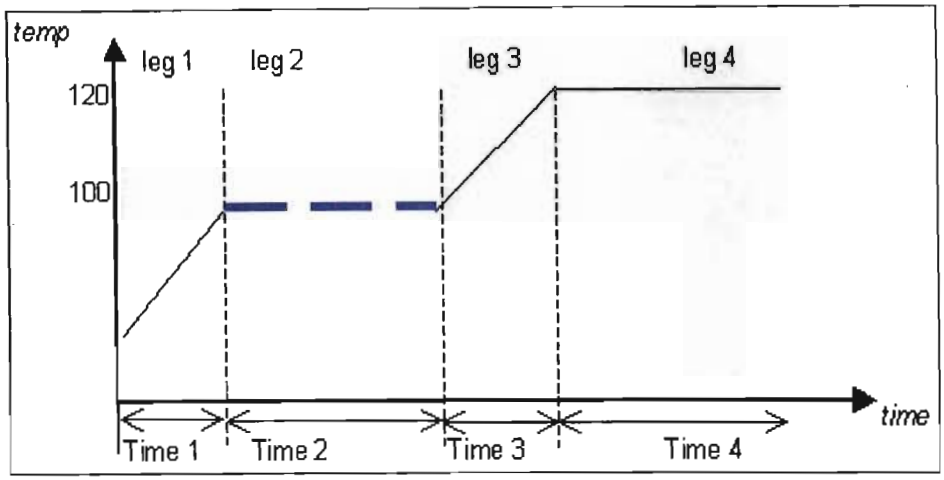

Figure 79 Schematic of heating cycle (Dwell leg highlighted).

Resin Flow at –80 kPa: Dwell Time - Flat samples

Experiment	Pressure	LEG 1	TIME 1	LEG 2	TIME 2	LEG 3	TIME 3	LEG 4	TIME 4
	kPa	° cel.	min	°cel.	min	° cel.	min	g cel	min
V11	80	100	20	100	15	120	10	120	30
V12	80	100	20	100	20	120	10	120	30
V13	80	100	20	100	25	120	10	120	30
V14	80	100	20	100	30	120	10	120	30
V15	80	100	20	100	35	120	10	120	30
V16	80	100	20	100	40	120	10	120	30
V17	80	100	20	100	45	120	10	120	30

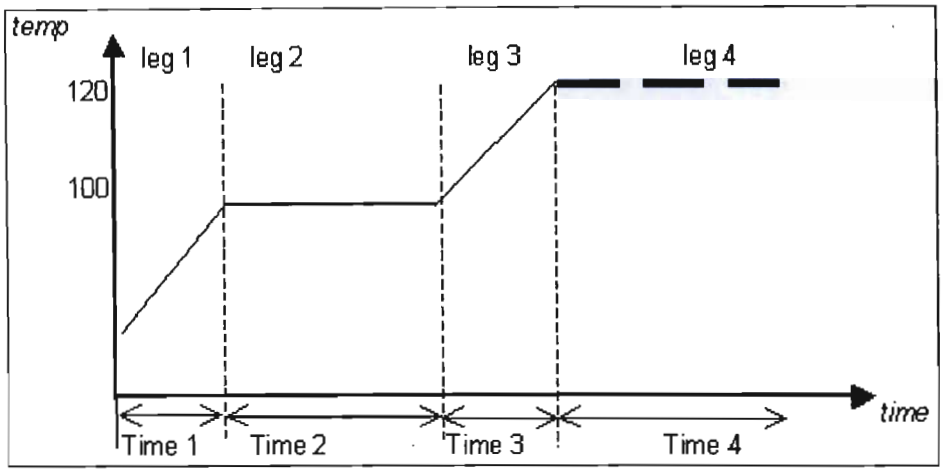

Figure 80 Schematic of heating cycle (Cure cycle highlighted)

Resin Flow at –80 kPa: Cure Time - Flat samples

Experi-ment	Press-ure	LEG 1	TIME 1	LEG 2	TIME 2	LEG 3	TIME 3	LEG 4	TIME 4
	KPa	° cel.	Min	° cel.	min	° cel.	min	° cel.	min
V31	80	100	20	100	20	120	10	120	15
V32	80	100	20	100	20	120	10	120	20
V33	80	100	20	100	20	120	10	120	25
V34	80	100	20	100	20	120	10	120	30
V35	80	100	20	100	20	120	10	120	35
V36	80	100	20	100	20	120	10	120	40
V37	80	100	20	100	20	120	10	120	45

Table 6Heating cycle for cure time samples (-80kPa)

Resin Flow at –90 kPa: Dwell Time - Flat samples

Experi-ment	Press-ure	LEG 1	TIME 1	LEG 2	TIME 2	LEG 3	TIME 3	LEG 4	TIME 4
	KPa	° cel.	min	° cel.	min	° cel.	min	° cel.	min
V21	90	100	20	100	15	120	10	120	30
V22	90	100	20	100	20	120	10	120	30
V23	90	100	20	100	25	120	10	120	30
V24	90	100	20	100	30	120	10	120	30
V25	90	100	20	100	35	120	10	120	30
V26	90	100	20	100	40	120	10	120	30
V27	90	100	20	100	45	120	10	120	30

Table 7 Heating cycle for dwell time samples (-90kPa)

Resin Flow at –90 kPa: Cure Time - Flat samples

Experi-ment	Press-ure	LEG 1	TIME 1	LEG 2	TIME 2	LEG 3	TIME 3	LEG 4	TIME 4
	kPa	° cel.	min	° cel.	min	° cel.	min	° cel.	min
V41	90	100	20	100	20	120	10	120	15
V42	90	100	20	100	20	120	10	120	20
V43	90	100	20	100	20	120	10	120	25
V44	90	100	20	100	20	120	10	120	30
V45	90	100	20	100	20	120	10	120	35
V46	90	100	20	100	20	120	10	120	40
V47	90	100	20	100	20	120	10	120	45

Table 8 Heating cycle for cure time samples (-90kPa)

Bend Test results.

Sample no.	Load 1	Load 2	Defl. (mm)	Width (mm)	Depth (mm)	y (mm)	I (mm^4)	L (mm)	M1 (Nmm)	Stress (MPa)
V11A	12	14.7	6.3	34.64	1.02	0.51	3.063	40.54	1216.2	202.478
V11B	12.3	16.4	6.4	37.34	1	0.5	3.112	40.54	1246.6	200.311
V11C	14.6	14.6	6.7	33.18	1.02	0.51	2.934	40.54	1479.7	257.188
V11D	15.1	16.2	6.5	36.62	1	0.5	3.052	40.54	1530.4	250.746
V11E	8.9	10.7	5.7	35.32	1	0.5	2.943	40.54	902.02	153.230
V12A	19.4	20.4	6.5	39.2	1.04	0.52	3.675	40.54	1966.2	278.243
V12B	14.5	18.2	6.5	34.14	1.06	0.53	3.388	40.54	1469.6	229.862
V12C	16.4	18.5	6.5	35.5	1.02	0.51	3.139	40.54	1662.1	270.016
V12D	15	18.8	6.6	35.68	1.02	0.51	3.155	40.54	1520.3	245.720
V12E	15.9	17.6	6.6	34.76	1.04	0.52	3.258	40.54	1611.5	257.173
V13A	36.1	37.3	6.6	37.34	1.08	0.54	3.92	40.54	3658.7	504.035
V13B	33.4	34.5	6.5	35.92	1.06	0.53	3.565	40.54	3385.1	503.238
V13C	34.4	36.6	6.4	35.06	1.06	0.53	3.48	40.54	3486.4	531.019
V13D	34.9	37.4	6.4	35.1	1.06	0.53	3.484	40.54	3537.1	538.123
V13E	35.2	37.2	6.4	35.88	1	0.5	2.99	40.54	3567.5	596.575
V14A	20.3	21.7	6.7	37.34	1.08	0.54	3.92	40.54	2057.4	283.432
V14B	19.4	20.7	6.7	35.8	1.06	0.53	3.553	40.54	1966.2	293.280
V14C	19.2	20.3	6.4	36.2	1.08	0.54	3.8	40.54	1945.9	276.516
V14D	16.4	18	6.8	34.68	1	0.5	2.89	40.54	1662.1	287.567
V14E	18	19.2	6.5	35.82	1.04	0.52	3.358	40.54	1824.3	282.524
V15A	11.3	13.6	6.5	35.86	1.04	0.52	3.361	40.54	1145.3	177.164
V15B	13.7	14.2	6.3	35	1.04	0.52	3.281	40.54	1388.5	220.070
V15C	13.6	14.1	7	35.72	1.06	0.53	3.545	40.54	1378.4	206.059
V15D	12.9	14.3	5.8	34.46	1.06	0.53	3.42	40.54	1307.4	202.599
V15E	14.8	14.9	6.8	35.78	1.02	0.51	3.164	40.54	1500	241.766
V16A	17.6	19.4	6.4	36.02	1.04	0.52	3.376	40.54	1783.8	274.712
V16B	19.5	21.6	6.3	34.72	1.1	0.55	3.851	40.54	1976.3	282.257
V16C	22	23.5	6.6	35	1.04	0.52	3.281	40.54	2229.7	353.397
V16D	22.2	25.3	6	35.88	1.24	0.62	5.701	40.54	2250	244.699
V16E	26.2	28.5	5.5	36.46	1.04	0.52	3.418	40.54	2655.4	404.011

Sample no.	Load 1	Load 2	Defl. (mm)	Width (mm)	Depth (mm)	y (mm)	I (mm^4)	L (mm)	M1 (Nmm)	Stress (MPa)
V17A	10.4	10.8	6.7	37.64	1.06	0.53	3.736	40.54	1054	149.536
V17B	10.7	11.2	6.5	34.14	1.04	0.52	3.2	40.54	1084.4	176.209
V17C	12	12.7	5.6	35.58	1.02	0.51	3.146	40.54	1216.2	197.129
V17D	12.8	13.7	6.3	34.92	1.04	0.52	3.273	40.54	1297.3	206.084
V17E	13.1	14.5	6.6	35.88	1.08	0.54	3.767	40.54	1327.7	190.347
V21A	27.4	32	7	36.56	1	0.5	3.047	40.54	2777	455.742
V21B	24.4	30	6.2	34.98	1.08	0.54	3.672	40.54	2472.9	363.662
V21C	23.2	28.8	6.3	35.64	1.02	0.51	3.152	40.54	2351.3	380.474
V21D	24.7	27.7	6.5	36.5	1	0.5	3.042	40.54	2503.3	411.509
V21E	22.8	25.8	6.3	35.14	1.06	0.53	3.488	40.54	2310.8	351.153
V22A	17.7	21.1	6.5	35.54	1.04	0.52	3.331	40.54	1793.9	280.004
V22B	20.1	22	6.7	35.36	1.06	0.53	3.51	40.54	2037.1	307.643
V22C	15.1	16.7	6.3	34.22	1.06	0.53	3.396	40.54	1530.4	238.814
V22D	14	14.8	6.4	35.6	1.04	0.52	3.337	40.54	1418.9	221.099
V22E	12.8	12.8	6.3	35.1	1.06	0.53	3.484	40.54	1297.3	197.363
V23A	21.7	23.4	6.3	35.58	1	0.5	2.965	40.54	2199.3	370.876
V23B	19.7	23.7	6.2	35.68	1.02	0.51	3.155	40.54	1996.6	322.713
V23C	21.6	23.7	8.2	35.2	1	0.5	2.933	40.54	2189.2	373.152
V23D	21.4	22.7	6.5	35.56	1	0.5	2.963	40.54	2168.9	365.954
V23E	21.1	22.9	6.5	35.64	1.1	0.55	3.953	40.54	2138.5	297.532
V24A	21	23.9	7	36.12	1	0.5	3.01	40.54	2128.4	353.547
V24B	17	21.5	6.1	34.74	0.99	0.5	2.809	40.54	1723	303.615
V24C	15.8	18.8	6.4	35.62	1.02	0.51	3.15	40.54	1601.3	259.261
V24D	15.8	17.6	7	35.38	1	0.5	2.948	40.54	1601.3	271.565
V24E	15	17	6.9	34.08	1	0.5	2.84	40.54	1520.3	267.650
V25A	12.5	14.1	6.9	34.06	1	0.5	2.838	40.54	1266.9	223.172
V25B	12.6	14.6	6.4	35.8	1.02	0.51	3.166	40.54	1277	205.713
V25C	13.7	15.8	7	36.66	1	0.5	3.055	40.54	1388.5	227.250
V25D	13.7	16.4	6.2	34.6	1	0.5	2.883	40.54	1388.5	240.779
V25E	15.6	17.8	7.6	35.44	1	0.5	2.953	40.54	1581.1	267.674

Sample no.	Load 1	Load 2	Defl. (mm)	Width (mm)	Depth (mm)	y (mm)	I (mm4)	L (mm)	M1 (Nmm)	Stress (MPa)
V26A	23	23.9	6.5	35	1.04	0.52	3.281	40.54	2331.1	369.461
V26B	24.6	25.1	6.6	35.74	1.02	0.51	3.161	40.54	2493.2	402.305
V26C	25.2	28.2	6.5	35.62	1.04	0.52	3.339	40.54	2554	397.754
V26D	28.2	30.9	6	35.38	1.06	0.53	3.512	40.54	2858.1	431.375
V26E	31.7	31.7	6.3	35.12	1.04	0.52	3.292	40.54	3212.8	507.473
V27A	22.4	28.2	6.6	36	1.04	0.52	3.375	40.54	2270.2	349.827
V27B	21.5	26.1	6.1	35.42	1.04	0.52	3.32	40.54	2179	341.270
V27C	22.4	27.1	6.2	35.44	1.1	0.55	3.931	40.54	2270.2	317.646
V27D	21	25	6.2	34.96	1.04	0.52	3.277	40.54	2128.4	337.720
V27E	22.4	26	6.6	35.3	1.06	0.53	3.504	40.54	2270.2	343.429
V31A	14.4	16	6.7	36.9	1.04	0.52	3.459	40.54	1459.4	219.404
V31B	13.8	15.2	6.2	34.5	1.02	0.51	3.051	40.54	1398.6	233.795
V31C	13.4	15.6	6.1	35.18	1	0.5	2.932	40.54	1358.1	231.624
V31D	14.3	16.2	6.6	35.66	1	0.5	2.972	40.54	1449.3	243.854
V31E	11.9	16.8	5.9	35.7	1	0.5	2.975	40.54	1206.1	202.700
V32A	17.4	21.6	6.1	34.2	1.04	0.52	3.206	40.54	1763.5	286.043
V32B	21.5	21.9	6.8	34.88	1.12	0.56	4.084	40.54	2179	298.814
V32C	22.2	23.1	6.4	35.4	1.11	0.56	4.035	40.54	2250	309.513
V32D	21.9	22.4	6.7	35	1.08	0.54	3.674	40.54	2219.6	326.215
V32E	23.3	24.2	6.5	38.06	1.11	0.56	4.338	40.54	2361.5	302.146
V33A	23.7	27.3	6.5	36.26	1.16	0.58	4.717	40.54	2402	295.379
V33B	22.7	27	6.1	35.88	1.06	0.53	3.561	40.54	2300.6	342.402
V33C	24.9	28	6.5	35.86	1.04	0.52	3.361	40.54	2523.6	390.389
V33D	24.8	28.2	6.4	34.11	1.06	0.53	3.385	40.54	2513.5	393.490
V33E	25.1	28.8	6.4	35.44	0.99	0.5	2.866	40.54	2543.9	439.425
V34A	18.7	20.1	6.1	34.92	1.18	0.59	4.781	40.54	1895.2	233.872
V34B	18.7	20.4	5.1	34.84	1.1	0.55	3.864	40.54	1895.2	269.745
V34C	18.5	20.6	6.1	35.6	1.08	0.54	3.737	40.54	1875	270.925
V34D	19.5	21.4	6.3	37.02	1.06	0.53	3.674	40.54	1976.3	285.077
V34E	18.1	20	6.4	34.86	1.06	0.53	3.46	40.54	1834.4	281.005

Sample no.	Load 1	Load 2	Defl. (mm)	Width (mm)	Depth (mm)	y (mm)	I (mm^4)	L (mm)	M1 (Nmm)	Stress (MPa)
V35A	11.8	13.8	6.1	33.24	1	0.5	2.77	40.54	1195.9	215.872
V35B	13.2	15.1	6.5	35.32	1.09	0.55	3.812	40.54	1337.8	191.283
V35C	12.7	14.3	6.1	34.86	1.06	0.53	3.46	40.54	1287.1	197.169
V35D	12.7	14.3	6.5	35.68	1.04	0.52	3.345	40.54	1287.1	200.118
V35E	12.6	13.6	7.1	34.7	1.14	0.57	4.284	40.54	1277	169.905
V36A	8.1	8.2	6.3	34.22	1.16	0.58	4.451	40.54	820.94	106.971
V36B	9.3	9.4	6.5	34.02	1.12	0.56	3.983	40.54	942.56	132.522
V36C	11.5	11.4	6.2	36.2	1.14	0.57	4.469	40.54	1165.5	148.646
V36D	12.2	12.2	6.1	35.24	1.1	0.55	3.909	40.54	1236.5	173.986
V36E	12.5	12.6	6.1	35.38	1.14	0.57	4.368	40.54	1266.9	165.317
V37A	20	22.4	6.6	36.12	1.15	0.58	4.578	40.54	2027	254.602
V37B	17.8	20	6.5	33.5	1.13	0.57	4.028	40.54	1804	253.042
V37C	18.8	21.9	6.3	36.26	1.1	0.55	4.022	40.54	1905.4	260.567
V37D	19	22	6	35.72	1.1	0.55	3.962	40.54	1925.7	267.320
V37E	19.8	23.5	6.1	35	1.02	0.51	3.095	40.54	2006.7	330.652
V41A	11.2	12.3	6.4	33.44	1.04	0.52	3.135	40.54	1135.1	188.304
V41B	11.9	13.5	6.3	36.08	1.06	0.53	3.581	40.54	1206.1	178.502
V41C	11.7	13.1	6.3	34.58	1.04	0.52	3.241	40.54	1185.8	190.226
V41D	12	13.6	6.4	35.64	1.16	0.58	4.636	40.54	1216.2	152.161
V41E	11.8	13.4	6.3	35.04	1.04	0.52	3.285	40.54	1195.9	189.333
V42A	14.7	18.4	5.6	37.06	1.08	0.54	3.89	40.54	1489.8	206.795
V42B	13.5	15.5	6.6	33.44	1	0.5	2.787	40.54	1368.2	245.495
V42C	14	17.4	5.9	36.3	1	0.5	3.025	40.54	1418.9	234.529
V42D	14	16.7	6.2	36.12	0.99	0.5	2.921	40.54	1418.9	240.483
V42E	16.6	18.7	7	35.51	1.02	0.51	3.14	40.54	1682.4	273.232
V43A	12.8	14	6	34.22	1.1	0.55	3.796	40.54	1297.3	187.983
V43B	11.8	14.1	6.2	34.14	1.03	0.52	3.109	40.54	1195.9	198.116
V43C	12.2	14.6	5.8	36.18	1.04	0.52	3.391	40.54	1236.5	189.583
V43D	10.8	8.4	6.1	35.39	1.08	0.54	3.715	40.54	1094.6	159.100
V43E	10.3	13.1	5.7	34.2	1	0.5	2.85	40.54	1043.9	183.141

Sample no.	Load 1	Load 2	Defl. (mm)	Width (mm)	Depth (mm)	y (mm)	I (mm^4)	L (mm)	M1 (Nmm)	Stress (MPa)
V44A	20.2	25.3	6.4	35.38	1.02	0.51	3.129	40.54	2047.3	333.709
V44B	20.3	25.6	6.1	34.48	1.1	0.55	3.824	40.54	2057.4	295.882
V44C	21.1	26.8	6	35.22	1.06	0.53	3.496	40.54	2138.5	324.232
V44D	21.2	26.1	6.2	35.6	1	0.5	2.967	40.54	2148.6	362.127
V44E	20.2	24.5	6.2	36.26	1.02	0.51	3.207	40.54	2047.3	325.610
V45A	23.3	28.1	6.4	35.74	1.14	0.57	4.413	40.54	2361.5	305.047
V45B	23.5	27.5	6.6	36.3	1	0.5	3.025	40.54	2381.7	393.674
V45C	21.1	24.5	6.6	35	1	0.5	2.917	40.54	2138.5	366.597
V45D	21	24.9	6.5	35.5	1	0.5	2.958	40.54	2128.4	359.721
V45E	19.5	23.4	6.4	34.5	1	0.5	2.875	40.54	1976.3	343.709
V46A	19.6	24.7	6.3	37.22	1.1	0.55	4.128	40.54	1986.5	264.648
V46B	21.4	26.9	6	35.58	1	0.5	2.965	40.54	2168.9	365.749
V46C	23.2	27.8	6.4	36.14	1.06	0.53	3.587	40.54	2351.3	347.427
V46D	21	20.7	6.7	34.52	1	0.5	2.877	40.54	2128.4	369.933
V46E	21.3	24.4	6.6	35.5	1	0.5	2.958	40.54	2158.8	364.860
V47A	22.8	27.8	6.3	36.7	1	0.5	3.058	40.54	2310.8	377.784
V47B	20.1	24.2	6.3	34.7	1	0.5	2.892	40.54	2037.1	352.242
V47C	18.3	23.7	6.6	35.5	1	0.5	2.958	40.54	1854.7	313.471
V47D	18.8	22.4	6.1	35.26	1.1	0.55	3.911	40.54	1905.4	267.957
V47E	19.1	23	6.1	35.24	1.1	0.55	3.909	40.54	1935.8	272.387

Table 9 Bend test results

Impact Test Results:

Sample no.	Energy [J]	Scale / Pin	Break
V11 A	1.67	11	Partial
V11 B	1.92	9	Partial
V11 C	2.2	6	Partial
V11 D	2.03	8	Partial
V11 E	2.03	8	Partial
V12 A	1.38	13	Partial
V12 B	1.67	11	Partial
V12 C	1.67	11	Partial
V12 D	1.67	11	Partial
V12 E	1.04	15	Partial
V13 A	1.38	13	Partial
V13 B	1.38	13	Partial
V13 C	1.67	11	Partial
V13 D	1.38	13	Partial
V13 E	1.38	13	Partial
V14 A	1.38	13	Partial
V14 B	1.21	14	Partial
V14 C	1.04	15	Partial
V14 D	1.21	14	Partial
V14 E	1.04	15	Partial
V15 A	1.53	12	Partial
V15 B	1.67	11	Partial
V15 C	1.53	12	Partial
V15 D	1.8	10	Partial
V15 E	1.53	12	Partial

Sample no.	Energy [J]	Scale / Pin	Break
V23 A	2.33	4	Partial
V23 B	1.8	10	Partial
V23 C	2.33	4	Partial
V23 D	2.03	8	Partial
V23 E	2.27	5	Partial
V24 A	1.04	15	Partial
V24 B	1.04	15	Partial
V24 C	1.21	14	Partial
V24 D	1.04	15	Partial
V24 E	1.21	14	Partial
V25 A	1.8	10	Partial
V25 B	2.33	4	Partial
V25 C	2.37	3	Partial
V25 D	2.33	4	Partial
V25 E	2.27	5	Partial
V26 A	1.21	14	Partial
V26 B	1.53	12	Partial
V26 C	1.67	11	Partial
V26 D	2.12	7	Partial
V26 E	2.03	8	Partial
V27 A	1.21	14	Partial
V27 B	1.38	13	Partial
V27 C	1.21	14	Partial
V27 D	1.21	14	Partial
V27 E	1.21	14	Partial

Sample no.	Energy [J]	Scale / Pin	Break
V16 A	1.21	14	Partial
V16 B	1.21	14	Partial
V16C	1.38	13	Partial
V16D	1.21	14	Partial
V16E	1.21	14	Partial
V17 A	1.53	12	Partial
V17 B	1.21	14	Partial
V17 C	1.21	14	Partial
V17 D	1.67	11	Partial
V17 E	1.67	11	Partial
V21 A	2.2	6	Partial
V21 B	2.37	3	Partial
V21 C	1.38	13	Partial
V21 D	1.8	10	Partial
V21 E	1.53	12	Partial
V22 A	2.12	7	Partial
V22 B	1.92	9	Partial
V22 C	2.03	8	Partial
V22 D	2.37	3	Partial
V22 E	1.21	14	Partial

Sample no.	Energy [J]	Scale / Pin	Break
V31 A	1.04	15	Partial
V31 B	1.04	15	Partial
V31 C	1.38	13	Partial
V31 D	1.04	15	Partial
V31 E	1.04	15	Partial
V32A	1.53	12	Partial
V32 B	1.21	14	Partial
V32 C	1.38	13	Partial
V32 D	1.38	13	Partial
V32 E	1.38	13	Partial
V33 A	1.21	14	Partial
V33 B	1.38	13	Partial
V33 C	1.38	13	Partial
V33 D	1.04	15	Partial
V33 E	1.04	15	Partial
V34 A	1.04	15	Partial
V34 B	1.04	15	Partial
V34 C	1.21	14	Partial
V34 D	1.21	14	Partial
V34 E	1.04	15	Partial

Sample no.	Energy [J]	Scale / Pin	Break
V35 A	1.04	15	Partial
V35 B	1.04	15	Partial
V35 C	0.85	16	Partial
V35 D	1.04	15	Partial
V35 E	1.04	15	Partial
V36 A	1.92	9	Partial
V36 B	1.8	10	Partial
V36 C	1.67	11	Partial
V36 D	1.8	10	Partial
V36 E	1.53	12	Partial
V37 A	1.04	15	Partial
V37 B	1.04	15	Partial
V37 C	1.04	15	Partial
V37 D	1.04	15	Partial
V37 E	1.04	15	Partial
V41 A	1.38	13	Partial
V41 B	1.04	15	Partial
V41 C	1.21	14	Partial
V41 D	1.04	15	Partial
V41 E	1.04	15	Partial
V42 A	1.04	15	Partial
V42 B	1.04	15	Partial
V42 C	1.04	15	Partial
V42 D	1.04	15	Partial
V42 E	1.04	15	Partial

Sample no.	Energy [J]	Scale / Pin	Break
V43 A	1.21	14	Partial
V43 B	1.04	15	Partial
V43 C	1.04	15	Partial
V43 D	1.04	15	Partial
V43 E	1.04	15	Partial
V44 A	1.21	14	Partial
V44 B	1.04	15	Partial
V44 C	1.21	14	Partial
V44 D	1.04	15	Partial
V44 E	1.04	15	Partial
V45 A	1.21	14	Partial
V45 B	1.04	15	Partial
V45 C	1.04	15	Partial
V45 D	1.04	15	Partial
V45 E	1.04	15	Partial
V46 A	1.21	14	Partial
V46 B	1.21	14	Partial
V46 C	1.04	15	Partial
V46 D	1.21	14	Partial
V46 E	1.04	15	Partial
V47 A	1.38	13	Partial
V47 B	1.53	12	Partial
V47 C	1.53	12	Partial
V47 D	1.67	11	Partial
V47 E	1.38	13	Partial

Table 10 Impact Test results

Tensile test results.

Sample Number	Cross - sectional area (mm^2)	Failure load (kN)	Failing Tensile Stress (MPa)	Young's Modulus (MPa)	Failing Tensile Strain
T13A	90.32	20.40	225.87	2773.82	0.0814
T13B	90.42	25.80	285.32	3120.73	0.0914
T13C	84.69	17.85	210.78	2837.36	0.0743
T26A	90.31	21.15	234.19	3035.84	0.0771
T26B	97.74	16.90	172.91	2521.60	0.0686
T26C	94.60	22.25	235.21	2655.60	0.0886
T27A	96.42	21.70	225.06	2716.22	0.0829
T27B	90.68	23.25	257.50	2954.94	0.0871
T27C	93.51	21.55	230.47	2644.72	0.0871
T31A	94.77	17.35	183.08	2135.98	0.0857
T31B	90.42	20.55	227.26	2696.35	0.0843
T31C	93.69	16.05	171.30	2067.45	0.0829
T32A	89.28	15.80	176.97	2294.04	0.0771
T32B	90.25	13.50	149.58	2094.15	0.0714
T32C	90.00	17.75	197.23	2465.37	0.0800
T33A	92.23	23.30	252.63	2720.63	0.0929
T33B	94.31	21.45	227.45	2793.26	0.0814
T33C	91.84	23.10	251.51	2750.91	0.0914
T45A	109.23	20.00	183.11	No Result	0.0000
T45B	92.20	14.25	154.56	2254.00	0.0686
T45C	89.11	20.65	231.73	No Result	0.0000

Table 11 Tensile test results

Surface Finish Grading

Series no.	Surface finish grade (out of 5)	Dwell / cure time (min)
Dwell	Vacuum –80kPa	
V11	2.80	15
V12	3.25	20
V13	4.00	25
V14	3.20	30
V15	2.40	35
V16	4.00	40
V17	2.40	45
Dwell	Vacuum -90kPa	
V21	4.00	15
V22	2.00	20
V23	2.60	25
V24	4.00	30
V25	4.10	35
V26	3.00	40
V27	4.00	45
Cure	Vacuum -80kPa	
V31	3.00	15
V32	3.00	20
V33	4.00	25
V34	4.00	30
V35	3.00	35
V36	1.00	40
V37	4.00	45

Series no.	Surface finish grade	Dwell / cure time
	(out of 5)	(min)
Cure	Vacuum –90kPa	
V42	4.00	20
V43	4.00	25
V44	4.00	30
V45	4.00	35
V46	4.00	40
V47	4.00	45

Table 12 Surface finish grading.

Burnout test results.

Table 13 Burnout test results

BURN-OFF TESTS							
Specimen	Mass of Dish (g)	Mass of Dish + Composite (g)	Mass of Dish + Glass (g)	Mass of Composite (g)	Mass of Glass (g)	Mass Fraction of Glass	Volume Fraction of Glass
V11	47.8981	48.9678	48.5753	1.0697	0.6772	0.633	0.480
V12	55.6361	57.1520	56.5774	1.5159	0.9413	0.621	0.467
V13	47.8977	48.9937	48.6180	1.0960	0.7203	0.657	0.507
V14	55.6364	56.9899	56.5986	1.3535	0.9622	0.711	0.568
V15	47.8950	49.2321	48.8084	1.3371	0.9134	0.683	0.536
V16	55.6345	57.1327	56.6761	1.4982	1.0416	0.695	0.550
V17	47.9051	49.3716	48.9132	1.4665	1.0081	0.687	0.541
V21	55.6393	57.2618	56.7757	1.6225	1.1364	0.700	0.556
V22	47.8995	49.8478	49.2873	1.9483	1.3878	0.712	0.570
V23	55.6395	57.2468	56.7402	1.6073	1.1007	0.685	0.538
V24	47.8971	49.9007	49.2950	2.0036	1.3979	0.698	0.553
V25	55.6355	58.1190	57.3438	2.4835	1.7083	0.688	0.541
V26	47.8944	48.9654	48.4853	1.0710	0.5909	0.552	0.397
V27	55.6360	57.0044	56.6003	1.3684	0.9643	0.705	0.561
V31	47.8958	49.7573	49.1822	1.8615	1.2864	0.691	0.545
V32	55.6340	56.9688	56.4851	1.3348	0.8511	0.638	0.485
V33	47.8972	49.3512	48.8759	1.4540	0.9787	0.673	0.524
V34	55.6350	57.0234	56.5302	1.3884	0.8952	0.645	0.493
V35	47.8967	49.4733	48.9879	1.5766	1.0912	0.692	0.546
V36	55.6352	57.4241	56.8332	1.7889	1.1980	0.670	0.521
V37	47.8967	49.3561	48.8666	1.4594	0.9699	0.665	0.515
V42F	55.6347	56.3499	56.1001	0.7152	0.4654	0.651	0.499
V43D	47.8969	49.1860	48.8018	1.2891	0.9049	0.702	0.558
V43F(1)	55.6352	56.2453	56.0386	0.6101	0.4034	0.661	0.511
V43F(2)	47.9000	48.9598	48.6167	1.0598	0.7167	0.676	0.528
V44F	55.6370	56.5317	56.2558	0.8947	0.6188	0.692	0.546
V45F	47.8982	48.6646	48.4279	0.7664	0.5297	0.691	0.545
V46F	55.6356	56.4454	56.1894	0.8098	0.5538	0.684	0.537
V47F	47.9011	48.6103	48.3917	0.7092	0.4906	0.692	0.546

Appendix D

PDEase

```
******************************
*    Post Release Notes      *
*  Professional Version 2.5  *
******************************
```

SYSTEM REQUIREMENTS

To Run the PDEase, it must be installed on a system running MS-DOS version 5.0 (or higher) and which meets the following minimum hardware requirements:

386 microprocessor with a 387 coprocessor
2 Mbytes of extended memory

PROGRAM NAME

pdease2

PDEase2 uses ordinary ASCII text files for problem input files. These files may be viewed, edited, and printed using any non-formatting text editor.

Appendix E

PDEase sample files.

PDEase Sample Files:

{ flux2.PDE }

```
title 'Viscous flow in porous networks'

select
        macsyma

variables
        P
                {Pressure in resin}


definitions
        Ti = 300
        {Initial Temperature in Mould}
        visc01 = 5.5e-5
        {Viscosity at Ti}
        D = 1.42e-12
        {Permeability of Preform}
        h = 1
                {Thickness of Preform}
        j = 0.001
        {external flux rate}
        tf = 1
                {Final time}
        Pc =-80000
        {External Vacuum Pressure}
        psi = 1034
        {visc. constant}
```

```
        rr = 5
                {Temperature ramp rate o / min}
        visc = visc01*exp[-psi/(Ti+rr*t/60)]                    {defining
equation for visc.}

initial values
        P = -80000

                {Initial pressure in resin = external vacuum
                pressure}
equations
        dx(P) = -j*visc/D
        {Darcy's Law}
Boundaries
        region 1
                start(0,0)
                                natural(P)=0
        {Boundary cond. that dp/dy = 0}
                line to (tf,0)
                                natural(P) = 0
        {Boundary cond. that dp/dx = 0}
                line to (tf,h)
                                value(P) = Pc
                {Boundary cond. that Pressure in Resin = external vacuum
pressure}
                line to finish
plots
        grid(x,y)
        contour(P)
                pause
        surface(P) interactive
        vector(dx(P),dy(P))

end
```

```
{ flux4.PDE }

title 'Viscous flow in porous networks'

{Single layer of reinforcement with one layer of resin film placed above}

select
        macsyma

variables
        P
        {Pressure in resin}
        v

definitions
        Pcomp = 1013e-6
                                        {compaction pressure on resin film}
        Ti = 300
        {Initial Temperature in Mould}
        visc01 = 5.5e-11
        {Viscosity at Ti}
        D = 1.42e-18
        {Permeability of Preform}
        h = 1
        {Thickness of Preform}

        {external flux rate}
        tf =1
        {Final time}
        Pc =-80000e-6
        {External Vacuum Pressure}
        psi = 1034                                              {visc.
constant}
```

```
        rr = 3
        {Temperature ramp rate o / min}
        visc = visc01*exp[-psi/(Ti+rr*t*10/60)]
                                        {defining equation for visc.}
        flow = D*dx(P)
        tu=tf/8
initial values
        P = 0

                        {Initial pressure in resin = external vacuum pressure}
        v = 0
equations

        dx[-dx(P)*D/visc-dy(P)*D/visc]+dy[-dx(P)*D/visc-dy(P)*D/visc]=0
                                                {0 = dx[(-visc/D)*dx(P)]
                {Darcy's Law}}

        dt(v)=(visc/D)*dx(P)

Boundaries
        region 1
                start (0,0)
          natural(v)=0
      line to (0,1)
          value (P)=Pcomp
      line to (10,1)
                        natural (v)=Pc
      line to (10,0)
         value(P)= Pc
      line to finish

Time
    0 to tf
```

```
monitors
                    line to (tf,h)
                                        value(P) = Pc
        {Boundary cond. that Pressure in Resin = external vacuum pressure}

line to finish

plots
    for t= tu, tu*2, tu*3, tu*4, tu*5, tu*6, tu*7, tu*8
        grid(x,y)
        contour(P)
                    pause
        surface(P)
                    interactive
        vector(dx(P),dy(P))

end
```

```
{ flux6.PDE }

title 'Viscous flow in porous networks'

{2 layers of reinforcement stacked on either side of a single layer of resin}

select
        macsyma

variables
        P
        {Pressure in resin}
        v
        {flux of resin}

definitions
        Pcomp = 1013e-6
        {compaction pressure on resin film}
        Ti = 300
        {Initial Temperature in Mould}
        visc01 = 5.5e-11
        {Viscosity at Ti}
        D = 1.42e-18
        {Permeability of Preform}
        h = 1
        {Thickness of Preform}

        {external flux rate}
        tf =0.1
        {Final time}
        Pc =-80000e-6
        {External Vacuum Pressure}
        psi = 1034                                              {visc.
constant}
```

```
        rr = 3
        {Temperature ramp rate o / min}
        visc = visc01*exp[-psi/(Ti+rr*t*10/60)]
                                                    {defining
                equation for visc.}
        flow = D*dx(P)
        tu=tf/8
initial values
        P = 0
                                    {Initial pressure in resin = external
vacuum pressure}

    v = 0
        {initial flux}
equations

        dx[-dx(P)*D/visc-dy(P)*D/visc]+dy[-dx(P)*D/visc-dy(P)*D/visc]=0
        dt(v)=(-visc/D)*dx(P)

Boundaries
        {Two resin surrounding one mat}
        region 1
                start (0,0)
                                    value(v) = 0
                line to (0,1)
                                    value(P) = Pc
                line to (2,1)
                                    natural(v) = -1
                line to (2,0)
                                    value(P) = Pcomp
                line to finish
        region 2
                start (0,1)
```

```
                                        value(P) = Pc
            line to (2,1)
                                        natural(v) = 1
            line to (2,2)
                                        value(P) = Pcomp
            line to (0,2)
                                        natural(v) = -1
            line to finish

Time
        0 to tf
monitors

plots
    {for t= tu, tu*2, tu*3, tu*4, tu*5, tu*6, tu*7, tu*8}
        for t= tu/4, tu/3, tu/2, tu, tu*2, tu*4, tu*6, tu*8
        grid(x,y)
        contour(P)
                pause
        surface(P)
                interactive
        vector(dx(P),dy(P))


end
```

Appendix F

Material Data Sheets

Material Specification sheets.

Redux 312

Description

Redux 312 is a high strength 120°C curing film adhesive, suitable for metal to metal bonding and sandwich constructions, where operating temperatures of up to 100°C may be experienced.

Features

Short cure cycle - cures in 30 minutes at 120°C
Good mechanical performance up to 100°C
Suitable for composite to composite bonding
Low volatile content(solvent-less process)

Applications

Metal to metal bonding
Sandwich constructions
Composite to composite bonding

Forms

Grey flexible film adhesive, available in 5 areal weights; 4 in unsupported form and one with woven nylon carrier.

Product Description	Areal weights g/m²	Roll Width mm	Standard Roll m²
Redux 312	70	533	60
Redux 312UL	100	533	60
Redux 312L	150	533	50
Redux312	300	533	40
Redux 312/5	293	533	40

We possess sample quantities of both Redux 312 (300 g/m²) and 312L (150 g/m²). Queries have been made to obtain more sample quantities for future tests.

Instructions For Use

Application

Allow sufficient time for the adhesive to warm to room temperature (15°C - 27°C) before removing the protective polythene.
Cut the film to the shape and size required.
Remove the release paper and position the adhesive on the prepared bonding surface.
Remove the polythene backing sheet.
Complete the joint assembly and apply pressure while the adhesive is being cured. For sandwich structures the pressure application should be selected to suit the type of core used. After the adhesive has cured it is advisable to maintain pressure on the bonded assembly until it has cooled to below 70°C before releasing.

Mechanical Properties

All the performance values given in this data sheet are based on experimental results obtained during testing under laboratory conditions. They are typical values expected

for Redux 312 prepared and cured as recommended and under the conditions indicated. They do not and should not constitute specification minima.

Storage

Redux 312 has been formulated for maximum storage life with its high performance. Certain precautions, however, will help to enhance that storage life as follows. When stored at room temperature (less than 27°C) it should be kept on a horizontal mandrel passed through the tube core on which the roll is wound. This avoids the risk of local thinning of the film under the weight of the roll.

When storing under refrigeration the original packaging should be retained if possible. When returning to the refrigerator after use it is essential to protect the film with a water vapour barrier packaging material such as polythene.

On withdrawal from the refrigerator the water vapour packaging should not be removed until the roll of adhesive has reached the room temperature. This may take up to 24 hours depending on the size of the roll and the temperature involved (failure to observe this will result in the film becoming damp).

The film should be handled with care whilst in the frozen state since it will be brittle and easily cracked.

On receipt Redux 312 will have a storage life of at least 12 months at -18°C plus an additional shop life o. 1 month at below 27°C.

Volatile content

Redux 312 has a very low volatile content, usually below 1%. In practice, the loss in weight when cured is negligible and emission of volatile products is not of practical significance.

Associated products

Redux 112 and Redux140 surface pre-treatment protection solutions (primer)
Redux 212/NA and Redux 206/NA foaming film adhesives

Handling and safety precautions

In common with all Redux adhesives in film form, Redux 312 is particularly free from handling hazards for the following reasons:

Film is covered on both sides by protective release paper and polythene sheet which are not removed until final component assembly. It should be cut to shape before removing the protective coverings and virtually no handling of the film is necessary.
Virtually tack-free (dry) at normal room temperature. The film is dependent on elevated temperature for wetting-out the adherent surfaces.
Volatile-free at normal room temperature.
Splash free, leak-free, and spillage-free.

However, the usual precautions necessary when handling synthetic resins should be observed.

Description

Redux 312 is a high strength 120°C curing film adhesive, suitable for metal to metal bonding and sandwich constructions, where operating temperatures of up to 100°C may be experienced.

A supported version, Redux 312/5, is available with a woven nylon carrier for bond line thickness control.

Features

- Short cure cycle - cures in 30 minutes at 120°C
- Good mechanical performance up to 100°C
- Suitable for composite to composite bonding
- Low volatile content (solventless process)

Applications

- Metal to metal bonding
- Sandwich constructions
- Composite to composite bonding

Forms

Grey flexible film adhesive, available in 5 areal weights; 4 in unsupported form and one with a woven nylon carrier.

Product Description	Areal Weights g/m²	Roll Width mm	Standard Roll m²
Redux 312	70	533	60
Redux 312UL	100	533	60
Redux 312L	150	533	50
Redux 312	300	533	40
Redux 312/5	293	533	40

Instructions For Use

Pretreatment

It is essential that all substrates to be used are free of contamination and are in as ideal a state for bonding as possible. As pretreatment varies significantly depending on the substrates used, please refer to the Hexcel Composites publication Redux Bonding Technology for optimum procedures.

If there is to be a delay between the pretreatment and bonding of aluminium, the pretreated surface should be protected with Redux 112 or Redux 140 surface pretreatment protection solution to conserve the optimum bonding surface. This will enable bonding to be delayed for up to 2 weeks without deterioration of the pretreated surface. The correct application of Redux 112 or Redux 140 should not alter the bonding performance of Redux 312 (for full application details consult the relevant data sheet).

Application

1. Allow sufficient time for the adhesive to warm to room temperature (15°C - 27°C) before removing the protective polythene.
2. Cut the film to the shape and size required.
3. Remove the release paper and position the adhesive on the prepared bonding surface.
4. Remove the polythene backing sheet.
5. Complete the joint assembly and apply pressure while the adhesive is being cured. For sandwich structures the pressure application should be selected to suit the type of core used. After the adhesive has cured it is advisable to maintain pressure on the bonded assembly until it has cooled sufficiently to be handled without discomfort.

Curing

Redux 312 should be cured at 120 ± 5°C for 30 minutes to obtain optimum properties. Enough time should be allowed for heat to penetrate through the assembled parts to ensure that the adhesive reaches that temperature before timing starts. Cure pressures of around 100 - 350 kPa and heat up rates of approximately 5°C per minute are recommended during cure. After curing it is recommended that components are cooled to below 70°C before releasing the pressure.

Mechanical Properties

All the performance values given in this data sheet are based on experimental results obtained during testing under laboratory conditions. They are typical values expected for Redux 312 prepared and cured as recommended and under the conditions indicated. They do not and should not constitute specification minima.

Metal Bonding Strengths

Redux 312 at areal weights of 70, 100, 150 and 300 g/m², and Redux 312/5 at areal weight 293 g/m² were used to bond Alclad 2024-T3 aluminium test specimens; the aluminium was pretreated in accordance with DTD 915B (iii) (chromic/sulphuric acid pickling). The honeycomb tests used Hexcel's 7.9-1/4-40 (5052) T aluminium honeycomb.

Test	Test Temperature °C	Redux 312 70g/m²	Redux 312 100g/m²	Redux 312 150g/m²	Redux 312 300g/m²	Redux 312/5
Lap Shear Strength MPa	22	37	39	42	43	38
	70	33	32	36	39	29
	90	27	32	33		
	100			17	36	
Bell Peel N/25mm	22		230	245	230	245
Climbing Drum Peel N/76mm	22		190	360	710	510
Flatwise Tensile MPa	22		5.4	7.0	9.1	8.3

Storage

Redux 312 has been formulated for maximum storage life consistent with its high performance. Certain precautions, however, will help to enhance that storage life as follows:

1. When stored at room temperature (less than 27°C) it should be kept on a horizontal mandrel passed through the tube core on which the roll is wound. This avoids the risk of local thinning of the film under the weight of the roll.

2. When storing under refrigeration the original packaging should be retained if possible. When returning to the refrigerator after use it is essential to protect the film with a water vapour barrier packaging material such as polythene.

3. On withdrawal from the refrigerator the water vapour barrier packaging should not be removed until the roll of adhesive has reached room temperature. This may take up to 24 hours depending on the size of the roll and the temperature involved (failure to observe this will result in the film becoming damp).

4. The film should be handled with care whilst in the frozen state since it will be brittle and easily cracked.

On receipt, Redux 312 will have a storage life of at least 12 months at -18°C plus an additional shop life of 1 month at below 27°C

Volatile content

Redux 312 has a very low volatile content, usually well below 1%. In practice, the loss in weight when cured is negligible and emission of volatile products is not of practical significance.

Associated products

Redux 110 and Redux 140 surface pretreatment protection solutions (primer)
Redux 212/NA and 206/NA foaming film adhesives

Handling and safety precautions

In common with all Redux adhesives in film form, Redux 312 is particularly free from handling hazards for the following reasons:

- Film is covered on both sides by protective release paper and polythene sheet which are not removed until final component assembly. It should be cut to shape before removing the protective coverings and virtually no handling of the film is necessar
- Virtually tack-free (dry) at normal room temperature. The film is dependent on elevated temperature for wetting-out the adherend surfaces.
- Volatile-free at normal room temperature.
- Splash-free, leak-free, spillage-free.

However, the usual precautions necessary when handling synthetic resins should be observed. A Material Safety Data Sheet for Redux 312 is available on request.

Release Certification

The Quality System at Hexcel Composites Duxford has been certified to ISO 9001 by Lloyd's Register Quality Assurance, and is approved by the UK Civil Aviation Authority and Ministry of Defence. Certificates of Conformity and Test Reports can be issued for batches of Redux 312 on request.

Important

All information is believed to be accurate but is given without acceptance of liability. Users should make their own assessment of the suitability of any product for the purposes required. All sales are made subject to our standard terms of sale which include limitations on liability and other important terms.

For More Information

Hexcel Composites is a leading worldwide supplier of composite materials to aerospace and other performance driven industries. Our comprehensive product range includes:

- Carbon, glass, aramid and hybrid prepregs
- Honeycomb cores
- Structural film adhesives
- Honeycomb sandwich panels
- Special process honeycombs
- RTM materials

For technical assistance, applications & procedures, or further information, please contact:

Hexcel Composites
Duxford, Cambridge CB2 4QD
United Kingdom
Telephone: 44-(0)1223 833141
Fax: 44-(0)1223 838808

Hexcel Composites
ZI La Plaine, B.P.27 Dagneux
F-01121 Montluel, France
Telephone: 33 (0)4 72 25 26 27
Fax: 33 (0)4 78 06 02 92

Hexcel Composites
Industriestr. 1
A-4061 Pasching, Austria
Telephone: 43-(0)7229 772-0
Fax: 43-(0)7229 772-229

Hexcel Composites
Rue Trois Bourdons, 54
B-4840 Welkenraedt
Belgium
Telephone: 32 87 307 411
Fax: 32 87 882 895

Hexcel Composites
Bruselas, 10 - 16
Polig. Ind. "Ciucad de Paria"
28980 Paria, Madrid, España
Telephone: 34 1 664 49 00
Fax: 34 1 698 49 14

Hexcel Composites
5794 W.Las Positas Blvd.
P.O. Box 8181, Pleasanton,
CA 94588-8781 USA
Telephone: 1 510 847 9500
Fax: 1 510 734 9042

Redux 312 Rheology

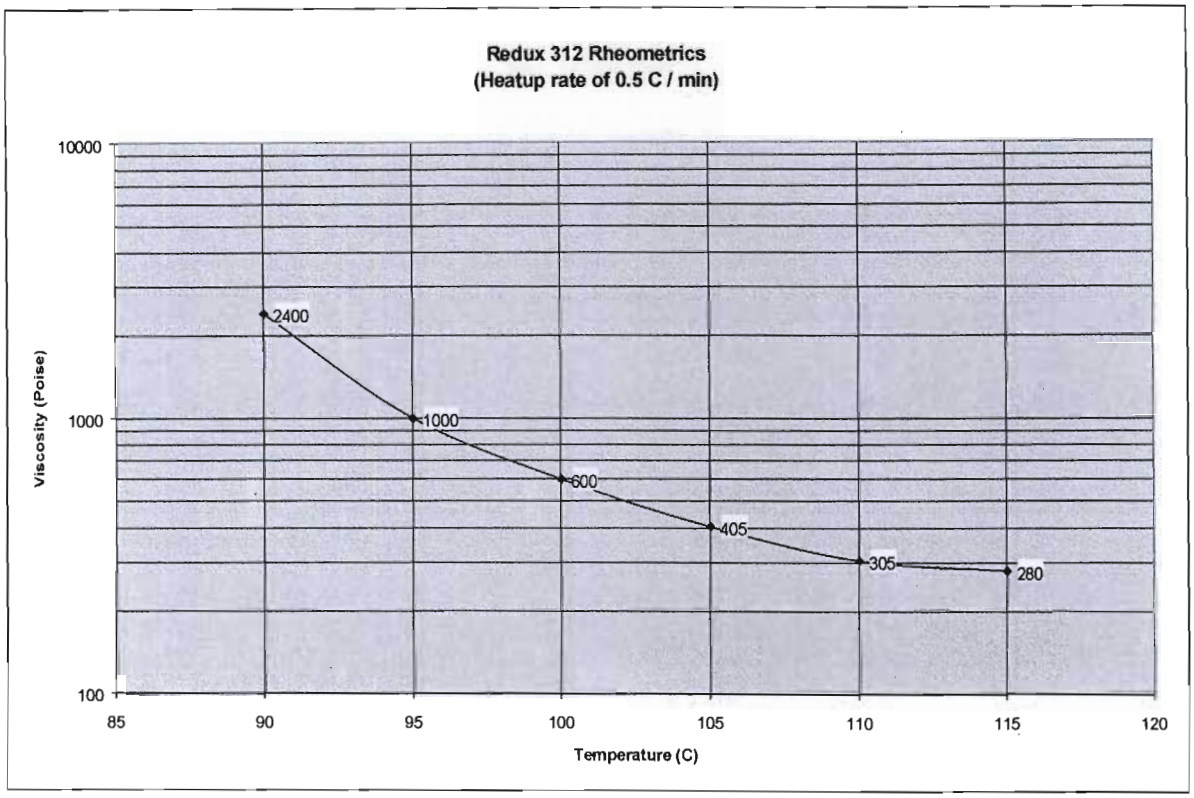

Figure 81 Redux 312 Viscosity curves.

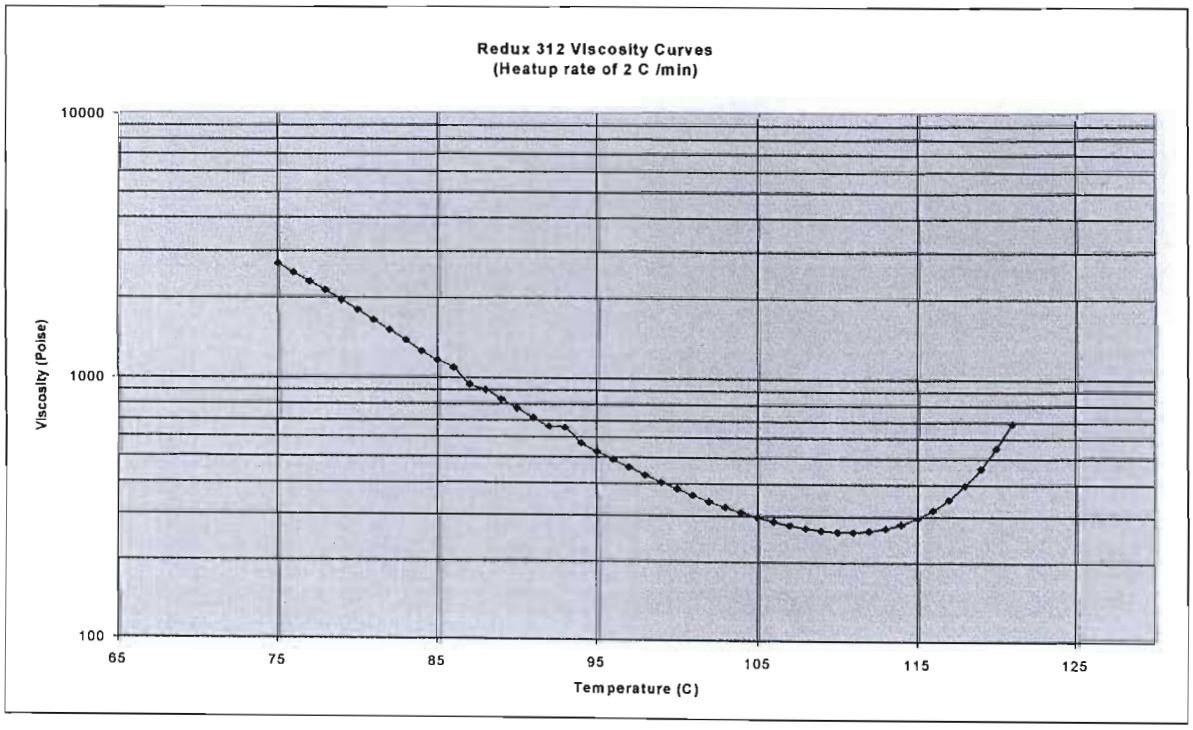

Figure 82 Redux 312 Viscosity Curves

Xiro film Adhesives

Technical Data Sheet
Xiro Adhesive Film V 587-1

Chemical and physical characteristics

Chemical basis	thermoplastic adhesive film based on modified polyolefins	
Melting range	85 - 105 °C / 185 - 220 °F	(Kofler bench)
Melt Flow Index (190 °C / 21.2 N)	8 - 15 g/10min	(DIN 53735)
Density	0.92 g/cm³	(DIN 53479)
Washing resistance	40 °C / 105 °F	(following DIN 53920)
Dry cleaning resistance	yes	(following EN ISO 3175)
Heat resistance	80 °C / 175 °F	(internal method)
Resistance to PVC plasticizers	none	(internal method)

Application parameters

Minimal bond line temperature	105 °C / 220 °F
Application machines and methodes	Can be processed with all established calendering, lamination and bonding techniques, except high frequency welding.
Standard rolls	available film weights on request available roll length on request available roll widths on request standard core diameter 76 mm
Storage conditions	for storage conditions see EC Safety Data Sheet
Safety instructions	for safety instructions see EC Safety Data Sheet
Remarks	none.

xiro

Special Fusible Films/Webs

Materials to be bonded

Guttacoll

Base	Type	minimum Bond Line temp. °C	Melting range °C	Heat Resistance °C	Washing Resistance °C	Plasticizer Resistance	Dry Cleaning Resistance	Density kg/dm³	Form of Delivery: weight g/m²	Form of Delivery: carrier
Polyolefin	Haroco	70	60-75	50	30	no	no	1.04	40-500	none. S
	P 90	105	85-105	85	40	no	no	0.92	40-500	
	XAF 2011	125	100-110	100	40	no	no	0.94	25-100	
	XAF 2031	115	92-102	90	40-60	no	yes	0.93	25-100	
	XAF 2061	105	85-95	85	40	no	no	0.94	25-100	
	XAF 2081	90	80-90	75	40	no	no	0.94	30-100	
	XAF 2211	140	120-130	110	60	no	yes	0.92	25-100	
	XAF 2221	150	120-130	120	60	no	yes	0.96	25-100	
	XAF 2301	160	134-144	130	95	no	yes	0.90	30-100	
	XAF 2311	165	140-150	135	60	no	yes	0.91	30-100	
	XAF 2321	165	135-145	130	60	no	yes	0.92	30-100	
	XAF 2331	155	140-150	130	60	no	yes	0.93	30-100	
Copolyester	P 51	130	115-135	90	90	part	yes	1.22	25-500	PE. S
	P 52	110	100-120	90	60	yes	part	1.20	25-500	PE. S
	P 55	135	115-130	110	60-95	yes	yes	1.10	25-500	PE
	P 71	80	65-80	50	30-40	yes	yes	1.24	25-500	PE. PP. S
	XIROWEB 8710	100	92-100	85	40	yes	yes		16-25	
Copolyamide	P 171	140	135-150	120	60-95	n. a.	yes	1.05	25-500	none. PE
	P 178	185	170-190	140-160	60-95	n. a.	yes	1.10	35-500	none. PE
	XIROCOLL 3400	130	100-110	100	40	no	yes	1.10	20-100	S
	XIROCOLL 3410	140	130-140	120	60	no	yes	1.10	20-100	S
	XIROCOLL 3420	90	75-85	75	40	no	yes	1.10	20-100	S
	XIROCOLL 3440	130	110-120	105	40-60	yes	yes	1.10	20-100	S
	XIROCOLL 3450	150	120-130	120	95	no	yes	0.97	25-100	S
	XIROWEB 8240	110	105-110	95	40	no	yes		15. 23. 30	
	XIROWEB 8250	100	80-85	75	40	no	yes		20. 30	
TPU	Poro I	90	65-85	60	30-40	yes	yes	1.16	25-500	PE
	Poro II	100	65-85	75	30-40	yes	yes	1.16	25-500	PE
	Poro III	100	65-85	80	40-60	yes	yes	1.21	25-500	PE [illegible]
	Poro X	135	100-130	90	40-90	yes	yes	1.18	25-500	PE. PP. S
	Poro E	150	130-155	130	95	yes	yes	1.20	25-500	PE

Materials to be bonded (Wood Products: Wood / chipboard, Paper / chipboard, Cork; Woven / Non woven / Felt: Wool, Cotton, Polyamide, Polyester, Aramide, Polypropylene; Foam plastics: PVC plasticized, PVC rigid, PUR rigid / non rigid, Polystyrene, PMI, PE)

Type	Metals	Aluminium	Leather	Wood / chipboard	Paper / chipboard	Cork	Wool	Cotton	Polyamide	Polyester	Aramide	Polypropylene	Glass	PVC plasticized	PVC rigid	PUR rigid / non rigid	Polystyrene
Haroco			●	●	●	●		●								●	●
P 90	●	●		●	●	●							●				
XAF 2011				●	●	●		●		●			●				
XAF 2031	●	●		●	●	●		●					●				
XAF 2061	●	●	●	●	●	●		●		●			●				
XAF 2081	●			●	●	●		●		●		●	●			●	
XAF 2211	●	●	●	●	●	●		●	●				●			●	
XAF 2221				●	●	●		●	●		●		●			●	
XAF 2301										○		●	●				
XAF 2311	●			●						●		●	●			●	
XAF 2321										●		●	●				
XAF 2331	●			●						●		●	●				
P 51			●	●	●	●	●	●	●	●				●	●	●	
P 52	●	●	●	●	●	●	●	●	●	●				●	●	●	
P 55	●	●		●	●	●	●	●	●	○	●			●	●	●	
P 71	●		●	●	●	●		●	●	○				●	●	●	
XIROWEB 8710					●			●		●				●			
P 171			●				●	●	●	●	●						
P 178							●	●	●	●			●				
XIROCOLL 3400			●	●	●	●			●								
XIROCOLL 3410			●	●	●				●								
XIROCOLL 3420			●	●	●				●								
XIROCOLL 3440	●		●	●	●	●			●	●				●	●	●	
XIROCOLL 3450				●	●	●		●	●				●			●	
XIROWEB 8240					●			●	●	●		●				●	
XIROWEB 8250			●	●	●				●								
Poro I			●	●	●	●		●	●	●	●		●	●	●	●	●
Poro II			●	●	●	●		●	●	●	●		●	●	●	●	●
Poro III			●	●	●	●		●	●	●	●		●	●	●	●	●
Poro X			●	●	●	●	●	●	●	●	●		●	●	●	●	
Poro E				●	●				●	●			●	●	●	●	

Materials to be bonded, continued (plastics)

Type	PMI	PE	PE	PP	Polyamide	Polyester	Polycarbonate	ABS	PMMA	PVC plasticized	PVC rigid	Cellulose Acetate	PS	Phenolics-Melamine	Rubber	SBR	Neoprene
Haroco		●							●						●		
P 90	●						●									●	
XAF 2011		●	●														
XAF 2031	●															●	
XAF 2061	●	●	●				●									●	
XAF 2081	●	●	●				●									●	
XAF 2211		●	●		●												
XAF 2221		●	●	●	●												
XAF 2301				●													
XAF 2311		●		●													
XAF 2321		●	●	●													
XAF 2331				●										●			
P 51																	
P 52										●					●		
P 55	●						●		●	●							
P 71							●			●	●						
XIROWEB 8710										●							
P 171														●			
P 178																	
XIROCOLL 3400																	
XIROCOLL 3410																	
XIROCOLL 3420																	
XIROCOLL 3440							●	●		●							
XIROCOLL 3450		●	●	●	●												
XIROWEB 8240																	
XIROWEB 8250																	
Poro I							●	●		●	●	●					●
Poro II							●	●		●	●	●					
Poro III							●	●	●	●	●	●					
Poro X							●	●			●	●		●			
Poro E								●			●	●					

Double Layer Films	XAF 2501 (P 55 / 2061)	XAF 2521 (3140 / 2211)	XAF 2531 (3140 / V 300)	Others on request

● = very good

○ = good

PE = Polyethylene
PP = Polypropylene
S = Siliconized paper

Form of delivery: Depending on the requirements, the Haroco, P and Poro types in widths from 10 mm – 2000 mm, [illegible] XAF types [illegible] widths [illegible] 10 mm – 1000 mm [illegible]

[illegible]

Capran high temperature vacuum bag material.

CAPRAN 526 HEAT STABILISED NYLON 6/6 - BLOWN TUBULAR FILM

DESCRIPTION

CAPRAN 526 is a heat stabilised blown film produced from nylon 6/6 resin. It is available both as lay flat tubing or as a slit tube laid at double width. Blown film is recommended as a bagging material for Advanced Composite fabrication by vacuum bag or autoclave techniques. The high elongation facilitates close conformation to complex shapes and minimises bridging. Nylon film manufactured from nylon 6/6 resin will operate at temperatures too high for nylon 6 film.

PHYSICAL PROPERTIES 20°C & 50% RH

CAPRAN 526	
Maximum Use Temperature	232°C
Colour	Blue
Tensile Strength	110.3 MPa
Yield Strength	34.5 MPa
Elongation	375%
Tear Strength	90g (ASTM D1922)
Shrinkage	1% (@ 177°C)
Flammability	Self extinguishing melts
Crystalline Melt Point	266°C

AVAILABILITY & PACKAGING

Thickness (nominal)	0.05mm or 0.076mm
Pack Size	Nominally 45 kgs
Yield	Nominally 17.4 m²/kg

WIDTHS

Up to 4.064 mts wide available.

STORAGE & HANDLING

All nylon films absorb water. The higher the moisture content the more flexible they become, conversely at low moisture levels flexibility is reduced. Capran 526 is despatched with an optimum moisture content to provide maximum performance and handleability. To preserve these characteristics during storage the roll should be wrapped in polyethylene and stored at around 65% RH and 20°C.

CAPRAN is a tradename of Allied-Signal Inc.

0790 03 06

HALAR E.C.T.F.E. FLUOROPOLYMER RELEASE FILMS

DESCRIPTION

HALAR film products are high strength high elongation release films which are ideal for use in vacuum bag/autoclave processing of composites. Halar will release cleanly from epoxy, polyester or phenolic resins and is intended for use up to 160°C (long term). It is available in non perforated and perforated forms in white or blue tints. Composite shops using both perforated and non-perforated styles often choose to colour code the different styles (perforated: blue non-perforated: white) enabling easy identification between the two by operatives.

The perforated film provides an effective pathway for removal of volatiles or to enable resin flow during cure. The low density results in a 22% greater surface area/kg of material compared to FEP films.

PHYSICAL PROPERTIES

HALAR PERFORATED AND NON PERFORATED	
Maximum Cure Temperature	160°C (long term)
Halar WNP/BNP*	Release film - non perforated
Halar WP1/BP1*	Release film - perforated 0.045" diameter holes ½" centres
Halar WP3/BP3*	Release film - pin pricked 0.015" diameter holes ½" centres
Release	Chemically inert to most commercial resins
Colour	White or Blue
Density	1.68 g/cm³
Elongation	200%
Melt point	240°C
Flammability	Non-flammable

AVAILABILITY & PACKAGING

Thickness	0.0127mm
Yield	47 m²/kg
Weight (nominal)	4.7 kg/roll
Roll size	1.22m wide x 183m long
Core size	75mm

STORAGE & HANDLING

Store in original packing.
No handling problems experienced.

* NOTE: W designates White Film
B designates Blue Film

0892 06 02

Aerovac Systems (Keighley) Ltd.
Bradford Road, Sandbeds, Keighley, West Yorkshire BD20 5LN, England.
Telephone: 0535 607457 Fax: 0535 609754

PRODUCT	DESCRIPTION
B2000P/P3	De bulking film - ambient use only.
HALAR WNP	Release film - high tear strength - impervious - to 160°C.
HALAR WP1	Release film - high tear strength - perforated - to 160°C.
HALAR WP3	Release film - high tear strength - pin pricked - to 160°C.
A5000	Release film - high elongation, impervious - to 260°C.
A5000 P1	Release film - high elongation, perforated - to 260°C.
A5000 P3	Release film - high elongation, pin pricked - to 260°C.
MR FILM	MR film - high elongation - to 315°C.
A5000SKA	Release film - high elongation - to 300°C.
A8888	Release fabric - silicone coated polyamide, porous - to 180°C.
B4444	Release fabric - smoother, silicone coated polyamide, porous - to 180°C.
E5555	Release / Bleed fabric - silicone coated glass, porous - to 475°C.
C6666	Release fabric (also bleed) - silicone coated glass, porous - to 475°C.
60001	Release fabric - synthetic, scoured and heat set, porous - to 200°C.
70001	Release fabric - synthetic, scoured and heat set, porous - to 200°C.
P9999	Release fabric - silicone resin coated polyester, porous - to 200°C.
A100	Peel ply - heat set and scoured - polyamide - to 180°C.
B100	Peel ply - heat set and scoured - smoother polyamide - to 180°C.
BR100	Peel ply - as B100 except fluorocarbon coated - to 180°C.
FF/03/PM	Bleed/release fabric - PTFE coated glass - to 320°C.
FF/03/PH	Bleed/release fabric - high porosity PTFE coated glass - to 320°C.
FF/03/A	Release fabric - impervious, PTFE coated glass - to 320°C.
FF/05/A	Release fabric - impervious, PTFE coated glass - special uses.
FF/010/PM	Bleed/release fabric - as FF/03/PM & PH but heavier & stronger.
FF/010/A	Release fabric - impervious, PTFE coated glass - special uses.
FF/0015/P	Bleed/release fabric - PTFE coated glass, for smoother finish - to 320°C.

NB. Please note that release films are available in several colours, more commonly clear, white, red and blue.

Appendix G

Impact tester calibration sheet.

Table for calculating impact energy.

IMPACT ENERGY IN JOULES

scale/pin	3	4	5	6	7
1:	12.09	8.58	5.11	2.42	0.63
2:	12.07	8.56	5.09	2.40	0.61
3:	12.04	8.53	5.06	2.37	0.58
4:	12.00	8.48	5.02	2.33	0.54
5:	11.94	8.43	4.96	2.27	0.48
6:	11.87	8.36	4.89	2.20	0.41
7:	11.79	8.27	4.81	2.12	0.33
8:	11.70	8.18	4.71	2.03	0.24
9:	11.59	8.07	4.61	1.92	0.13
10:	11.47	7.96	4.49	1.80	0.01
11:	11.34	7.83	4.36	1.67	———
12:	11.20	7.68	4.22	1.53	———
13:	11.05	7.53	4.06	1.38	———
14:	10.88	7.37	3.90	1.21	———
15:	10.71	7.19	3.72	1.04	———
16:	10.52	7.00	3.54	0.85	———
17:	10.32	6.80	3.34	0.65	———
18:	10.11	6.60	3.13	0.44	———
19:	9.89	6.38	2.91	0.22	———
20:	9.67	6.15	2.68	———	———
21:	9.43	5.91	2.44	———	———
22:	9.18	5.66	2.20	———	———
23:	8.92	5.41	1.94	———	———
24:	8.66	5.14	1.67	———	———
25:	8.38	4.87	1.40	———	———
26:	8.10	4.58	1.12	———	———
27:	7.81	4.29	0.83	———	———
28:	7.51	4.00	0.53	———	———
29:	7.21	3.69	0.23	———	———
30:	6.90	3.38	———	———	———
31:	6.58	3.06	———	———	———
32:	6.26	2.74	———	———	———
33:	5.93	2.41	———	———	———
34:	5.59	2.08	———	———	———
35:	5.25	1.74	———	———	———
36:	4.91	1.39	———	———	———
37:	4.56	1.05	———	———	———
38:	4.21	0.70	———	———	———
39:	3.86	0.34	———	———	———
40:	3.50	———	———	———	———
41:	3.14	———	———	———	———
42:	2.78	———	———	———	———
43:	2.42	———	———	———	———
44:	2.06	———	———	———	———
45:	1.70	———	———	———	———
46:	1.33	———	———	———	———
47:	0.97	———	———	———	———
48:	0.61	———	———	———	———
49:	0.25	———	———	———	———
50:	———	———	———	———	———